TECHNICAL REPORT ARBRL-TR-02347

APPLICATION OF DIGITAL FILTERS AND THE FOURIER TRANSFORM TO THE ANALYSIS OF BALLISTIC DATA

James N. Walbert

July 1981

US ARMY ARMAMENT RESEARCH AND DEVELOPMENT COMMAND
BALLISTIC RESEARCH LABORATORY
ABERDEEN PROVING GROUND, MARYLAND

REPORT DOCUMENTATION PAGE	READ INSTRUCTIONS BEFORE COMPLETING FORM

1. REPORT NUMBER	2 GOVT ACCESSION NO.	3. RECIPIENT'S CATALOG NUMBER
TECHNICAL REPORT ARBRL-TR-02347		

4. TITLE (and Subtitle)	5. TYPE OF REPORT & PERIOD COVERED
APPLICATION OF DIGITAL FILTERS AND THE FOURIER TRANSFORM TO THE ANALYSIS OF BALLISTIC DATA	Technical Report
	6. PERFORMING ORG. REPORT NUMBER

7. AUTHOR(s)	8. CONTRACT OR GRANT NUMBER(s)
James N. Walbert	

9. PERFORMING ORGANIZATION NAME AND ADDRESS	10. PROGRAM ELEMENT, PROJECT, TASK AREA & WORK UNIT NUMBERS
U.S. Army Ballistic Research Laboratory ATTN: DRDAR-BLI Aberdeen Proving Ground, MD 21005	1L161102AH80

11. CONTROLLING OFFICE NAME AND ADDRESS	12. REPORT DATE
U.S. Army Armament Research & Development Command U.S. Army Ballistic Research Laboratory ATTN: DRDAR-BL Aberdeen Proving Ground, MD 21005	JULY 1981
	13. NUMBER OF PAGES
	91

14. MONITORING AGENCY NAME & ADDRESS(if different from Controlling Office)	15. SECURITY CLASS. (of this report)
	UNCLASSIFIED
	15a. DECLASSIFICATION/DOWNGRADING SCHEDULE

16. DISTRIBUTION STATEMENT (of this Report)

Approved for public release; distribution unlimited.

17. DISTRIBUTION STATEMENT (of the abstract entered in Block 20, if different from Report)

18. SUPPLEMENTARY NOTES

19. KEY WORDS (Continue on reverse side if necessary and identify by block number)

digital filter	cepstral analysis
Fourier transform	differentiator
spectral analysis	transition band
convolution	pass band
transfer function	stop band

20. ABSTRACT (Continue on reverse side if necessary and identify by block number)   jmk

Special numerical techniques are described which permit productive utilization of digital filters in the analysis of ballistic data. Specific examples are given which demonstrate the use of these techniques.

DD FORM 1473 1 JAN 73   EDITION OF 1 NOV 65 IS OBSOLETE

TABLE OF CONTENTS

3

LIST OF ILLUSTRATIONS

LIST OF ILLUSTRATIONS (Continued)

LIST OF ILLUSTRATIONS (Continued)

I. INTRODUCTION

The application of digital filter techniques has had a substantial impact on numerical analysis of test data in recent years. In a previous report, reference (1), the author described software available on the BRL CYBER system for the design of multiple band digital filters and differentiators. It is the purpose of this report to illustrate the techniques by which such filters may be exploited in the analysis of time series data taken during various types of ballistic experiments. This report will also describe numerical methods for verification of results obtained through the use of digital filters.

It is important to define carefully the type of data to which these techniques apply. In a general sense, any analog data taken from a system which has governing differential equations with solutions in terms of Fourier series is a candidate for such analysis. More specifically, these techniques assume the data to consist of a discrete set of points sampled from an analog signal at equal time intervals. In addition, it will be assumed that sufficient care has been taken in the sampling process to avoid aliasing, (i.e., the data has not been biased by over or under-sampling) and that no component of the recording or playback system has been "overdriven" in frequency response or amplitude.

Finally, it should be noted that there will be instances in which all of the above assumptions are satisfied, and yet Fourier analysis fails to provide the desired information. This report contains at least one such example. The important point to be remembered is that these techniques cannot be used as "black box" processes. Moreover, it is possible to obtain seemingly reasonable results which are in fact totally erroneous if insufficient care is given to the analysis process.

II. FREQUENCY ANALYSIS VIA THE FAST FOURIER TRANSFORM

It is not the purpose of this report to relate in detail the theory of the Fast Fourier Transform (FFT). The reader will be assumed to have some knowledge of the subject, and is referred to various texts, references (2, 3), for additional information. It suffices to say that FFT subroutines are readily available, and provide the background for this report, since

---

[1] *J.N. Walbert, "Computer Algorithms for the Design and Implementation of Linear Phase Finite Impulse Response Digital Filters", BRL Technical Report (to be published).*

[2] *Bede-Liu, editor, Digital Filters and the Fast Fourier Transform, Halsted Press, 1975.*

[3] *L.R. Rabiner, B. Gold, Theory and Application of Digital Signal Processing, Prentice-Hall, 1975.*

Fourier analysis without the FFT is far too time-consuming computation-
ally to be feasible. One additional comment should be made: in
analyzing ballistic data, one deals generally with relatively small
numbers of data points (say 1000 to 2000) during a specific event. For
this reason, an FFT routine based on powers of 2 is not as useful as
one which can transform a data set of arbitrary length. The subroutine
used for the analysis presented in this report is one given to the
author by Dr. Carl de Boor at the Mathematics Research Center, Madison,
Wisconsin*. A listing of this subroutine in BASIC is given in Appendix
A.

There are numerous methods for using the FFT to compute a frequency
spectrum of a time series, and perhaps even a greater number of techniques
by which one may emphasize certain spectral characteristics. References
4,5, and 6 provide a great deal of insight into the various methods which
can be used. For the processes used in this analysis of the data
discussed in this report, it is not necessary to obtain the most precise
spectral estimates possible, either in frequency or amplitude. One need
only be able to determine the frequency ranges within which certain
phenomena of interest occur in order to design filters to isolate them.
Once these individual components are separated, a more precise frequency
analysis on each component of the original data can be performed, if
desired. It suffices, therefore, to use a simple amplitude spectrum,
normalized either to the spectral peak or by some other suitable means.

For example, if x(t) are the data, sampled at intervals equally
spaced in time t, then the discrete Fourier transform of x(t), X(f), is
a complex valued function

$$X(f) = R(f) + iI(f),$$

where $i^2 = -1$ and R and I are real valued functions of the discrete
frequencies f. The magnitude of X(f), denoted by $|X(f)|$, is given by

$$|X(f)| = \sqrt{R^2(f) + I^2(f)}.$$

Private communication during a visit by the author in May, 1979.

[4] *R.B. Blackman, J.W. Tukey, The Measurement of Power Spectra, Dover
Publications, 1958.*

[5] *C.K. Yuen, D. Fraser, Digital Spectral Analysis, Pitman Publishing,
1979.*

[6] *J.S. Bendat, A.G. Piersol, Random Data: Analysis and Measurement
Procedures, Wiley Interscience, 1971.*

Let

$$M = \max |X(f)|,$$

taken over all f. Then at each frequency f, the value S(f) of a normalized amplitude spectrum is defined by

$$S(f) = |X(f)|/M.$$

This admittedly crude spectrum will be shown to be entirely adequate for the first stage of data analysis.

The remainder of this report will demonstrate the process of spectral analysis on 5 types of data curves. These same five examples will be used to illustrate the application of digital filters. In each example, the data has not been converted to engineering units; the vertical axis has been labeled signal amplitude for reference. This was deliberately done to illustrate the fact that the vertical scaling of the data is not important in the process of the analysis. Moreover, each example is taken from test data; since the analysis of this data will appear in other reports, a discussion here concerning magnitudes of signal components in engineering units would serve no purpose.

III. EXAMPLE 1: THE HALF SINE PULSE ANALYSIS

The data curve in this example, shown in Figure 1, is the record of the response of a force gage mounted on a small mass as this mass impacts an essentially infinite mass. One would expect the force to be a half sine pulse, as indeed it is, but there is an additional sinusoidal component present in the signal. It is the purpose of the present analysis to separate the two components in the data.

The first step is the computation of the Fourier spectrum, shown in Figure 2. Some preliminary comments concerning the appearance of a spectrum are in order. In general terms, the more one-sided the time series, (i.e., the larger the absolute value of its mean) the larger the magnitude of the spectrum near zero on the frequency axis. In this example, one therefore expects to see the large zero Hz component. In some cases, this component may in fact be so large that it obscures other components in the spectrum. One solution frequently mentioned in the literature is to adjust the data so that it has zero mean prior to computing the spectrum. This technique works quite well when the amplitude of the data is nearly symmetric about its mean; in other instances, such as the present example, mean adjustment has little or no effect on the spectrum. At any rate, it is not a goal of this analysis to determine the precise amplitude spectrum; to identify the frequency ranges of the

11
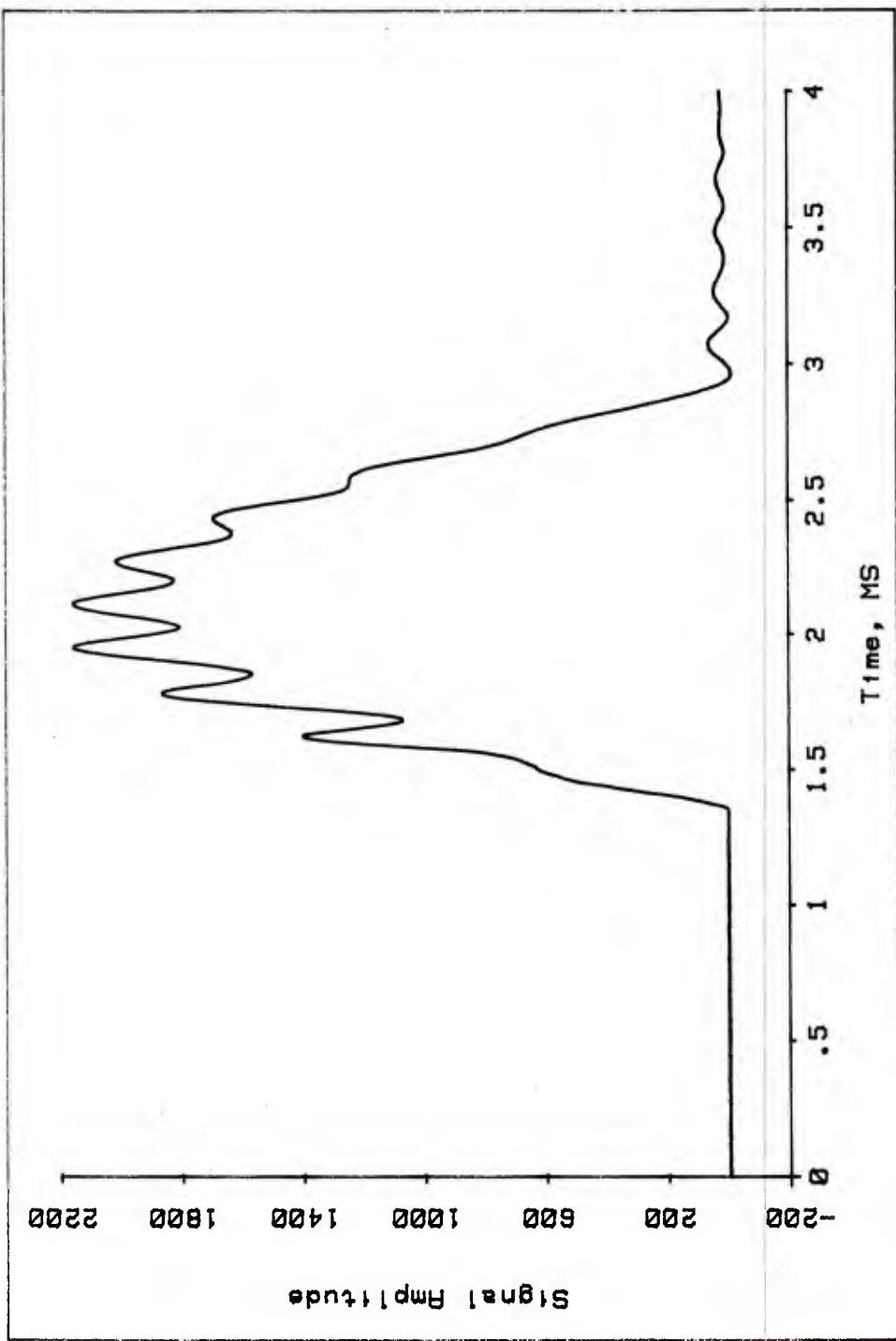
Figure 1.   The Half Sine Pulse: Raw Data

12
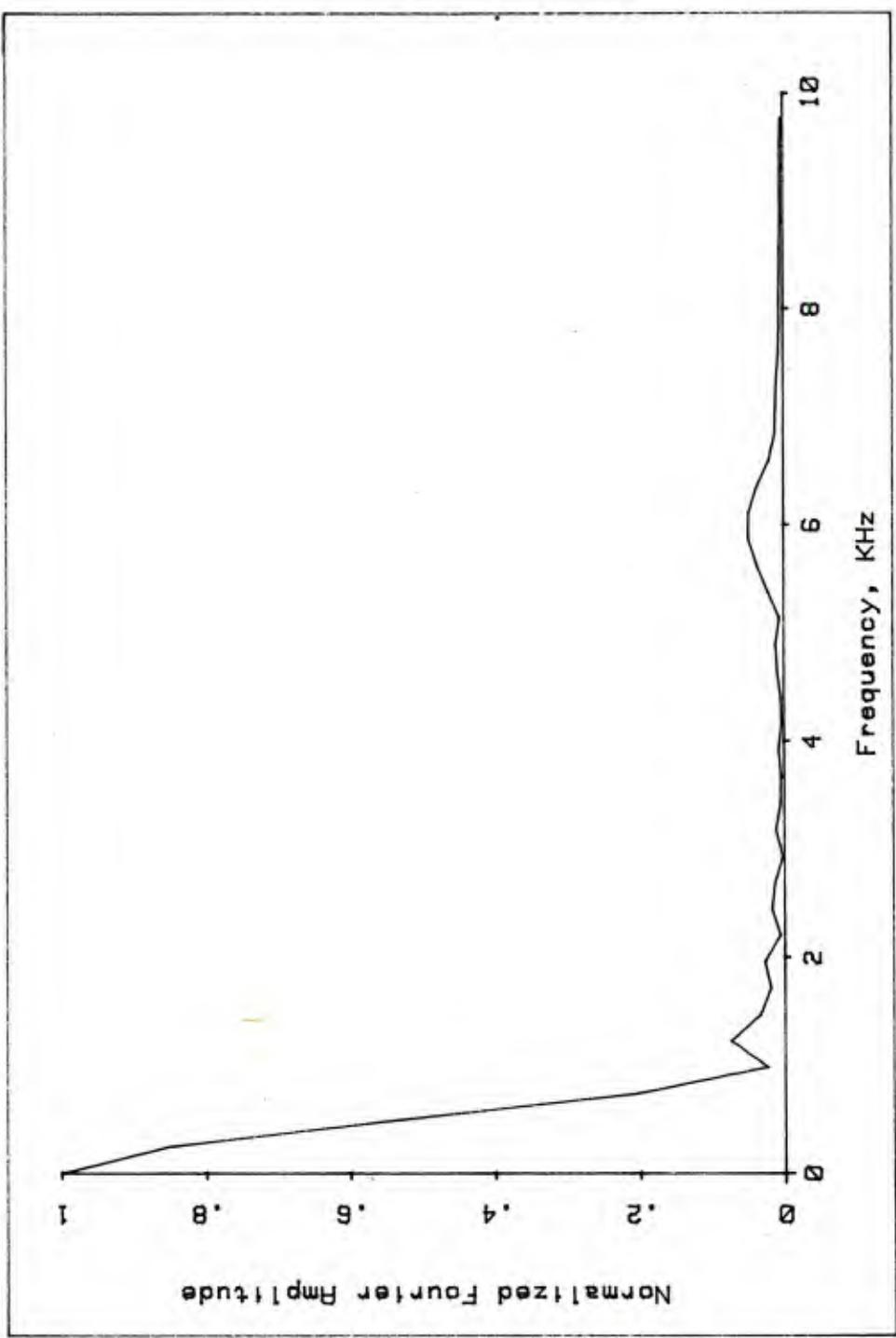
Figure 2. The Half Sine Pulse: Normalized Amplitude Spectrum

13

signal components the spectrum of Figure 2 is entirely adequate. Moreover, for analysis of trends or other baseline variations in ballistic data, such as in Example 4, adjustment of the data for zero mean may actually obscure the phenomenon which is to be detected.

Returning to the spectrum of Figure 2, one notes the peak at zero Hz, and the side lobes steadily decreasing in amplitude out to about 4.1 kHz. This portion of the spectrum is the classic shape generated by a pure half sine pulse. The rounded peak centered at 6 kHz is the component of interest here. It represents that portion of the data which is extraneous to the half sine pulse. One feature of this peak which should be noted here is that it is not sharp. This is an indication that more than one isolated frequency is present in this data component.

There are two possible causes for this resolution problem:

1) there are numerous data components present with frequency responses too close together to be distinguishable in the spectrum.

2) there is one data component, the frequency of which varies over the duration of the spectrum.

In the first case, the data was not sampled at a sufficiently high rate; in the second case, the spectral duration must be shortened for more precise determination of frequency content.

From Figure 1, it can be seen that there is probably only one component which must therefore have a time-varying frequency. At this stage of the analysis, there is no need to recompute the spectrum; application of a low pass filter with a cutoff frequency somewhere in the range of 2 to 4 kHz will effectively remove the higher frequency component. In this instance, choosing a cutoff frequency of 2 kHz with a transition band* from 2 to 4 kHz, the resulting filtered curve is shown in Figure 3. Depending on the reason for conducting the analysis, this curve may be entirely satisfactory. There is, however, one obvious difference between the curve in Figure 3 and that anticipated from Figure 1: in the original data curve, the start of the pulse is defined by a rather sharp corner; whereas in the filtered curve, this corner appears rounded. If this portion of the curve is important to the analysis, then this distortion is not acceptable.

The "rounding" is an undesirable side effect of the filtering process; a technique for eliminating this problem is the main purpose of the present example. To begin with, one must understand how and why the problem occurs. It is vital to realize that only digital data can have sharp corners; no analog system has components with the infinite response

---

*All filters used in this report were designed and applied using the software described in Reference 1. The reader is assumed to be familiar with this material or with filter design in general.

14
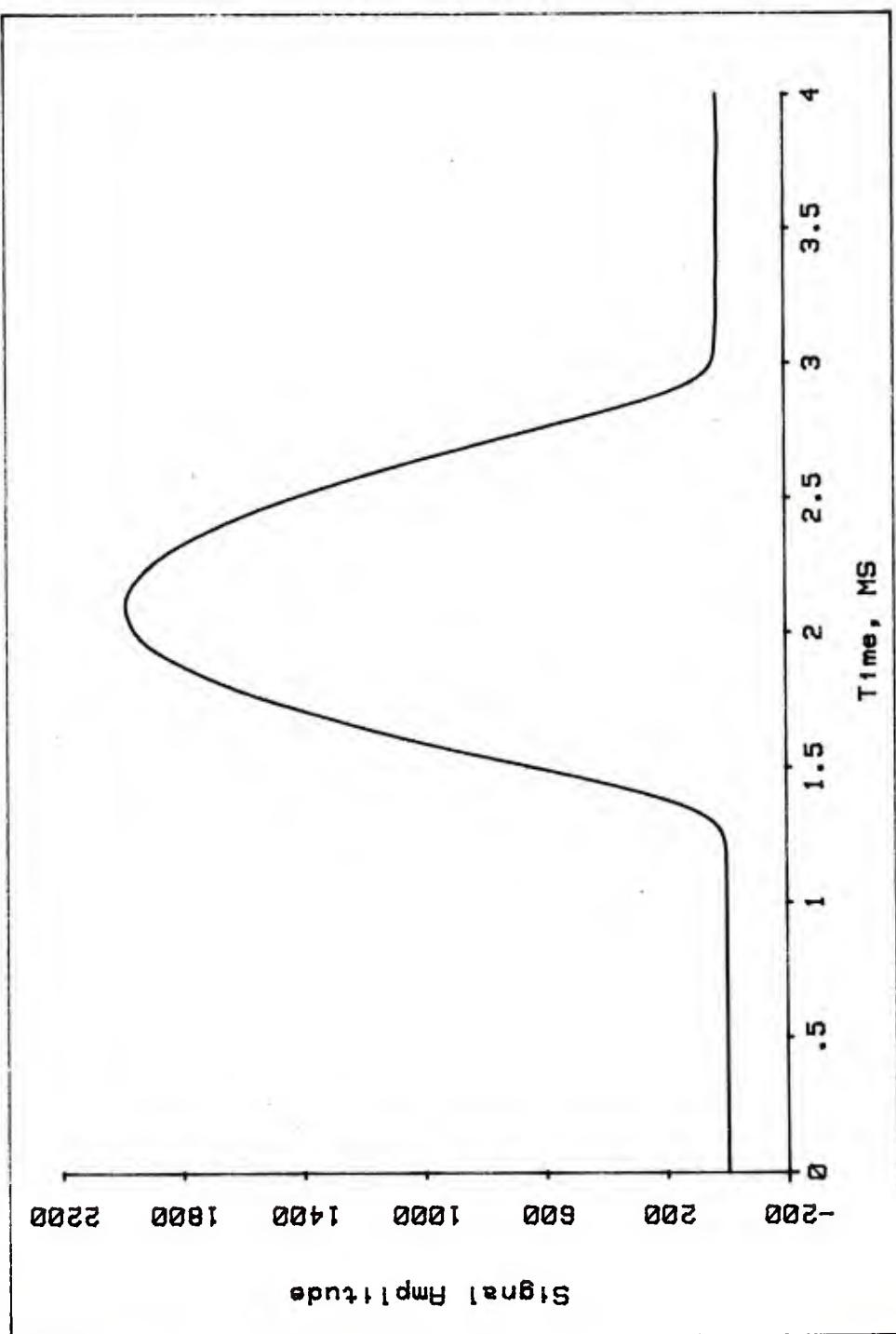
Figure 3. The Half Sine Pulse Low Pass Filtered with Cutoff Frequency 2 KHz

15

necessary to produce such output. The analog systems are nevertheless presumed to have a sufficiently rapid response to record the event, and any useful digital filtering technique should not degrade the quality of that response. The implication is, then, that the response of the digital filter is at fault.

Those familiar with this type of problem in numerical analysis will realize that there are two solutions: use more data points in the vicinity of the "corner", or use a shorter filter, i.e.: one with fewer coefficients. Each of these solutions has drawbacks. The first solution requires sampling the data at a higher rate, which may be physically or economically impossible for some types of data. One might, of course, sample at a higher rate only in the vicinity of the corner, but non-constant sampling rates pose a myraid of analysis problems and are best avoided altogether. In addition, increasing the sampling rate increases the bandwidth of the data. This means that, as a percent of bandwidth, any low pass filter of a specified cutoff frequency has smaller pass band and transition band, which may in general lead to a degradation of the filter amplitude response. The second solution, shortening the filter, may also cause degradation of amplitude response. In this case, one is required to design a filter response with what may prove to be an inadequate number of points.

There is a third option. The major underlying assumption in Fourier analysis is that the data to be analyzed is periodic. This assumption is violated by the half sine component of the raw data curve. Since the corner point in the raw data set can be identified easily by numerical search, one can reflect the data set through this point, to obtain a curve which is more periodic. Such a reflection is shown in Figure 4. Assuming no data of interest occurred prior to the reflection point no information is lost. Using the same low pass filter as before on this reflected curve, and then zeroing out the reflected portion and truncating the data set to its original length, one obtains the filtered curve shown in Figure 5. The corner is now preserved to the same degree of accuracy with which it appeared in the raw data. This reflection process, or odd periodic extension, is trivial to implement in a computer and avoids the problems encountered with changes in filter design or data sampling. One could treat the trailing end of the half sine pulse in a similar fashion although it will subsequently be shown that this may be inappropriate.

Although Figure 5 shows that the extraneous component has been completely removed, this example is obviously simple. How one can determine the adequacy of the process in a more complex data set will be demonstrated in other examples, but one such method can be shown in this example. The Fourier spectrum of the curve in Figure 5 is shown in Figure 6. In comparison with the spectrum in Figure 2, it will be seen that the spectra are virtually identical out to about 4.1 kHz, beyond which the spectrum of the filtered data set shows no significant content, as desired. Thus, post-filter spectral analysis (with the same normalization as the original spectrum) will verify not only that the appropriate components have been

16
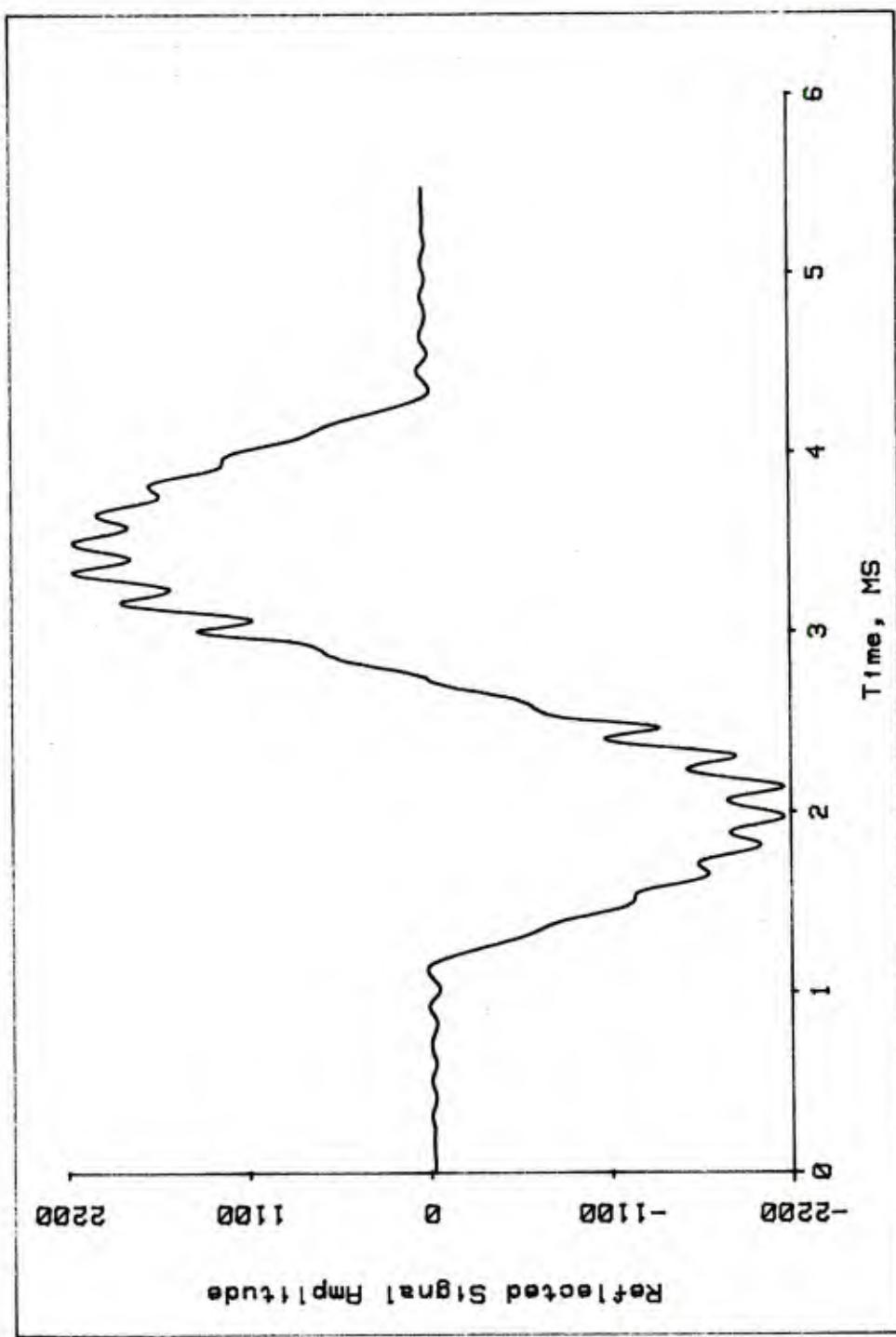
Figure 4. The Half Sine Pulse Reflected

17
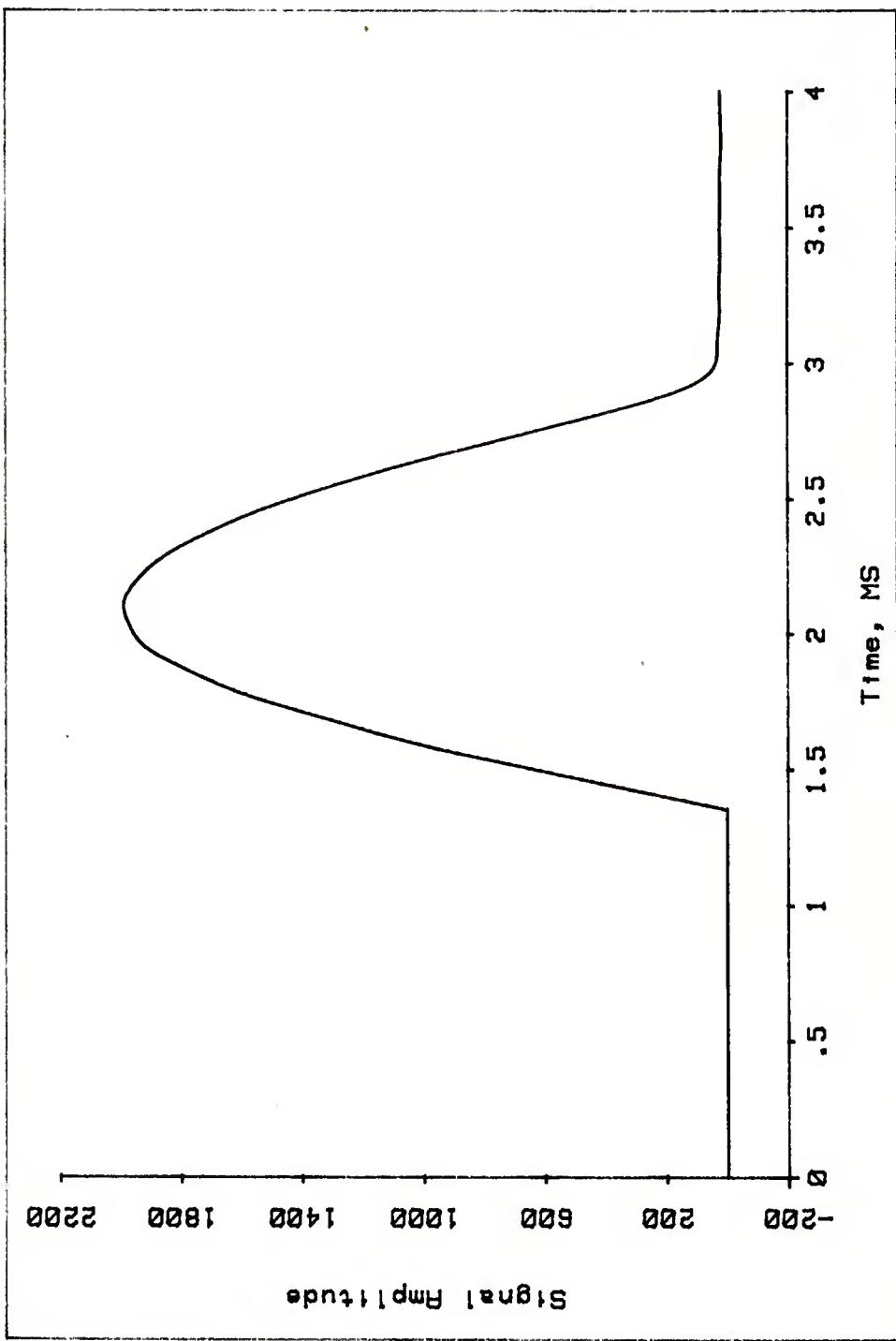
Figure 5. The Half Sine Pulse Low Pass Filtered Using the Reflection Technique
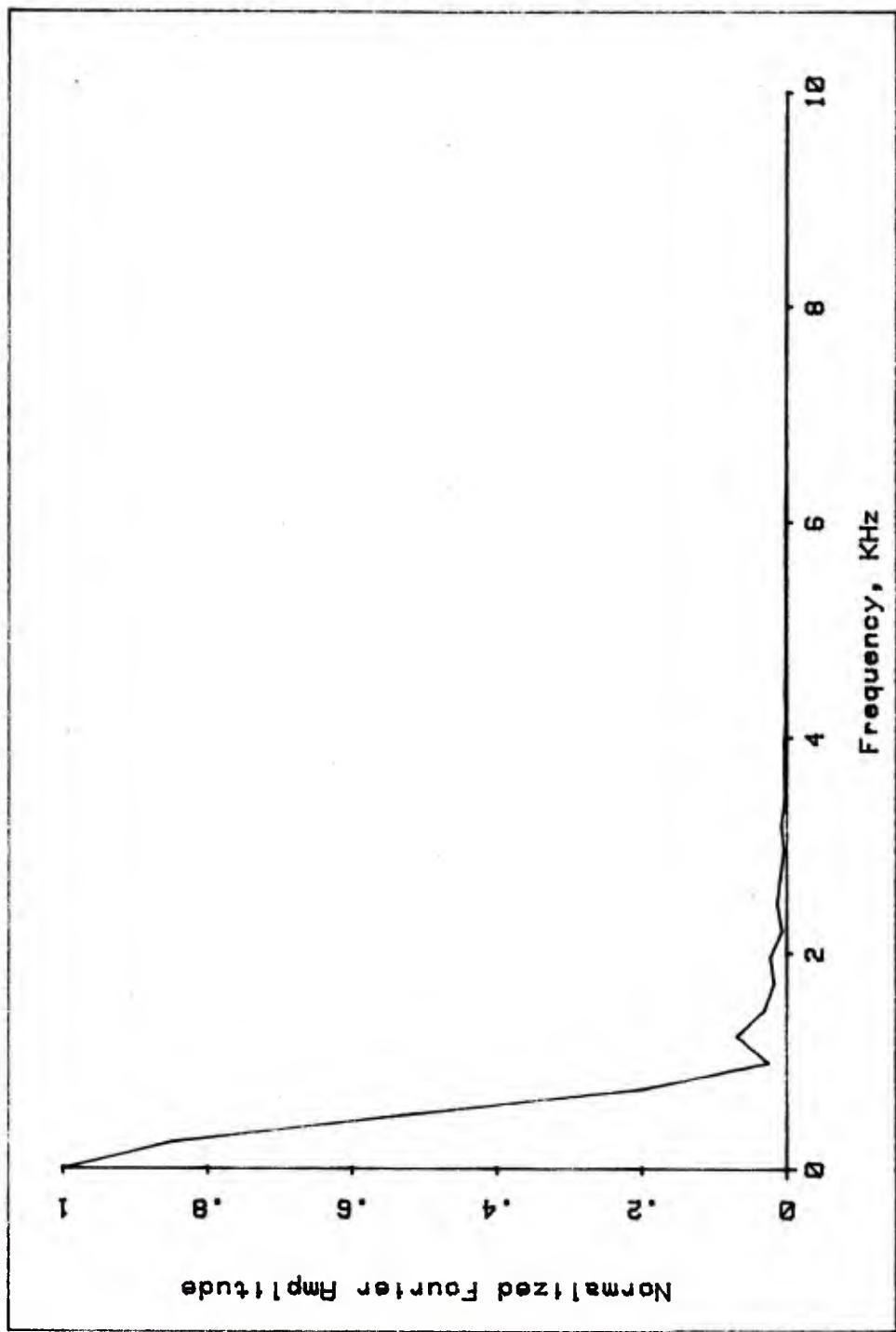
Figure 6. Normalized Amplitude Spectrum of the Filtered Half Sine Pulse

19

removed, but also to what extent, if any, the remaining components have been altered.

It is an indisputable truth that any analysis of this type of data must be done with an understanding of the physical and mechanical aspects of the experiment. In the present example, a small cylindrical deformable mass impacted an infinite nondeformable mass. A careful examination of Figures 1 and 5 with the aid of a straight edge will reveal the fact that the force curve did not return to zero after the event. This is evidence of the fact (physically measured) that the small mass was deformed during the impact. If one does a numerical point-by-point subtraction of the curve in Figure 5 from the curve in Figure 1, one obtains the curve in Figure 7. This component is obviously the sinusoidal shockwave, decaying in both amplitude and frequency, generated internally in the small mass by the impact.

Two parts of this curve, at the beginning and end of the half sine pulse, seem to deviate from its otherwise clean appearance. This curve is quite useful in analysis of the material properties of the small mass. The envelope of the curve is a measure of the damping; the frequency decay, used in conjunction with the physical dimensions of the mass, is a measure of the velocity of the shock through the mass, as well as an indication of the compression during impact. The deviation at the beginning of the curve may have been caused by the impacting surfaces not being parallel initially, setting off more than one shock wave, with phase differences. The deviation near the end of the half sine pulse may be due to the rounded corner in Figure 5, but a numerical simulation of this impact by a Duhamel integral produced a curve with an initial sharp corner and a terminal rounded corner. For this reason, it may not be appropriate (or possible) to obtain a sharp terminal corner.

IV. EXAMPLE 2: DAMPED VIBRATION ANALYSIS

The data curve of this example, shown in Figure 8, is from a force gage mounted on the elevation link of a weapon system. The impulse of recoil sets off vibrations in the link which damp out in time. It is of interest to isolate vibration modes and, if possible, the actual impulse. The spectrum of the data, Figure 9, shows peaks of interest at about 9, 24, and 47 Hz. There is also a poorly defined peak at 5 or 6 Hz, which suggests the impulse component. The spectrum near 9 Hz shows two peaks, but these are so close it seems doubtful they can be separated using filters. In this analysis, they will be treated as a single component.

Using a band pass filter* passing frequencies from 3 to 7 Hz, one obtains the curve shown in Figure 10. This is the impulse. It should

---

*Throughout this report, band pass filtering is accomplished in two stages, using a low pass and a high pass filter. The process is described in detail in section VIII.
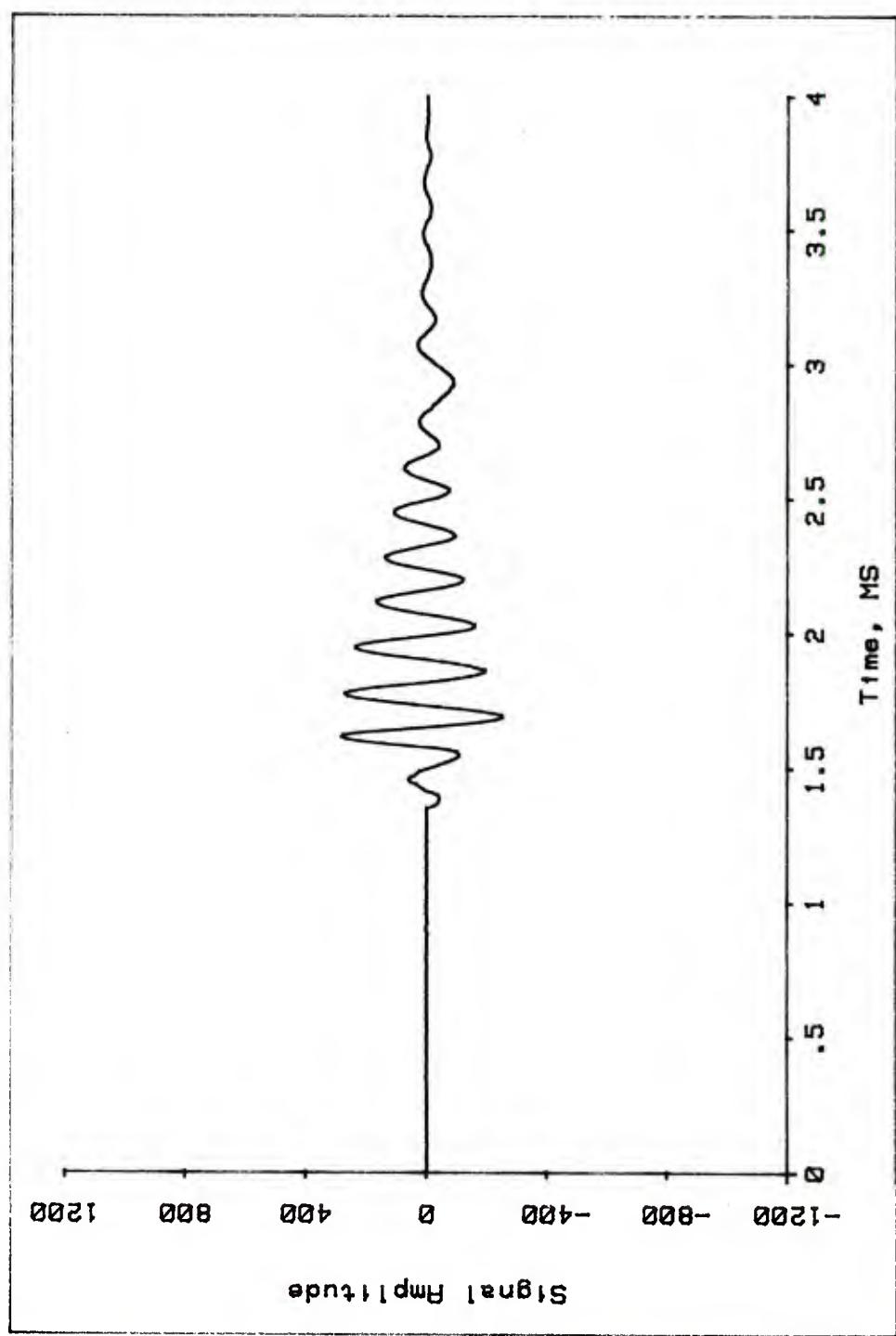
Figure 7. Shock Wave Component Isolated from the Half Sine Pulse

21
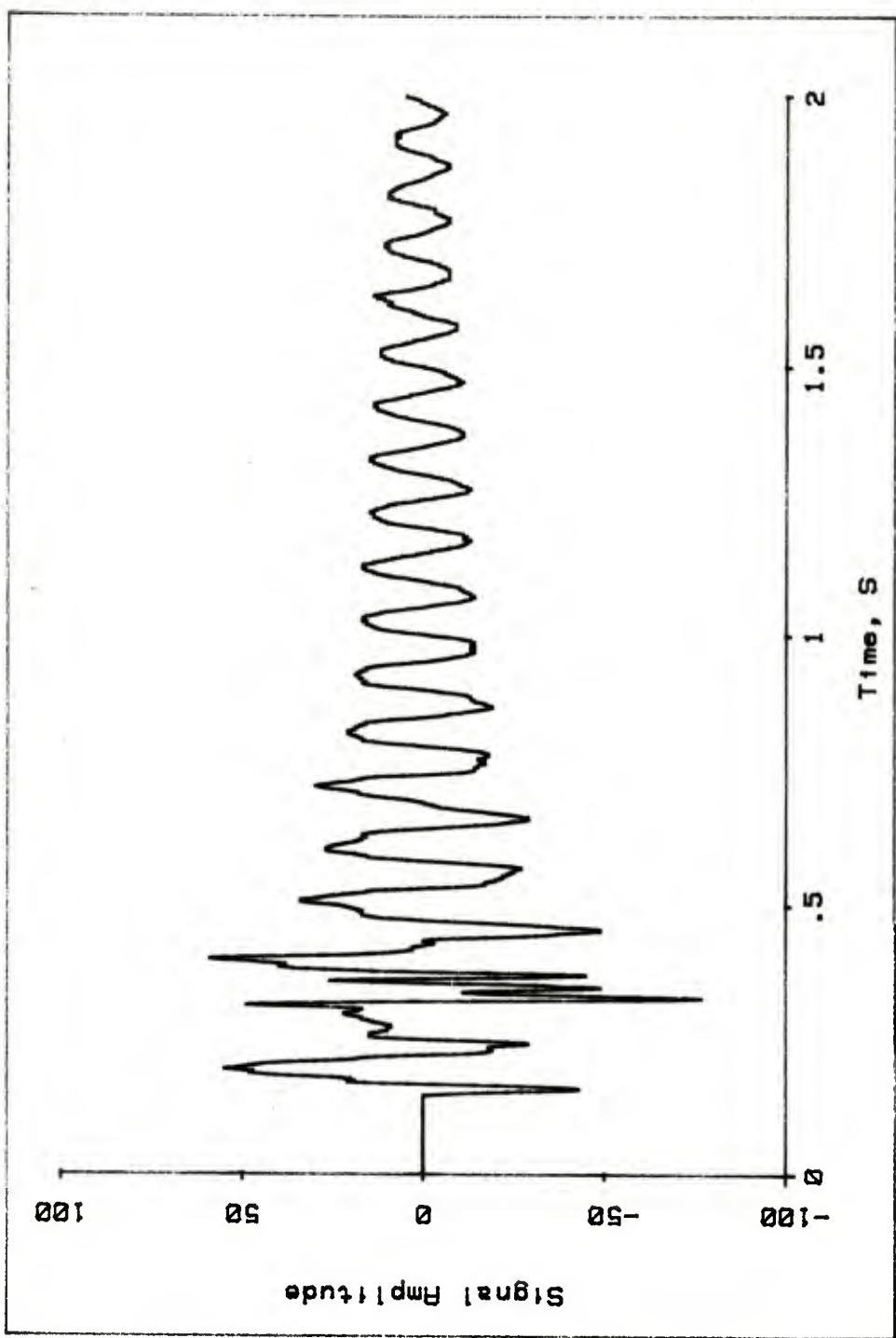
Figure 8. Elevation Link Recoil Force: Raw Data

22
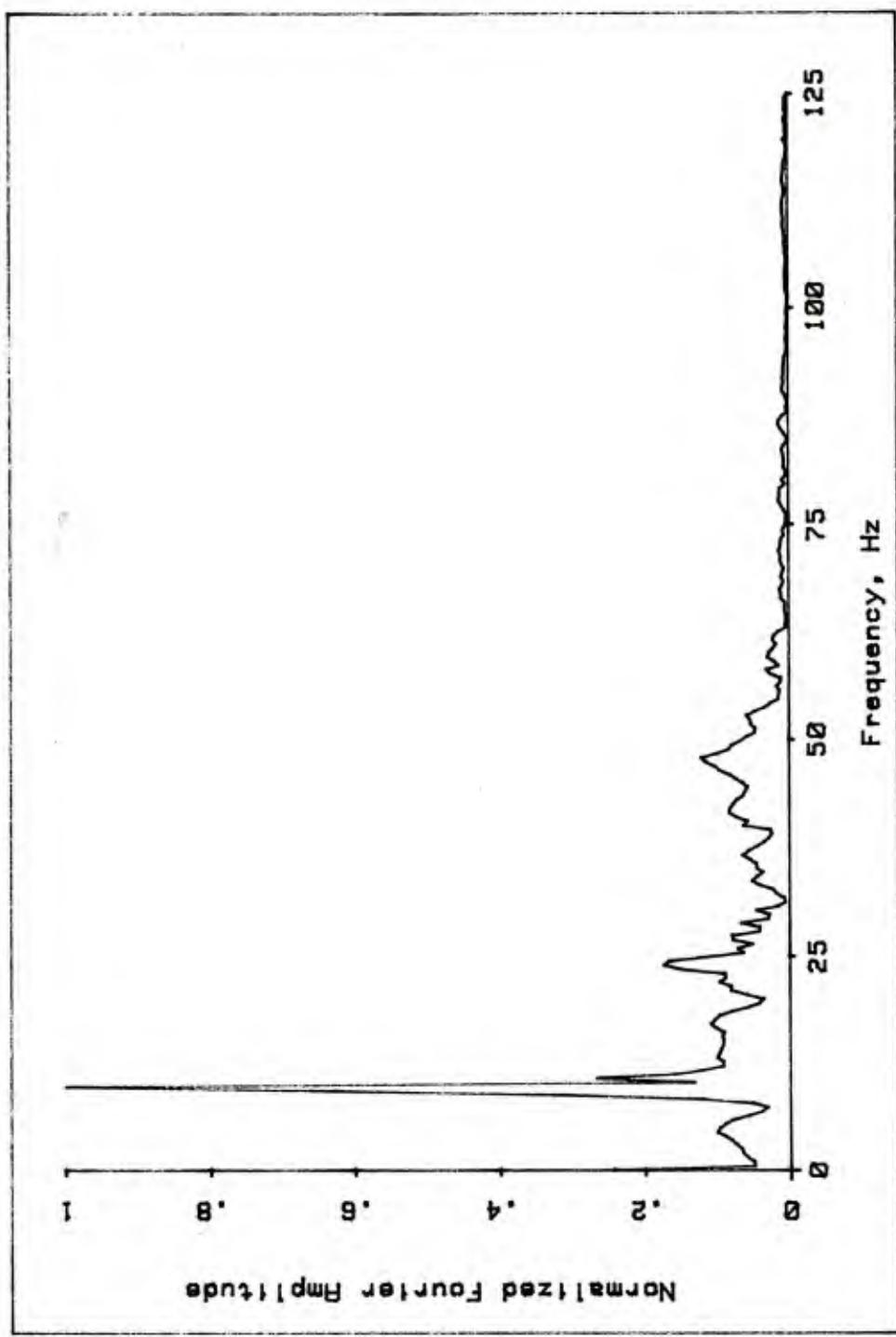
Figure 9. Recoil Force: Normalized Amplitude Spectrum

23
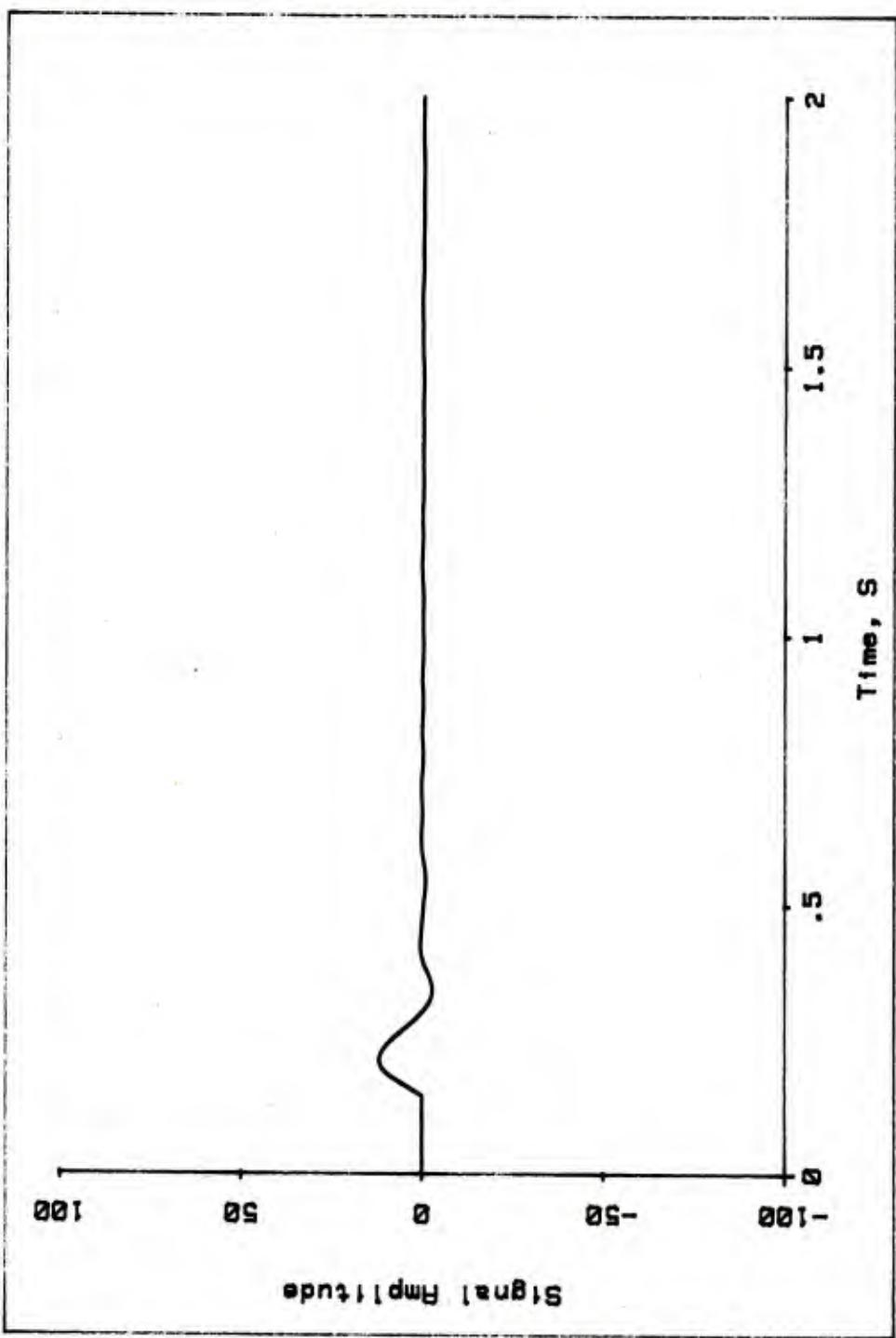
Figure 10. Recoil Force Impulse

24

be noted that in isolating each component in this example, the reflection process demonstrated in example 1 was used. This provides an accurate common reference point on each curve. The accuracy of this particular data curve can be verified by the fact that a numerical simulation of the weapon system recoil predicted an impulse on the elevation link which agrees with the curve to within 1%. Applying a band pass filter passing frequencies from 8 to 12 Hz produces the output shown in Figure 11. This represents the first mode of vibration and shows clearly the mode shape and the damping.

The output of a band pass filter passing frequencies from 22 to 25 Hz is shown in Figure 12. This curve represents a higher vibration mode, with at least one phase change early in the record. The particular item instrumented in this case has numerous mechanical stops to prevent free vibrations; these stops produce the phase shifts in the higher modes. A band pass filter passing frequencies from 44 to 50 Hz has the output shown in Figure 13. This mode shows at least two phase changes. One feature of the modes shown in Figures 11-13 is the symmetry about the zero amplitude level. This symmetry is one indication that these modes have been isolated correctly by the filtering process.

There is another method by which one can determine whether all significant portions of the data have been identified, and to what extent the amplitudes of the vibration modes are correct. This method is simply to form a point-by-point sum of all the components. Adding the curves in Figures 10-13 produces the curve of Figure 14. It will be noted that this curve bears a reasonable resemblance to the raw data curve of Figure 8, particularly from 0.5 seconds on. It is clear, however, that some significant amplitudes are absent prior to that point. A re-examination of the spectrum in Figure 9 reveals the presence of other peaks which are evidently of sufficient significance to merit further study. In particular, the peak at 18 Hz has somewhat higher amplitude than the peak due to the impulse.

A band pass filter passing frequencies from 15 to 20 Hz produces the output of Figure 15. This plot shows a rapidly decaying signal, with amplitude concentrated in precisely the area in which the reconstructed curve of Figure 14 was deficient. Adding this curve point-by-point to that of Figure 14 produces the curve of Figure 16. With the exception of some higher frequency content, this reconstructed data agrees quite well with the raw data in Figure 8, providing good confidence in the results. One might continue the analysis by isolating the spectral peaks at 35, 40, and 53 Hz, and so on. It is clear at this point, however, that the major components have been identified.

V.   CLOSED COMPARTMENT BLAST PRESSURE ANALYSIS

As was indicated earlier in this report, the techniques of Fourier analysis and digital filtering are not always completely successful. This next example illustrates the point. Figure 17 is a plot of pressure vs.

25
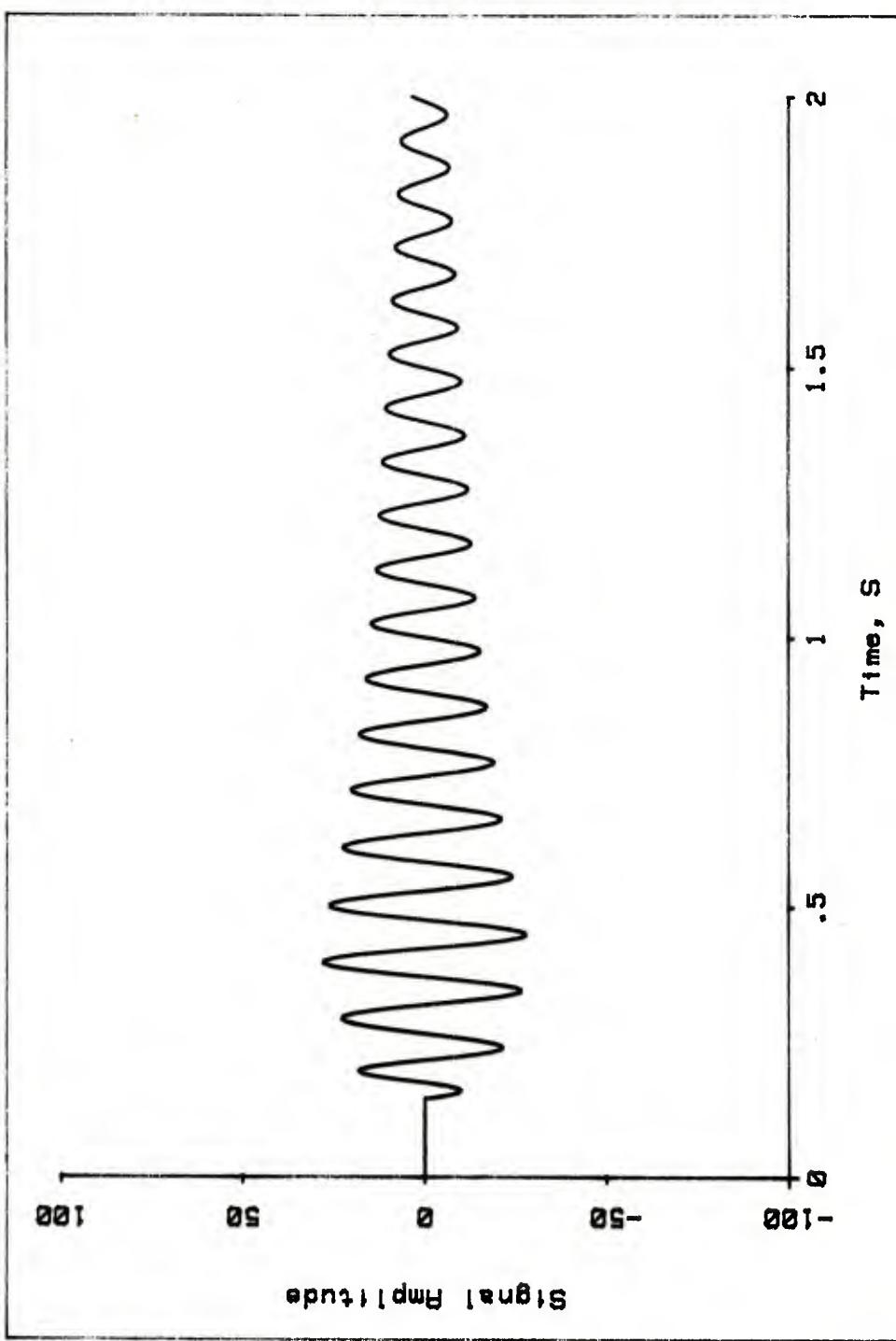
Figure 11. Elevation Link: 10 Hz Vibration Mode

26
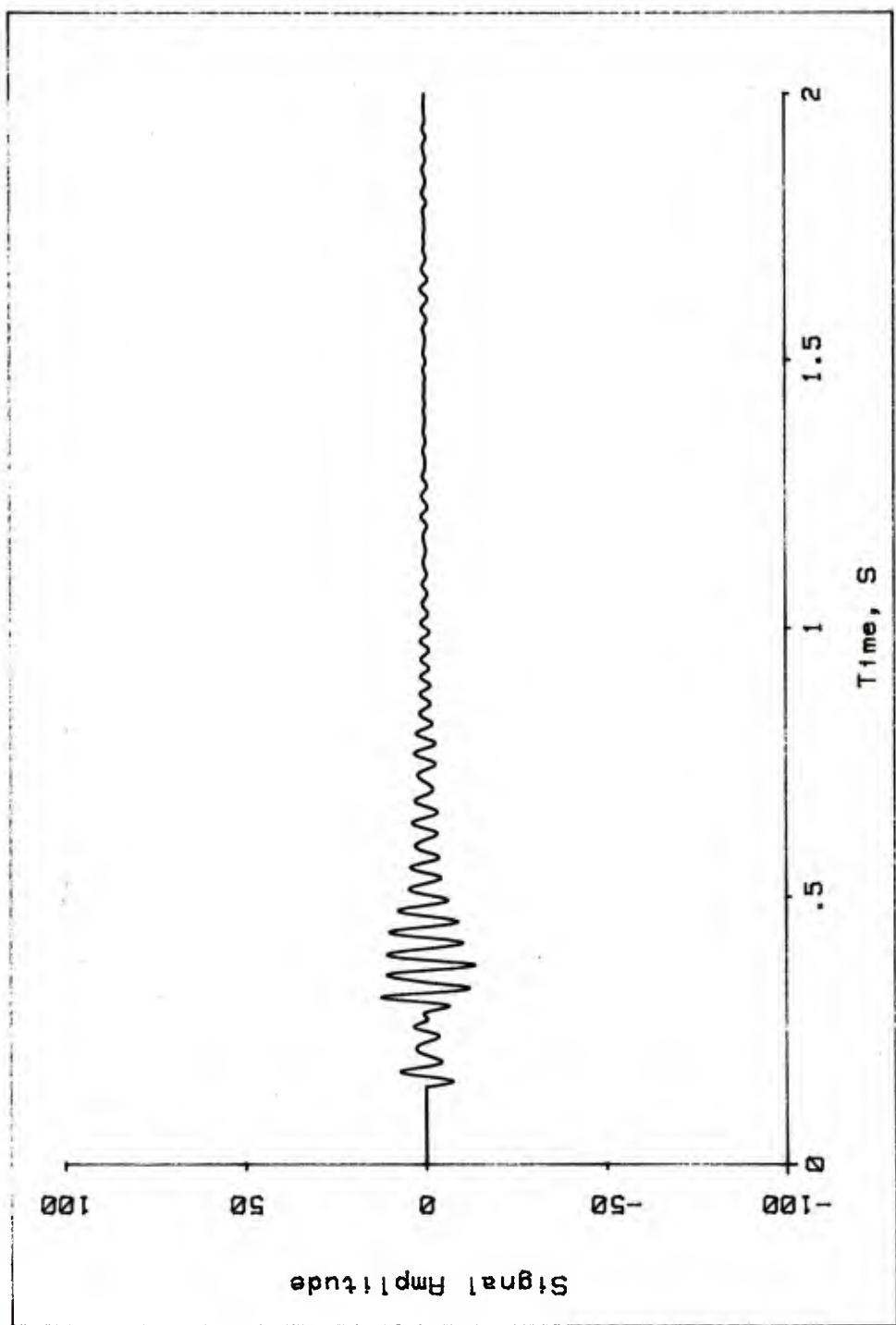
Figure 12. Elevation Link: 24 Hz Vibration Mode

27
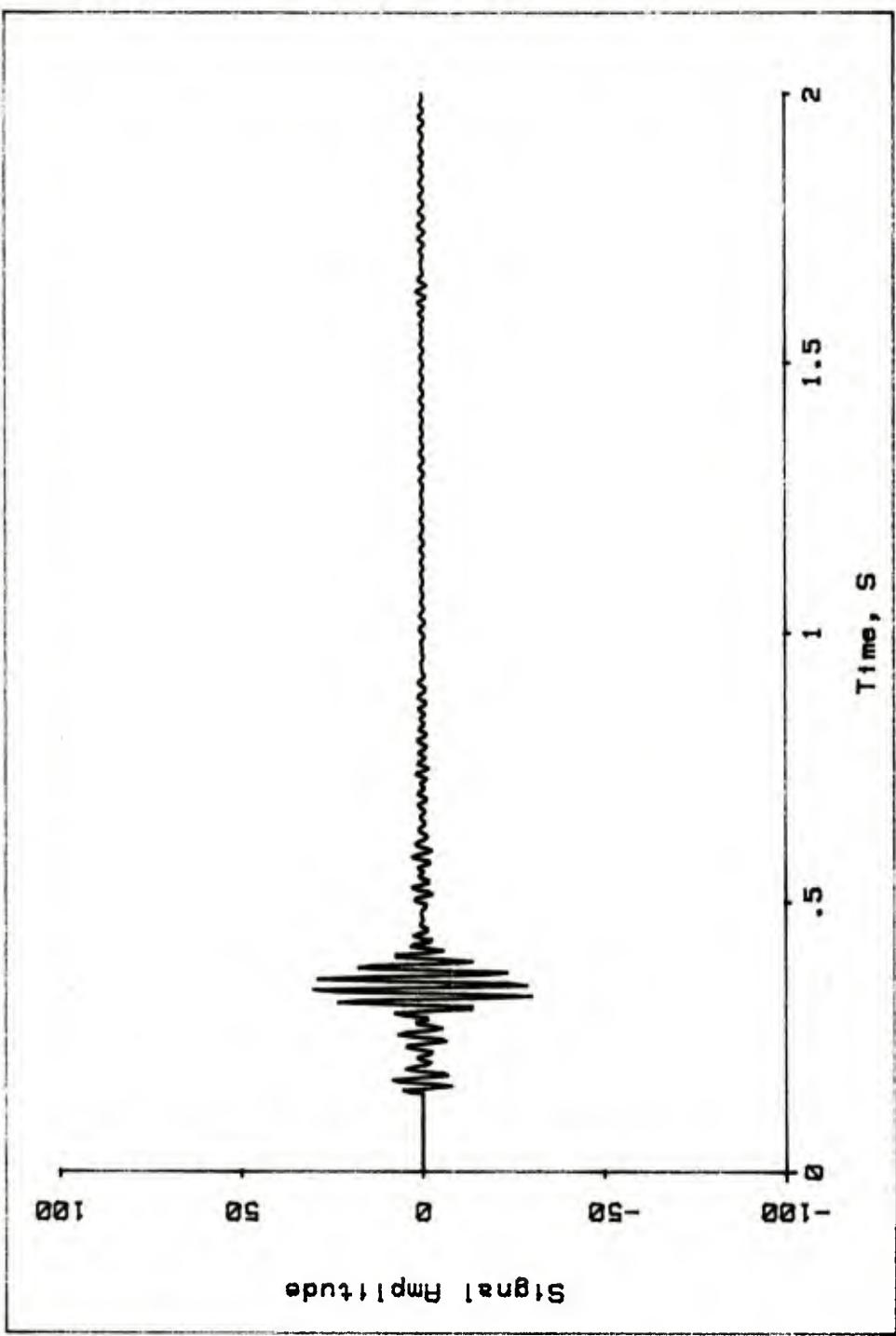
Figure 13. Elevation Link: 47 Hz Vibration Mode

28
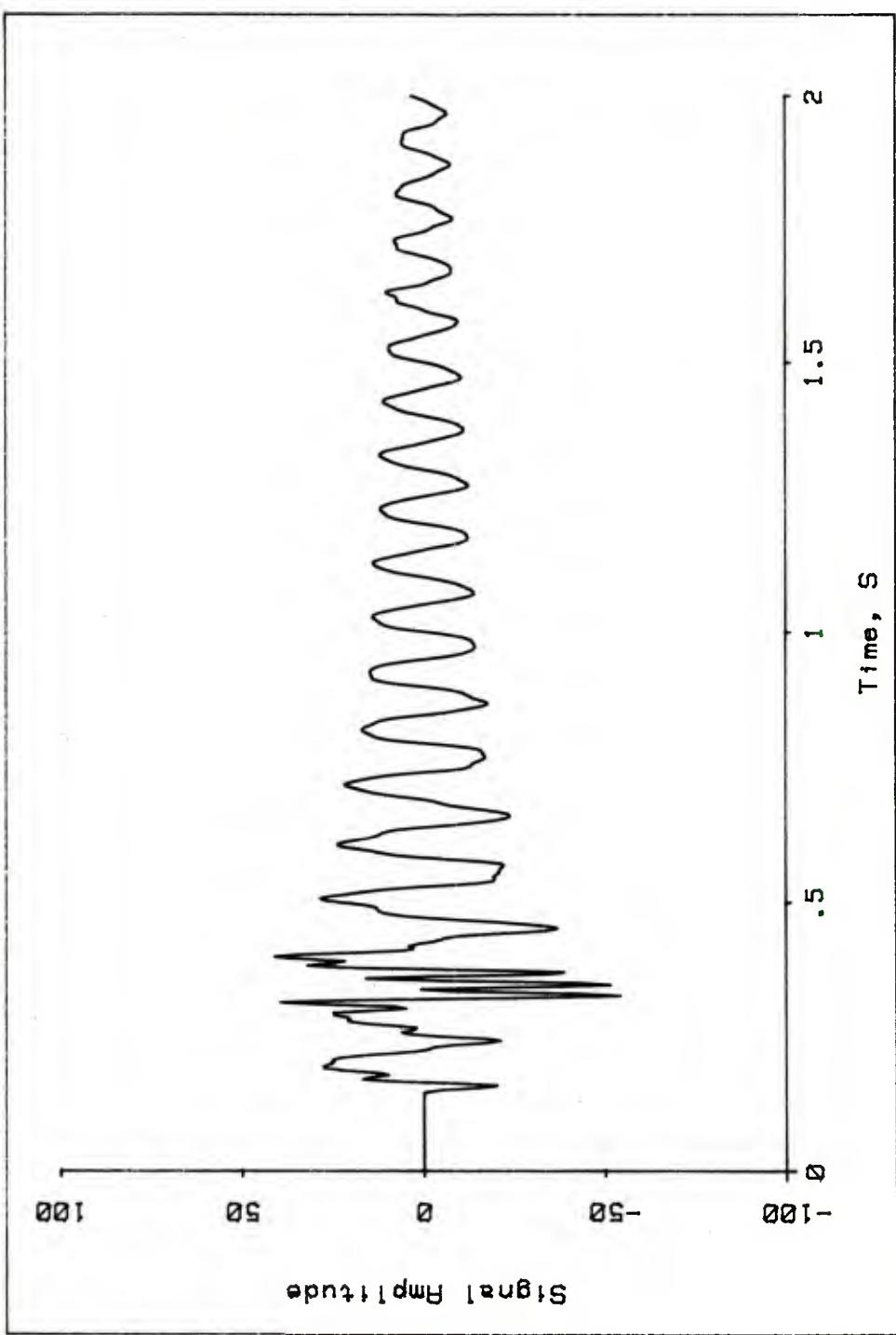
Figure 14. Sum of Impulse and 10, 24, and 47 Hz Vibration Modes

29
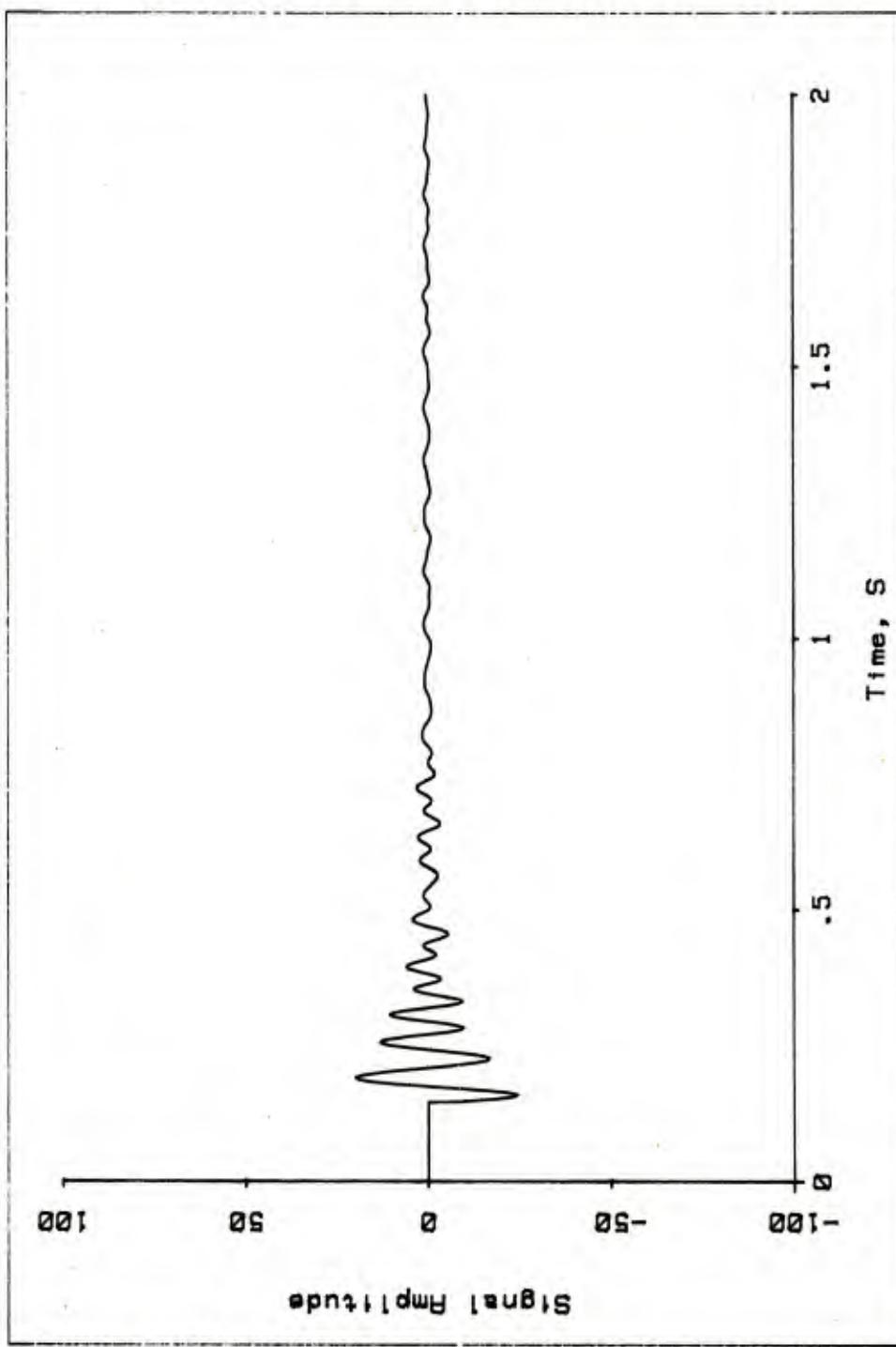
Figure 15. Elevation Link Recoil Force 18 Hz Component
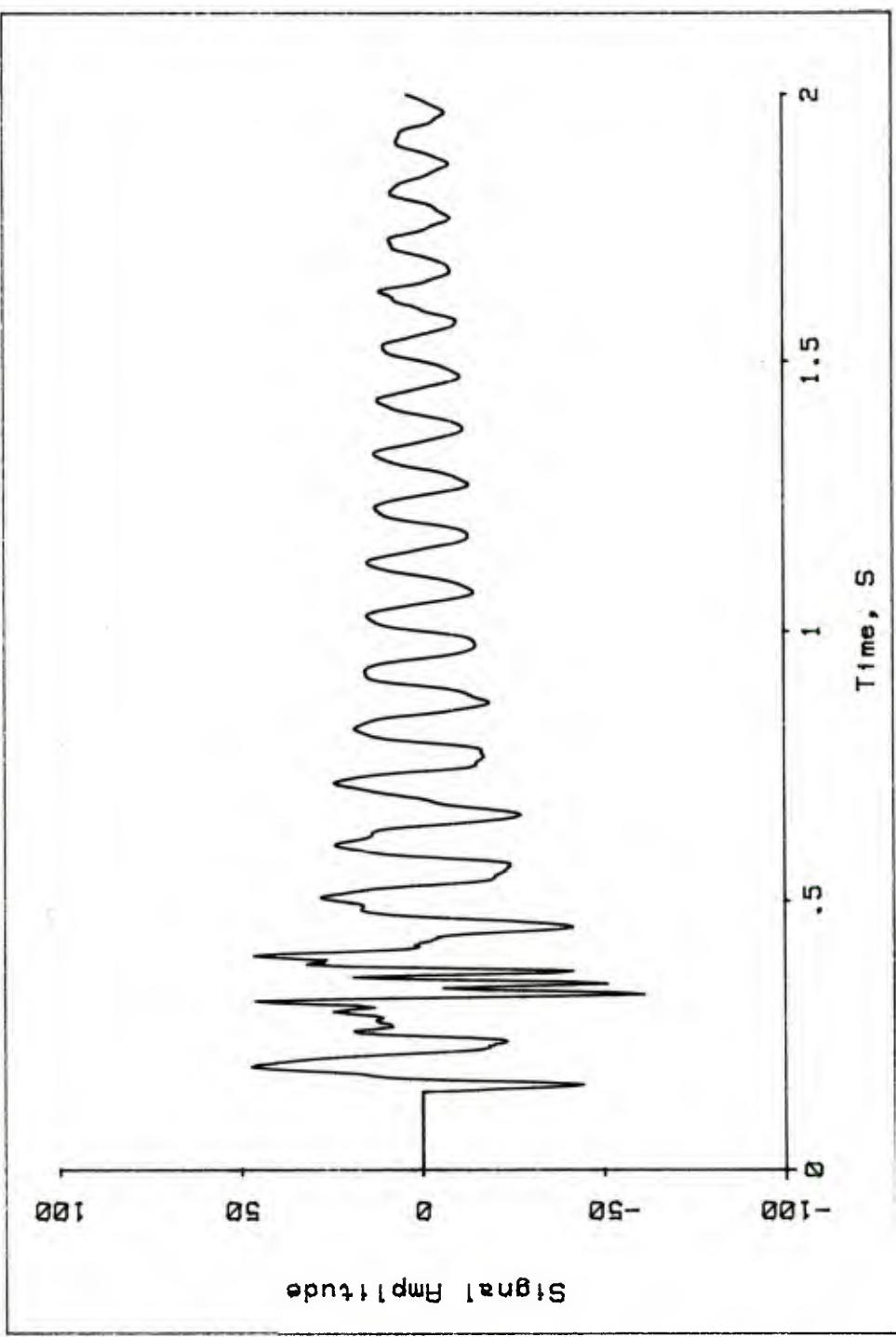
Figure 16. Data Curve Reconstructed from Impulse and 10, 18, 24, and 47 Hz Components

31
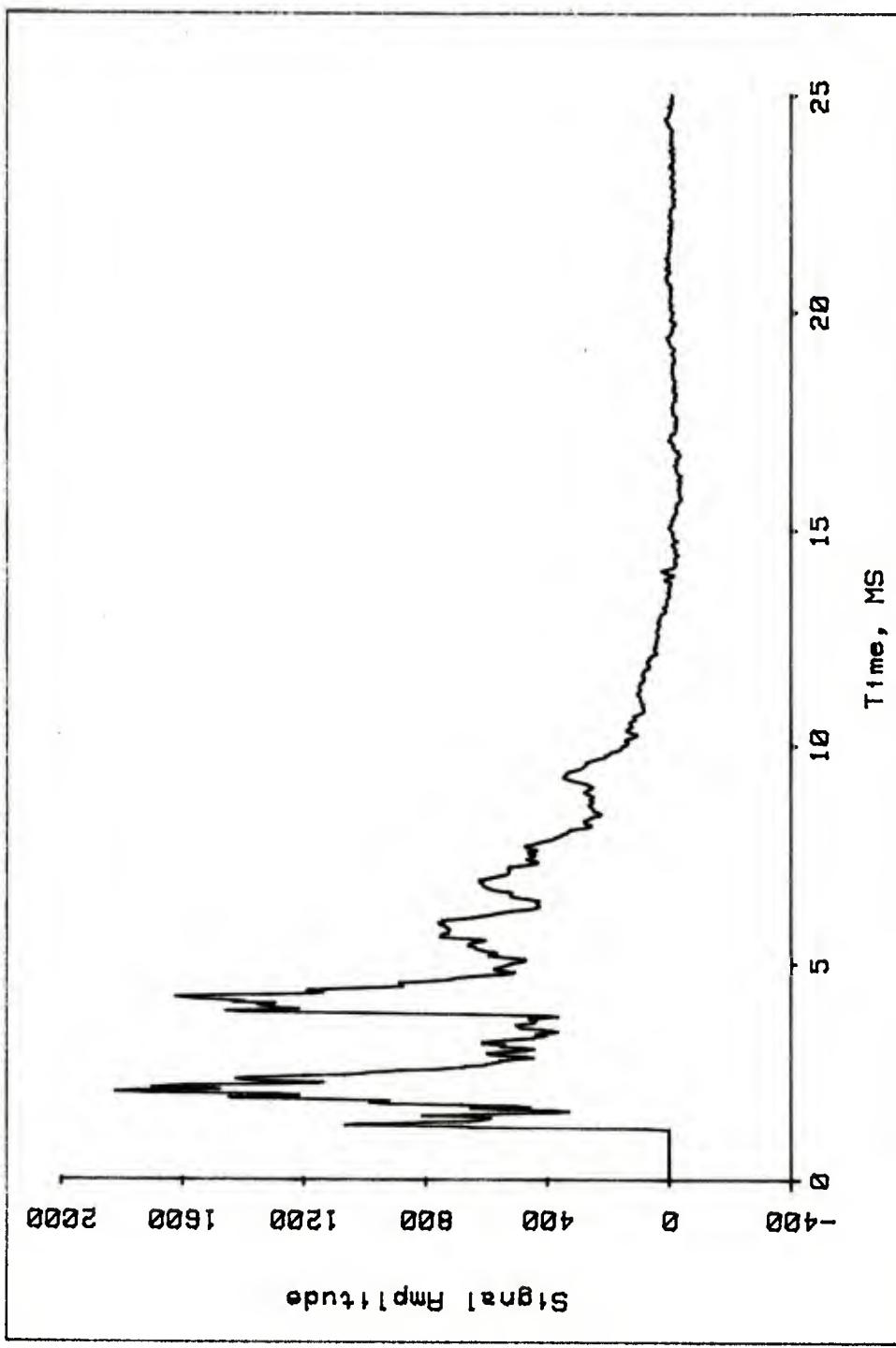
Figure 17. Closed Compartment Blast Pressure: Raw Data

32

time recorded interior to a closed chamber. The chamber, which held several containers of propellant of the type used for the ballistic launch of projectiles, was subjected to penetration by a shaped charge jet; this in turn ignited the propellant. The data therefore contains a pressure component due to the burning of the propellant, a blast component with probably several reflections from the chamber walls, and quite possibly some pressure waves.

Figure 18 is the spectrum of the raw data, showing the main non-periodic contribution at zero Hz and two secondary components at about 450 Hz and 1 kHz. In an attempt to isolate the nonperiodic zero Hz component, a low pass filter with cutoff frequency of 200 Hz is applied to the data. The problem which arises is that the transition band of the filter is not sufficiently narrow to eliminate all of the higher frequency components. As a result, the filtered curve appears as in Figure 19, which shows the pressure component from the burning propellant with some additional residual higher frequency components.

There are several options available. First, one could design a filter with a more narrow transition band. One possible consequence is greater deviation from the design specification in the filter pass band, as described in reference 1; this could result in undesirable amplitude distortion. A second option is presented by the fact that, having low pass filtered the data, the data can be processed at an increment. For example, the bandwidth in the spectrum of Figure 18 is 10 kHz. If one uses every other point (increment by 2) in the data of Figure 19, then the bandwidth of the incremented data is 5 kHz. The significance of this fact is that, since the filters are designed based on fractions of band-width rather than on actual frequencies, the range between the 200 Hz cutoff point and the 450 Hz spectral component is now twice as great. At increment 4, the range is 4 times larger, and so on. Thus, using the same filter, the transition band is effectively narrowed by incrementing the data.

While this second option works in this example, there is one drawback: incrementing the data means a loss of data points. While there is no information lost when incrementing is done in conjunction with low pass filtering, one can no longer perform point-by-point operations on the incremented data with some other component at a different increment, without resorting to interpolation. Depending on the goal of the analysis, this option may be perfectly acceptable.

A third option will be pursued here, to demonstrate another useful technique in digital data analysis. The previous example demonstrated that components A, B, C, and D of a raw data curve R could be summed point-by-point, with the sum being nearly equal to the curve R. That is,

$$A+B+C+D \simeq R$$

33
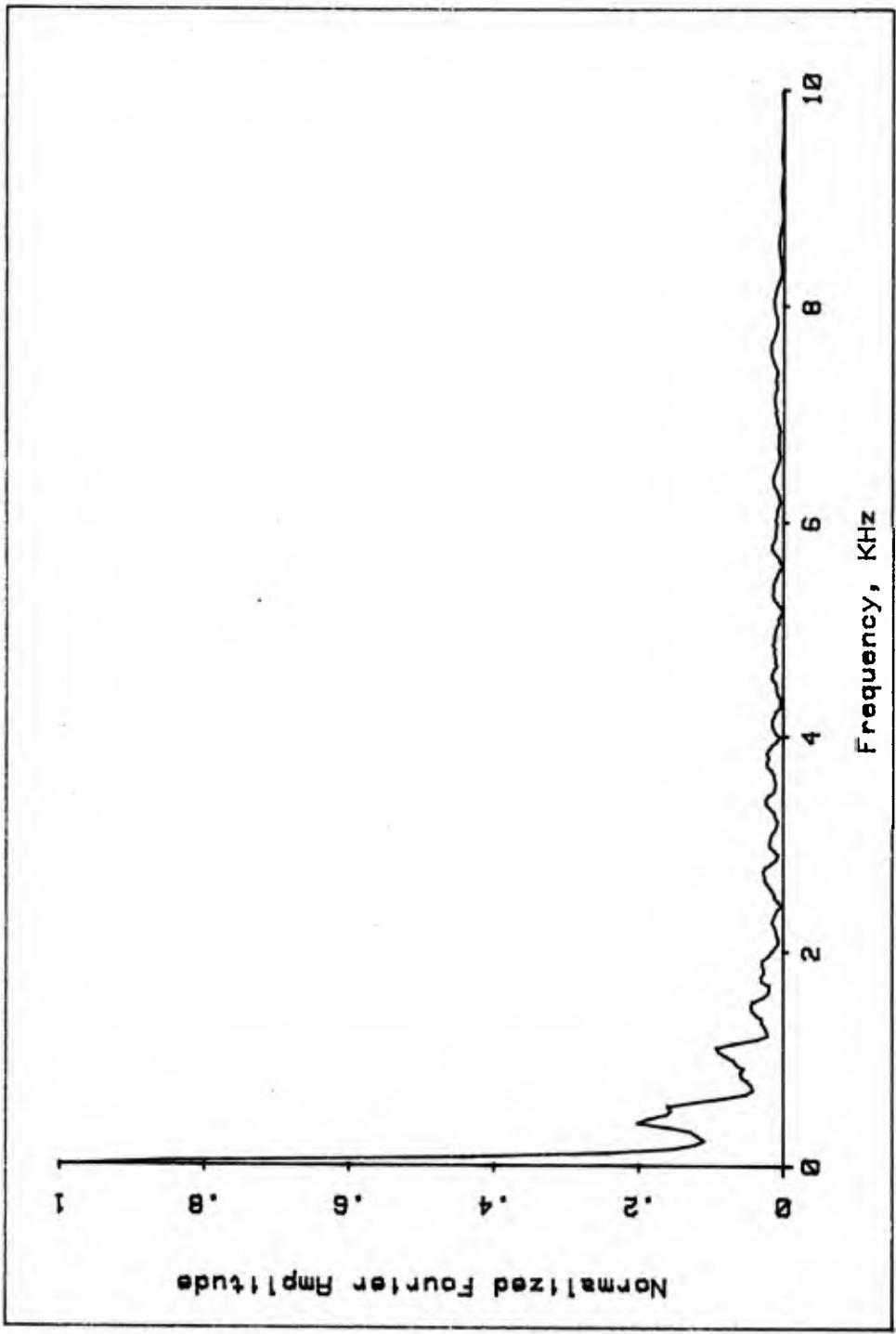
Figure 18. Spectrum of Blast Pressure Data
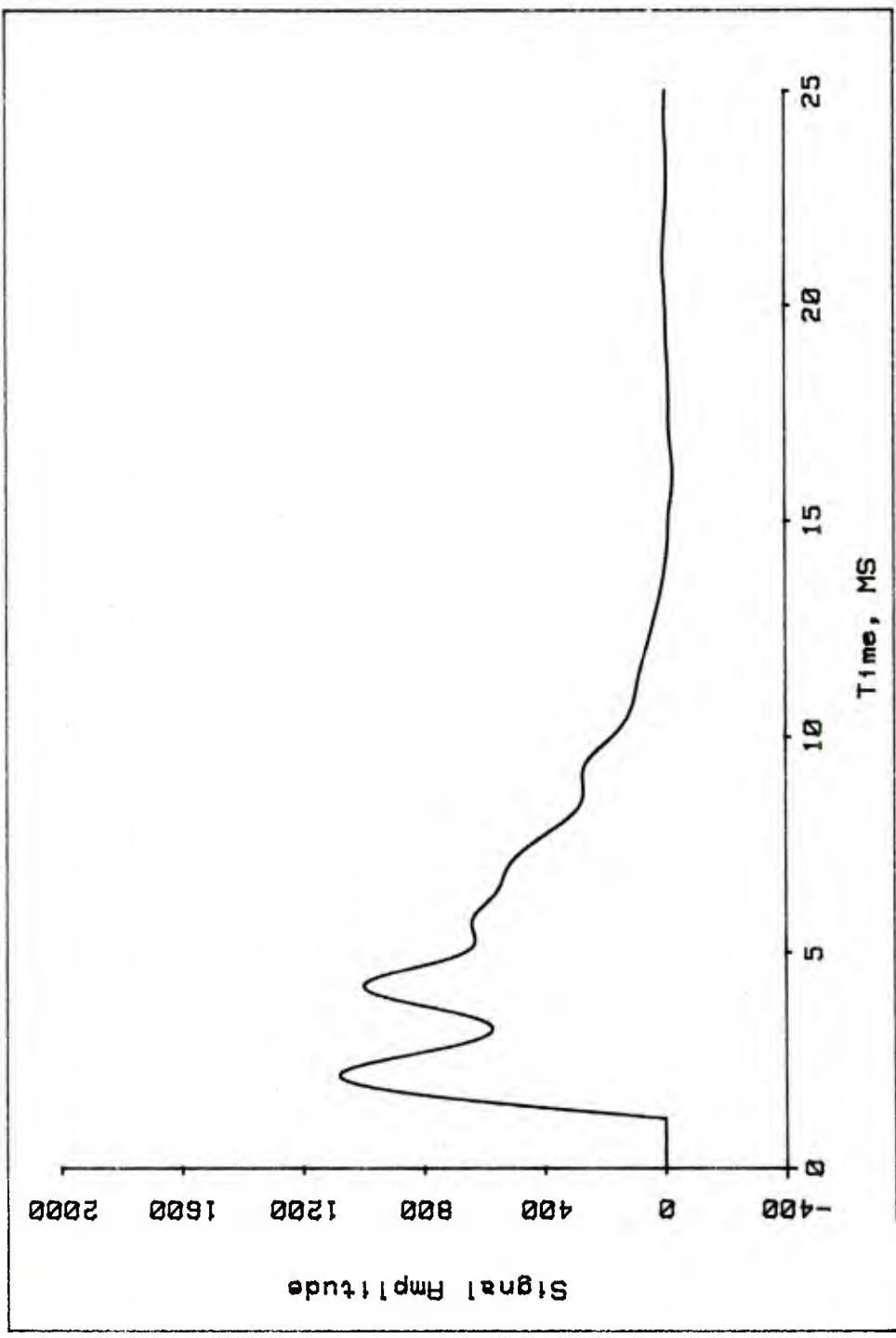
Figure 19. Output of a 200 Hz Low Pass Filter on the Blast Pressure Data

35

It would seem reasonable to expect that this expression can be manipulated so that, for example,

$$A \simeq R-B-C-D$$

That is, to isolate component A, one could just as well isolate components B, C, and D, and subtract them point-by-point from the original data R, leaving an approximation to A.

This method works especially well in cases like the present one, where there is a large amplitude component near zero Hz with numerous low amplitude components close by. In particular, the low amplitude peaks can be separated out one at a time by high pass filtering, beginning with the highest frequency. Using this method, one applies a high pass filter with cutoff frequency of 950 Hz to the raw data. A copy of the output at this stage is stored for future use, and then, the output is low pass filtered at a cutoff frequency of 1.2 kHz. The output of this 2-stage band pass filtering process is shown in Figure 20.

This curve contains several features of interest. The initial part of the curve, the first three positive and two negative peaks, show a nicely decaying wave. Just beyond the third positive peak, this pattern is disturbed in both phase and amplitude by the second of the two main peaks seen in the raw data in Figure 17. Beyond this point, the curve has little recognizable regularity. The important fact to note is that the clean symmetry of some of the components in the previous example is absent here.

Continuing the analysis, by subtracting the output of the highpass filter with cutoff frequency of 950 Hz from the raw data, the output of Figure 21 is obtained. Comparing Figure 21 with Figure 19, one sees that the data in Figure 19 does not contain the full 450 Hz component. In order to separate the two remaining parts of the data, use is made of the incrementing technique described earlier. It turns out that by incrementing the data in Figure 21 by two (i.e., using every other point) the two components can be separated using a high pass filter with a cutoff frequency of 200 Hz. Since the original data, with bandwidth 10 kHz, has had all content above 950 Hz removed, one could take increments as high as 10 (a bandwidth of 1 kHz) without aliasing the data. Using increment 2 simply means that for a frequency of say 500 Hz, one has 20 points per cycle instead of the original 40. The implication is that linear interpolation after filtering should be entirely adequate.

Incrementing the data in Figure 21 by two, applying a high pass filter with cutoff frequency 200 Hz, and using linear interpolation on the output to obtain the same number of points as the original data set, results in the curve in Figure 22. This curve also shows a well defined envelope of waves up to the end of the third negative peak, at which
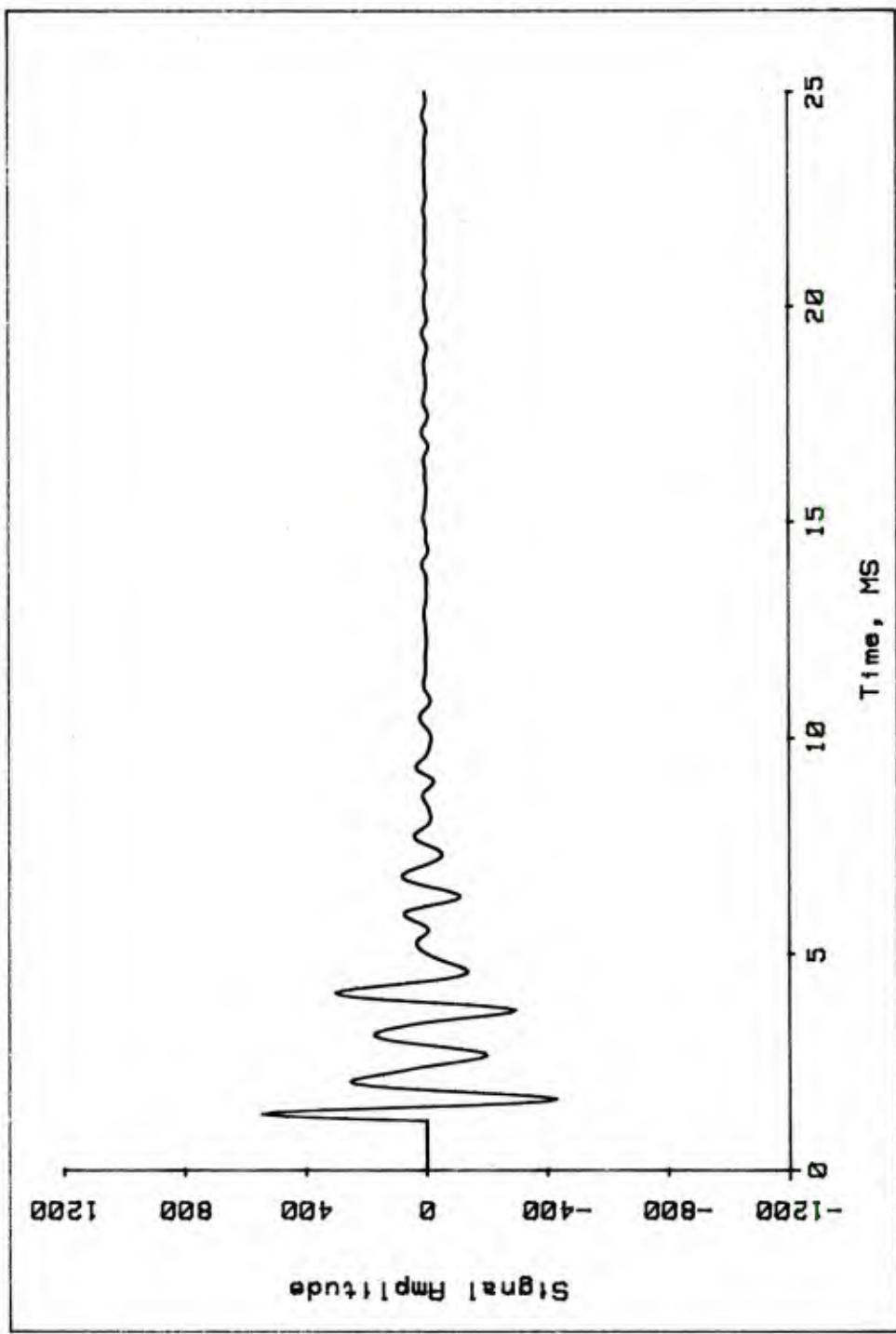
Figure 20. Blast Pressure Data: 1 KHz Component
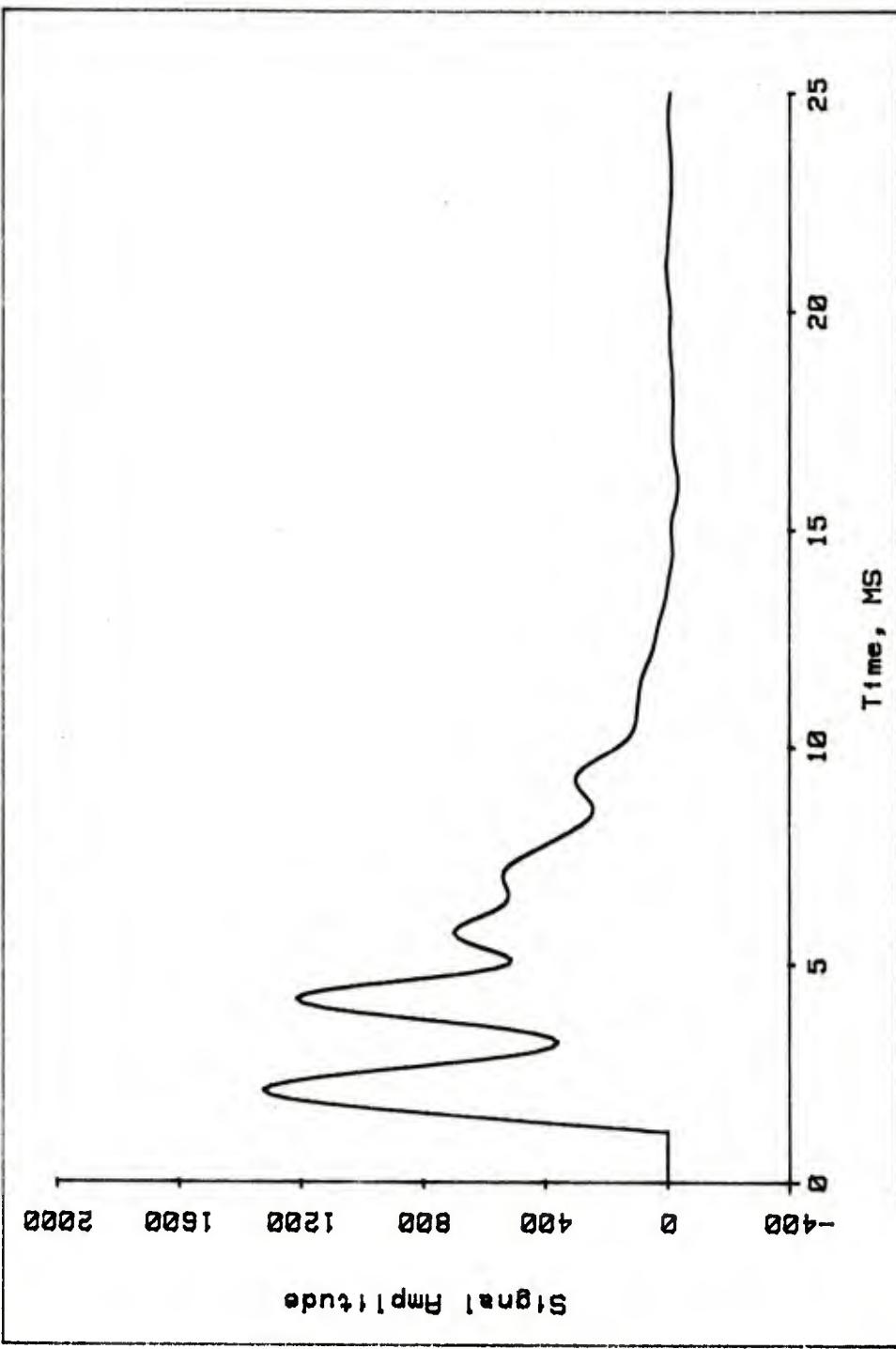
Figure 21. Blast Pressure Data With All Components Above 950 Hz Removed

38
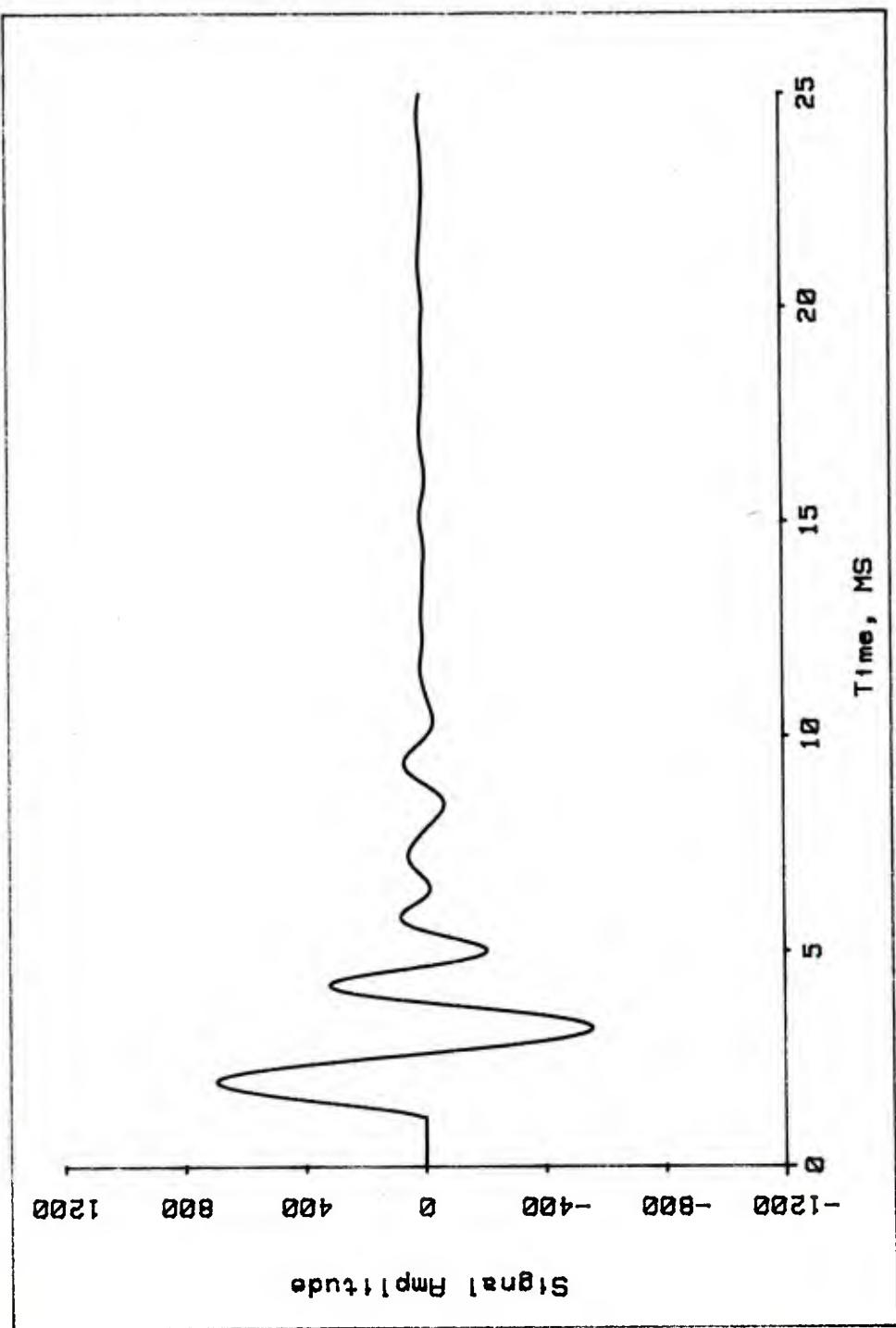
Figure 22. Blast Pressure Data: 450 Hz Component
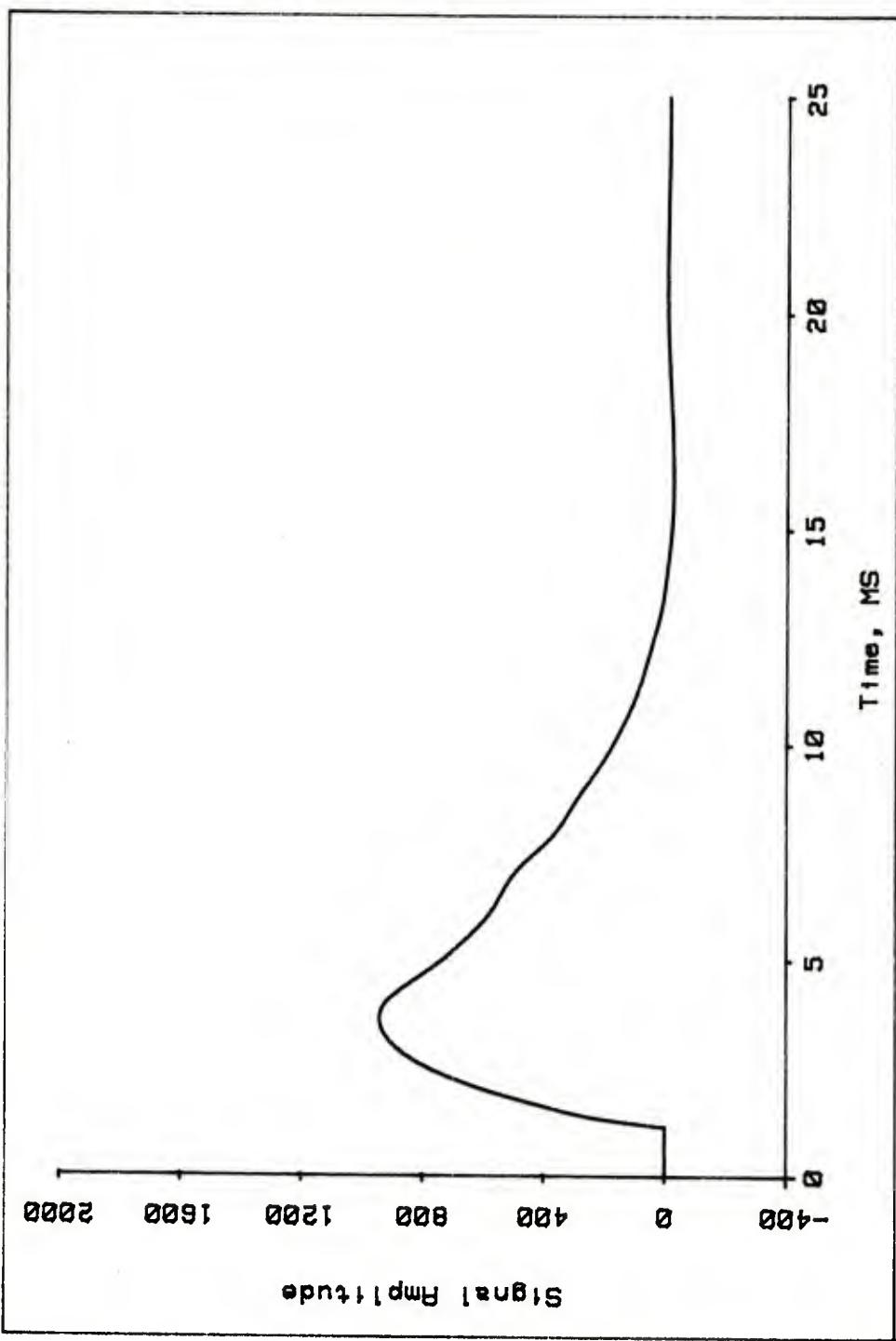
Figure 23. Blast Pressure Data: Pressure due to Propellant Burning

40

point there is a phase change and a loss of symmetry. This curve bears some resemblance to the first part of the curve in Figure 20, with one major difference; in Figure 22, the waves seem to increase in frequency, rather than decrease as one might expect. As the temperature increases inside the chamber, the wave velocity (and hence frequency) will also increase; this may in fact explain the increase seen here.

At any rate, subtracting the data in Figure 22 from that in Figure 21 results in the curve shown in Figure 23. There are two features of this curve which lead one to question its accuracy. First, on the downward slope there appears to be some residual variation from the 450 Hz component. More importantly, the pressure decreases to a level below zero amplitude for a short time, and then returns to zero. This negative pressure level is really a part of the blast wave, an idealization of which is shown in Figure 24. The data of this example contain parts of two such curves, one at each of the main peaks in Figure 17. Thus, the analysis here has failed to isolate the data in Figure 23 properly, and the actual blast curve shape is partially in the data of Figures 20, 22, and 23.

The curve in Figure 25 is the sum of the curves in Figure 20, 22, and 23, and shows that the mathematical, if not physical, components have been isolated properly. Thus, this particular example demonstrates that not all physical phenomena are amenable to Fourier analysis. The above analysis was not totally in vain, however. First, the data in Figure 23 is a reasonable representation of the desired curve. Conceivably, one could use a filter with a slightly lower cutoff frequency to remove the residual higher frequency content on the down slope of this data curve. The peak value would seem to be reliable, as well as the maximum value of the integral of this pressure curve. Finally, were it possible to isolate the blast pressure curve similar to that of Figure 24, the integral of this curve should approach a constant value which is a measure of the force applied to the chamber by the blast. If one integrates the 450 Hz component, the result is the curve shown in Figure 26. Although there are some early cyclic variations, the integral does finally attain a fairly constant value. This value may in fact be a measure of the blast impulse. It should also be noted that the fact that the final constant value of this integral is nonzero is proof that the 450 Hz component does not consist solely of pressure waves.

VI. EXAMPLE 4: ACCELEROMETER BASELINE CORRECTION

A frequent problem occurring in acceleration data is an apparent change in baseline (zero level) during the event. A typical example is shown in Figure 27. In this case, the level change is obvious; in some cases it may not be so apparent. There is a way of checking for baseline variations which is simple yet effective: the physical component being studied has a velocity which returns to zero after the data event. That is, the integral of the acceleration must return to zero. In Figure 28, which is the integral of the data in Figure 27, one sees that there is

41
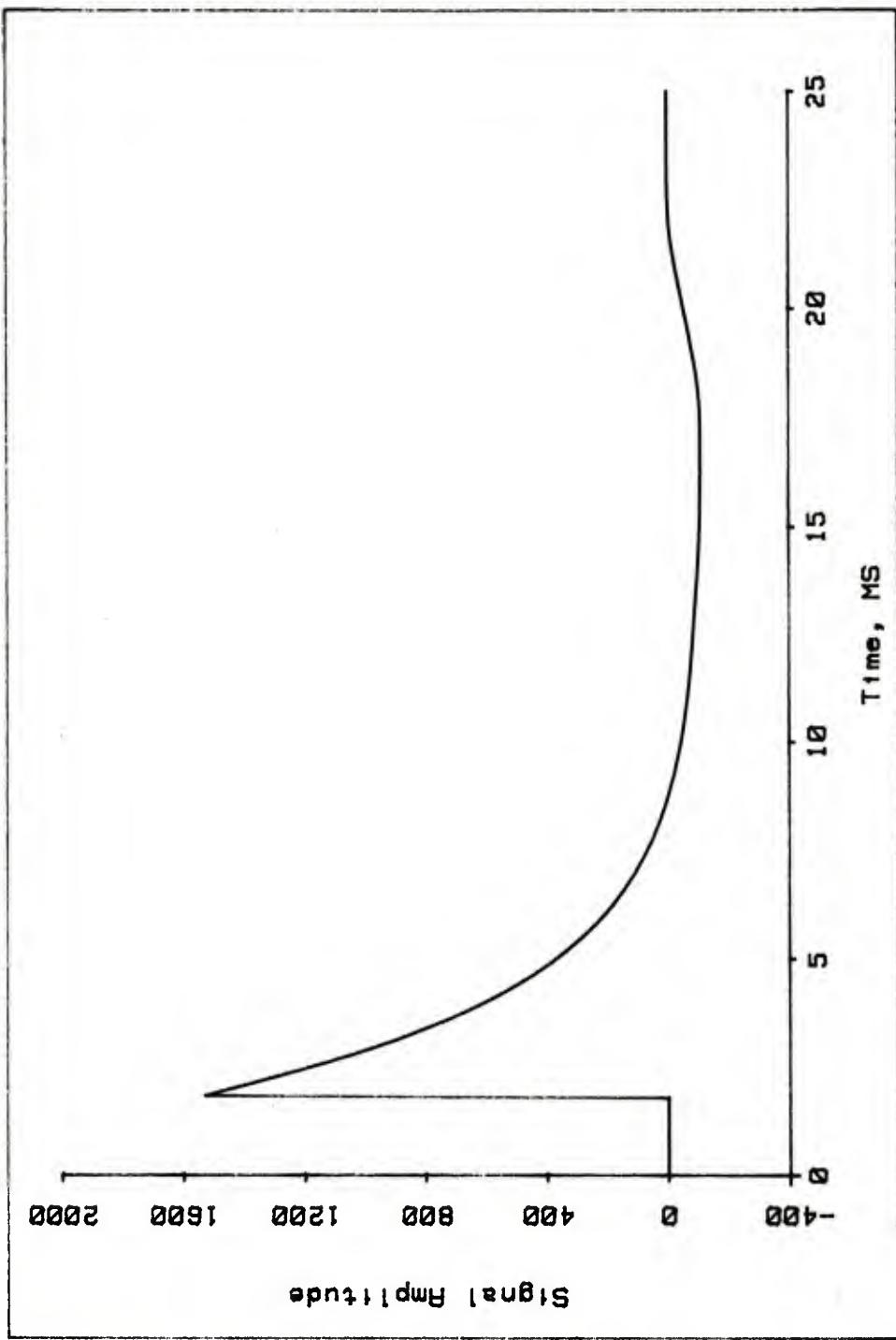
Figure 24. An Idealized Blast Pressure Curve

42
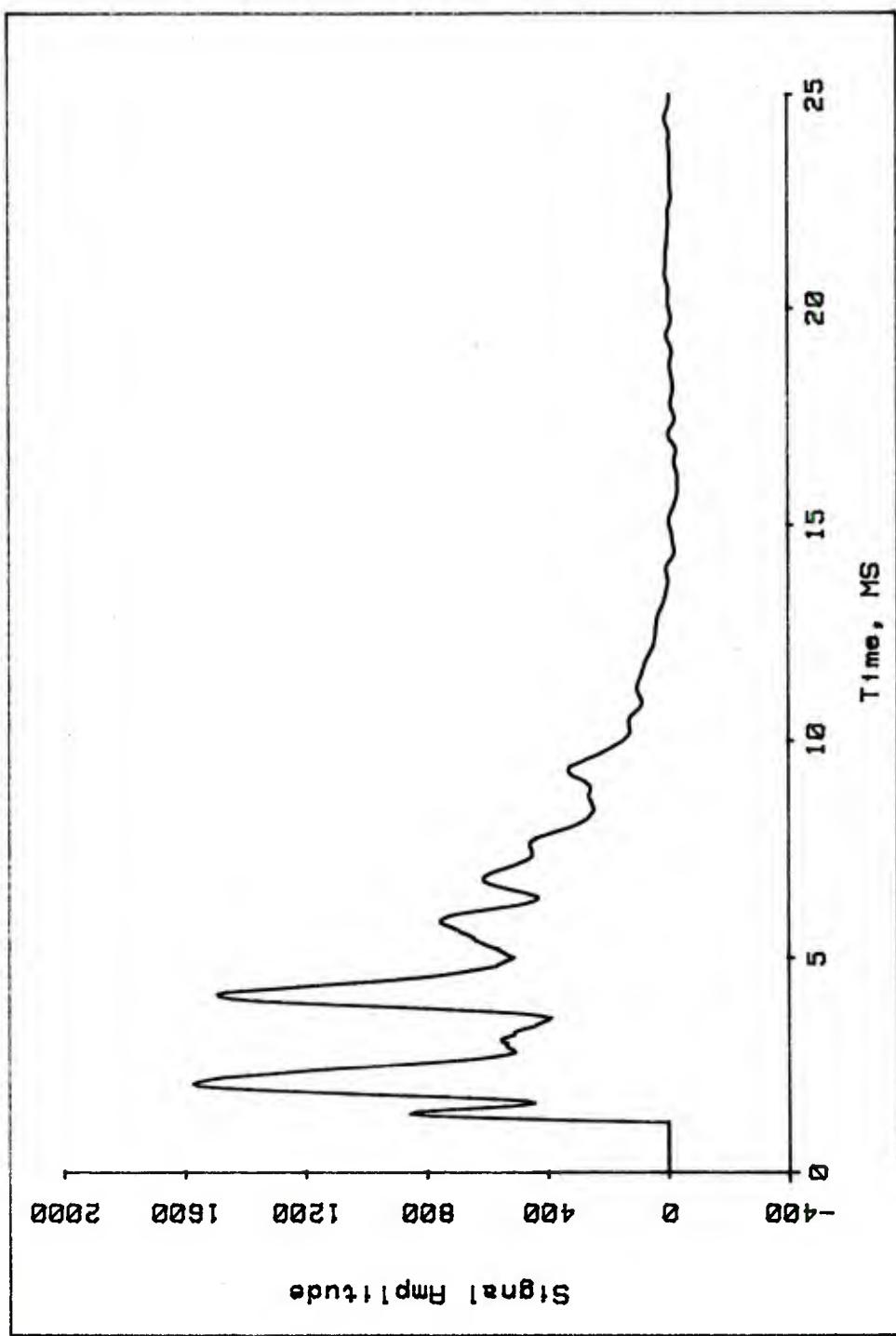
Figure 25. Blast Pressure Data: Sum of the 1 KHz, 450 Hz, and Non-periodic Components

43
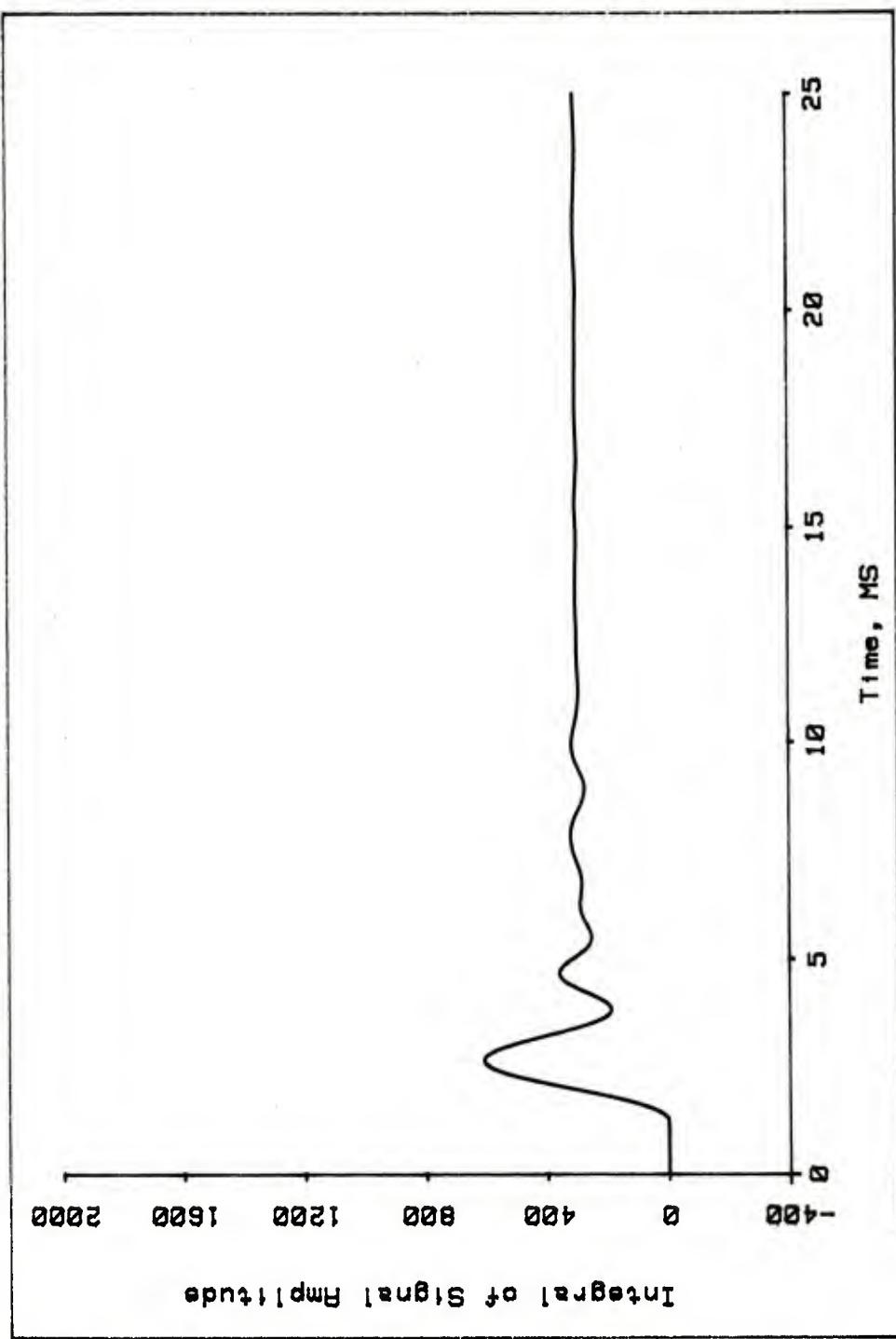
Figure 26. Integral of 450 Hz Component

44
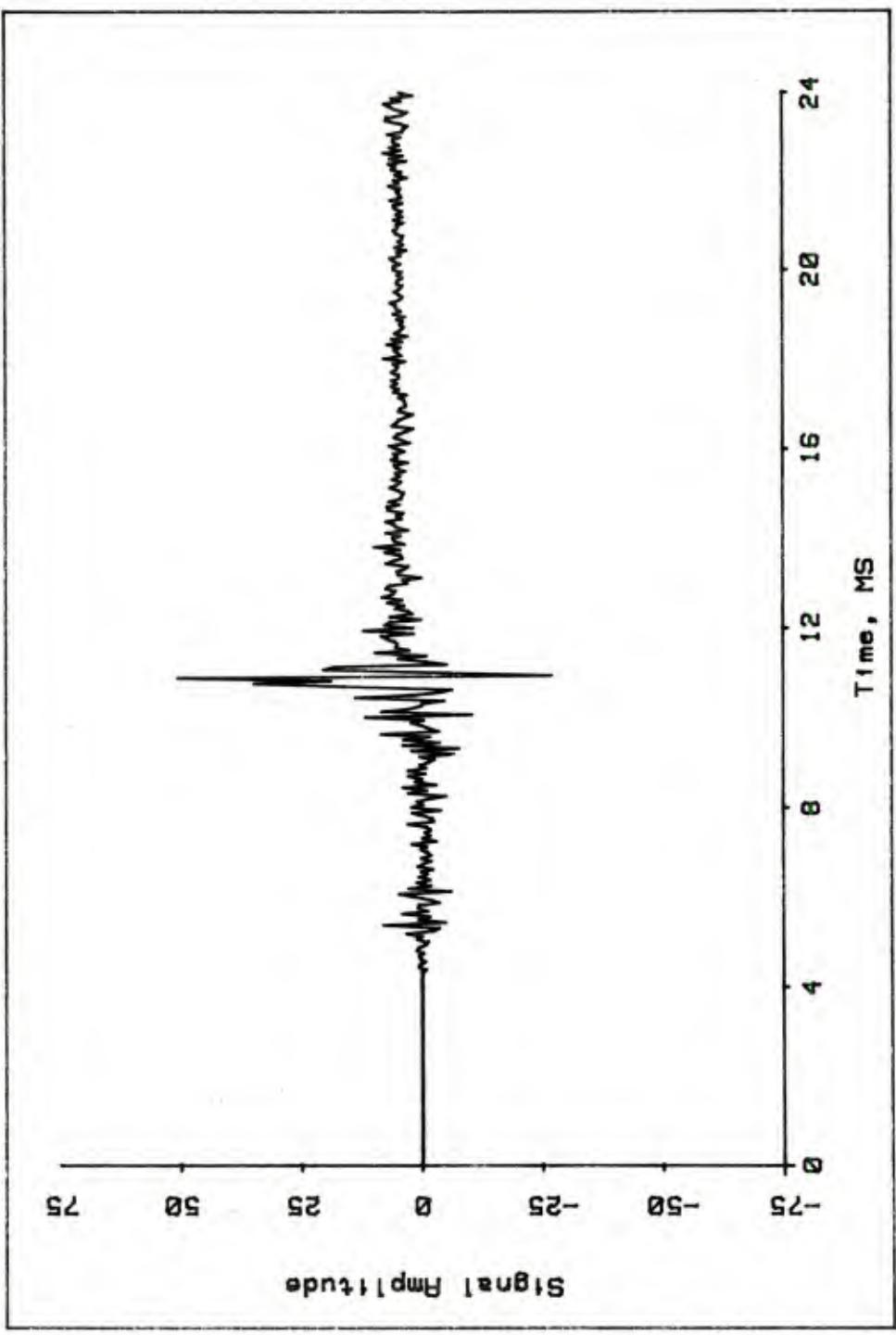
Figure 27. Acceleration Data with Baseline Shift
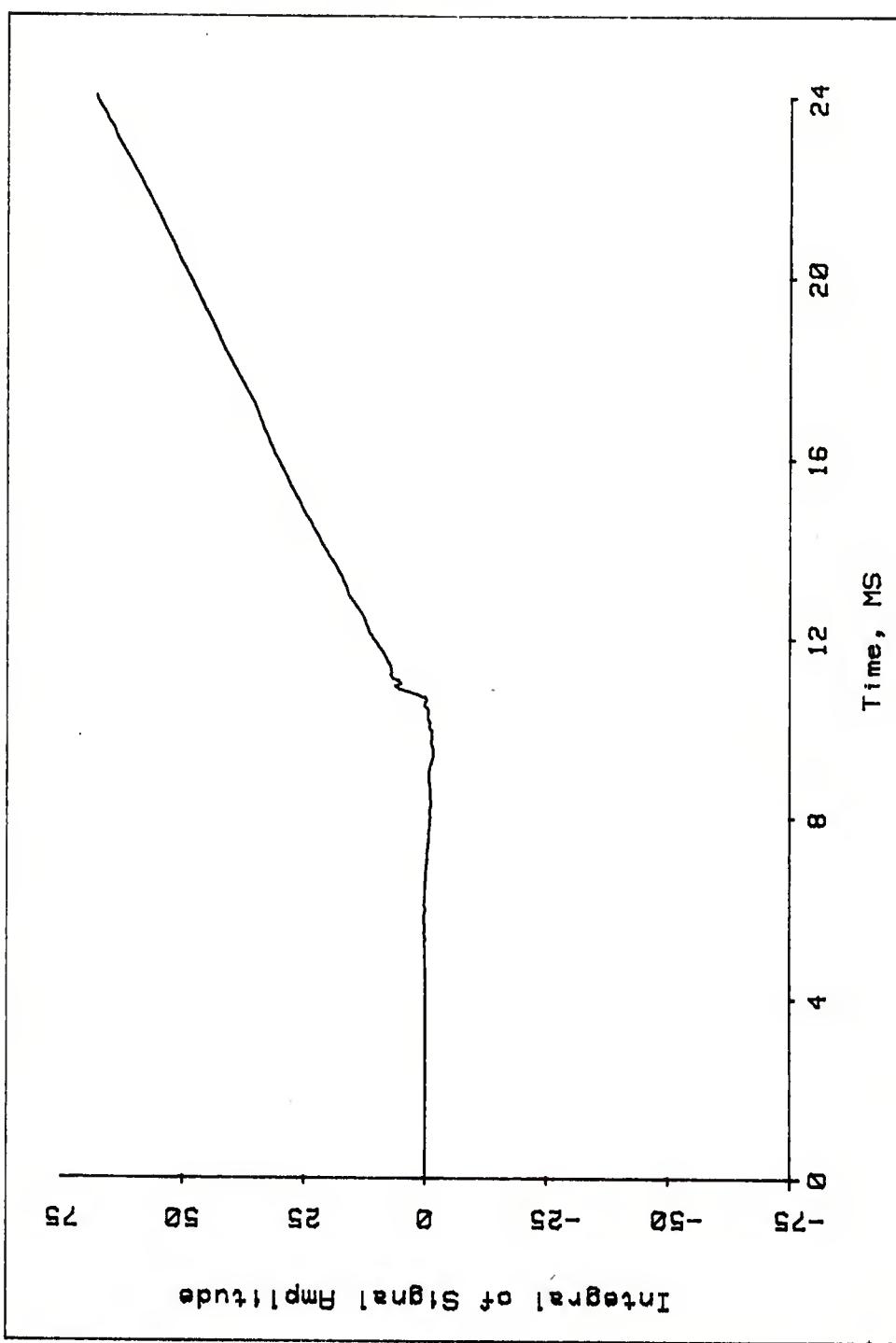
Figure 28. Integral of Uncorrected Acceleration

indeed a problem.

In analyzing this particular difficulty, one commonly made mistake is to assume that at some point during the data event an abrupt level change occurred, giving the baseline the appearance of a step function. While this is possible (although the change can occur no faster than the fastest response of any part of the transducer/recording/playback system) it is more likely that the analog components responded in a "smooth" fashion. Specifically, if a step function such as that in Figure 29 is applied to the input of an analog device, an output of the form of that in Figure 30 is likely to occur. Alternately, it may be that a "spike" will occur at the top of the input step, as seen in Figure 31. This overshoot may result in an analog response such as that seen in Figure 32. The point is that one should anticipate that the actual baseline variation has the appearance of the curves in Figures 30 or 32, or some combination thereof.

A further indication of a problem in the raw data is given by the presence of a large peak at zero Hz in its spectrum, shown in Figure 33. The spectral contribution of this component includes side lobes similar in appearance to the spectrum of Figure 6. To remove the component, a low pass filter with a cutoff frequency of 80 Hz was used. This cutoff frequency is well below the frequency of the first vibration mode of the system. The output of this filter is shown in Figure 34. The similarity of this curve to that of Figure 32 is readily apparent. If this curve is subtracted point-by-point from that in Figure 27, the result is the corrected acceleration data shown in Figure 35.

It indeed appears that the level shift has been removed by this process, and in fact, the spectrum of the data, Figure 36, shows the zero Hz component and its side lobes to be absent. The real proof of the matter, however, is the integral of the corrected acceleration data, shown in Figure 37. Whereas the final value of the integral in Figure 28 was about 75 units, the final value of this integral is indeed zero (precisely, the computed value was 0.3 units, although had the integration been stopped earlier, say at 22 milliseconds, the computed value would have been 0.01 units). In any event, this integral provides immense confidence in the baseline correction process. Moreover, the shape of this velocity curve is exactly as expected.

VII. EXAMPLE 5: PRESSURE WAVE ANALYSIS

This final example demonstrates the fact that it is not always possible to detect the presence of signal components by looking in the time domain. Figure 38 is a plot of the numerical difference between the aft and fore chamber pressures in a particular gun tube. One phenomenon frequently present in this pressure difference is waves reflecting between the base of the projectile and the rear face of the tube. In this particular example, it would appear that one or both of the pressure curves may have failed to correctly represent the physical
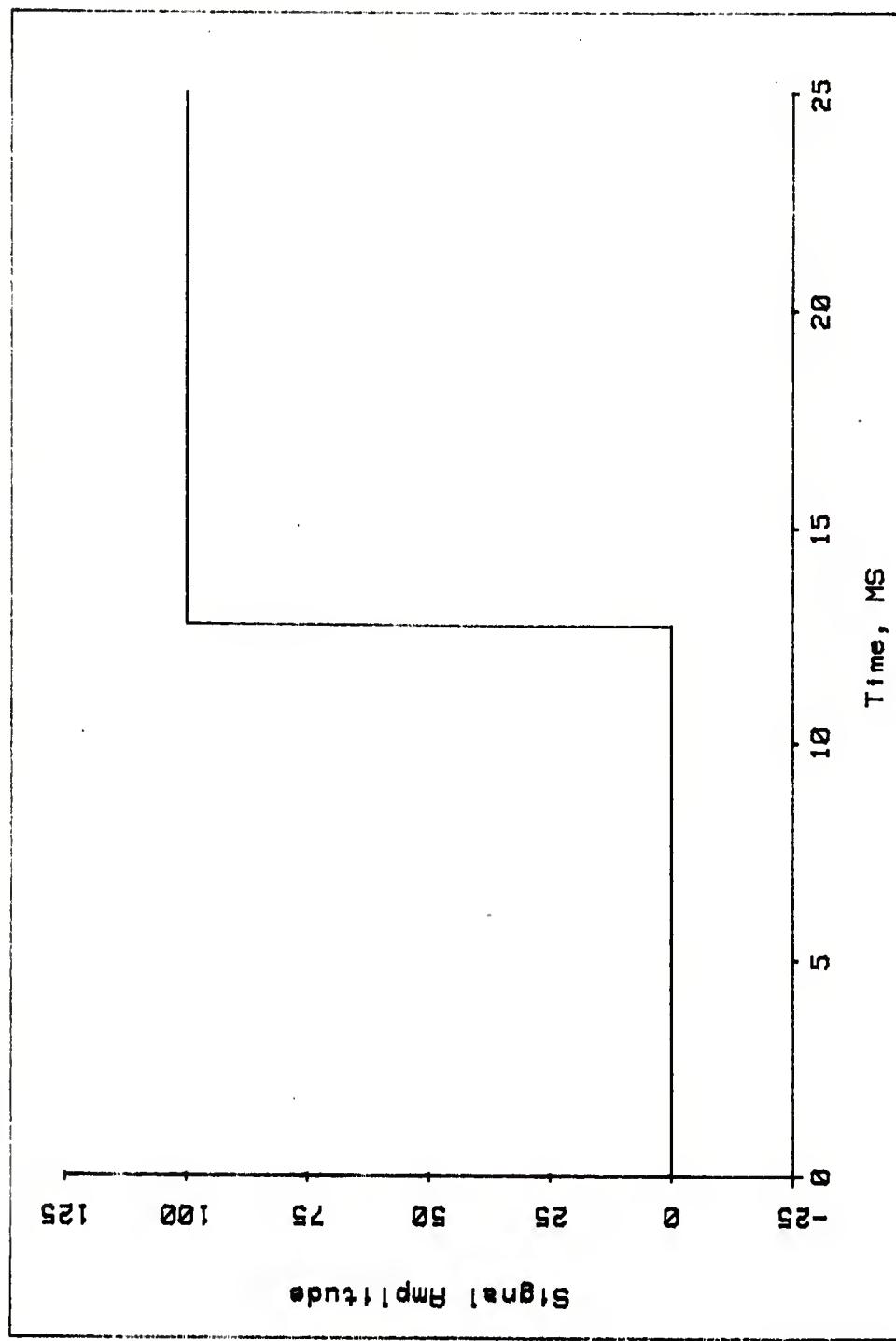
Figure 29. A Step Function

48
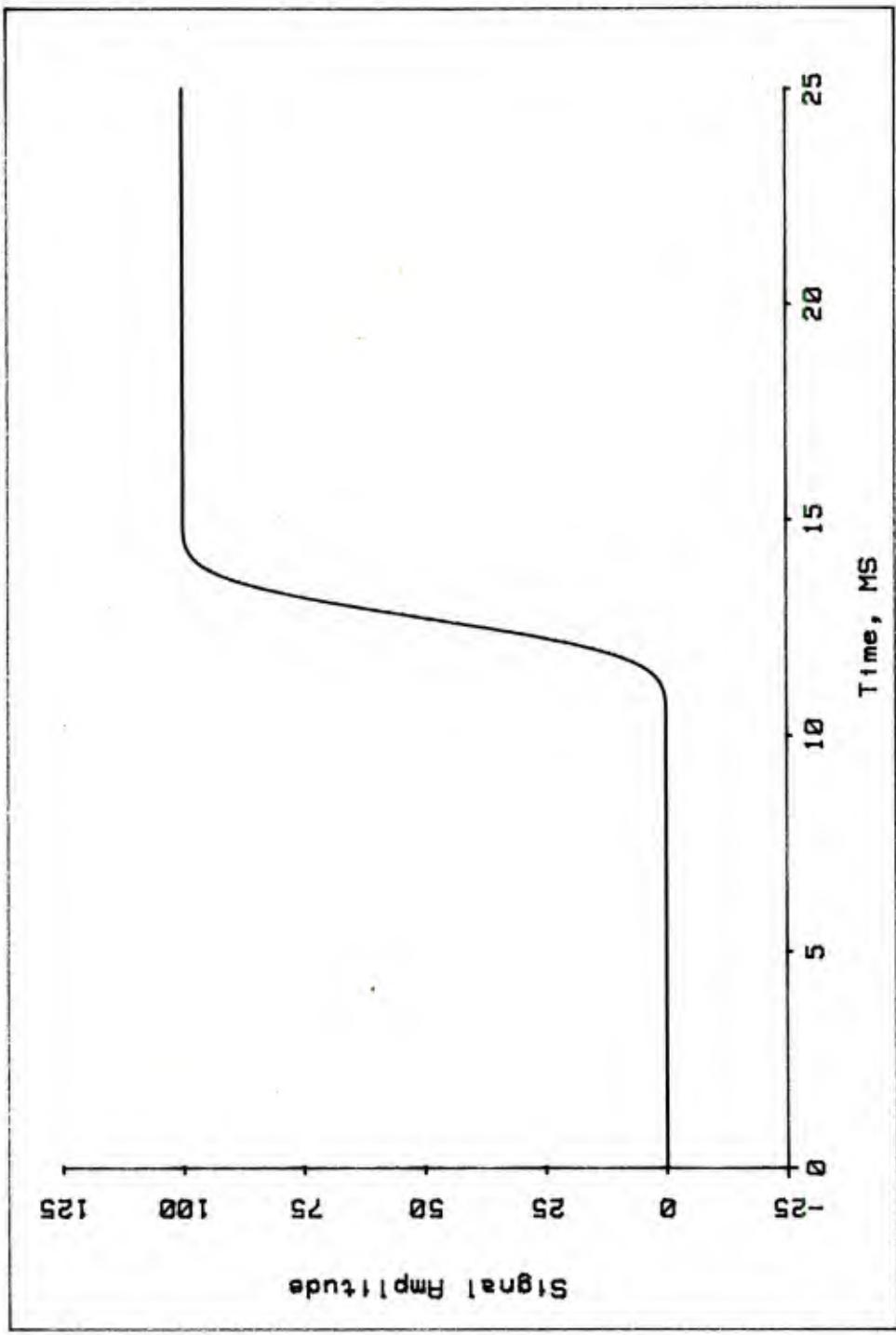
Figure 30. Analog Response to a Step Function

49
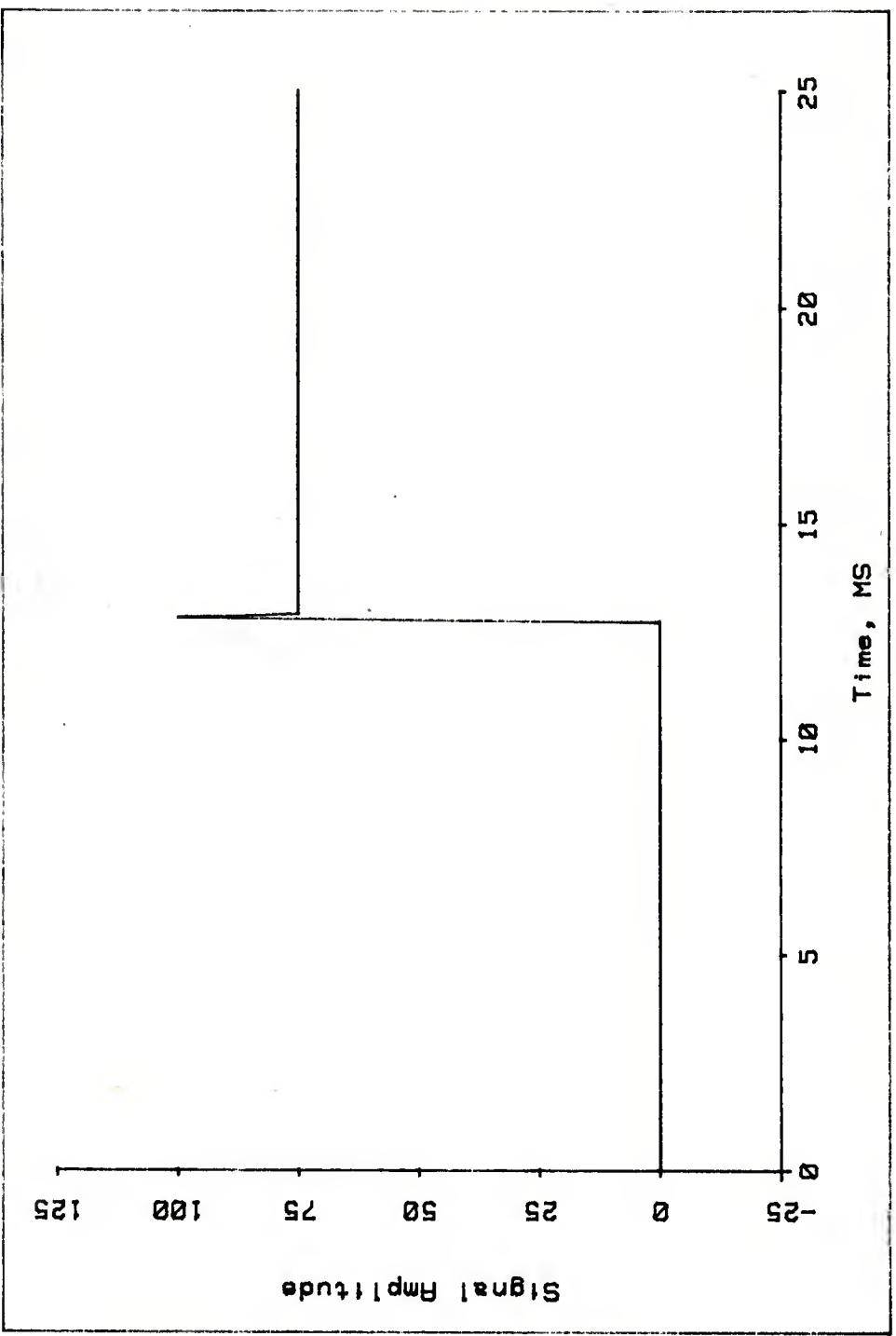
Figure 31. Step Function with Overshoot

50
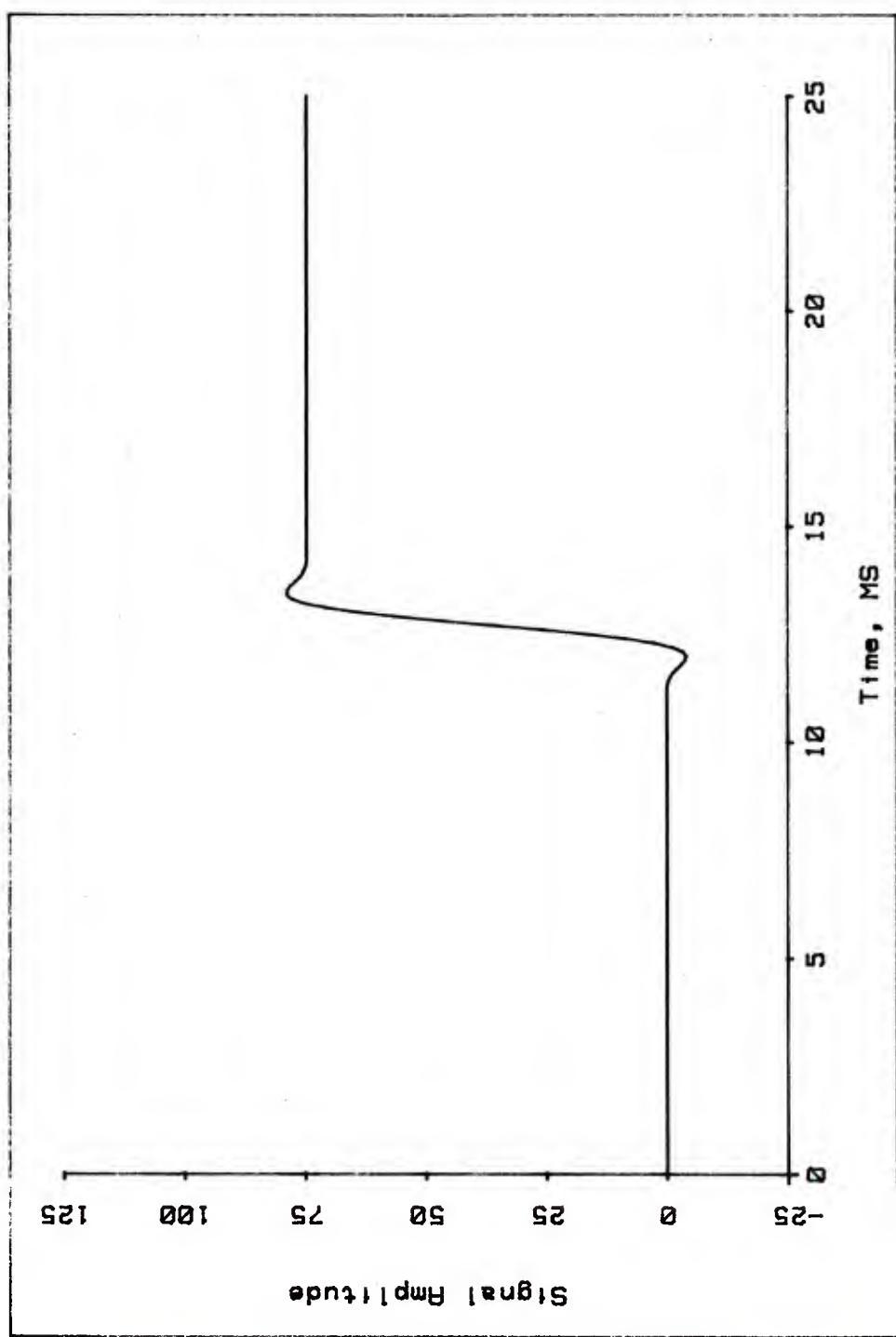
Figure 32. Analog Response to Step Function with Overshoot

51
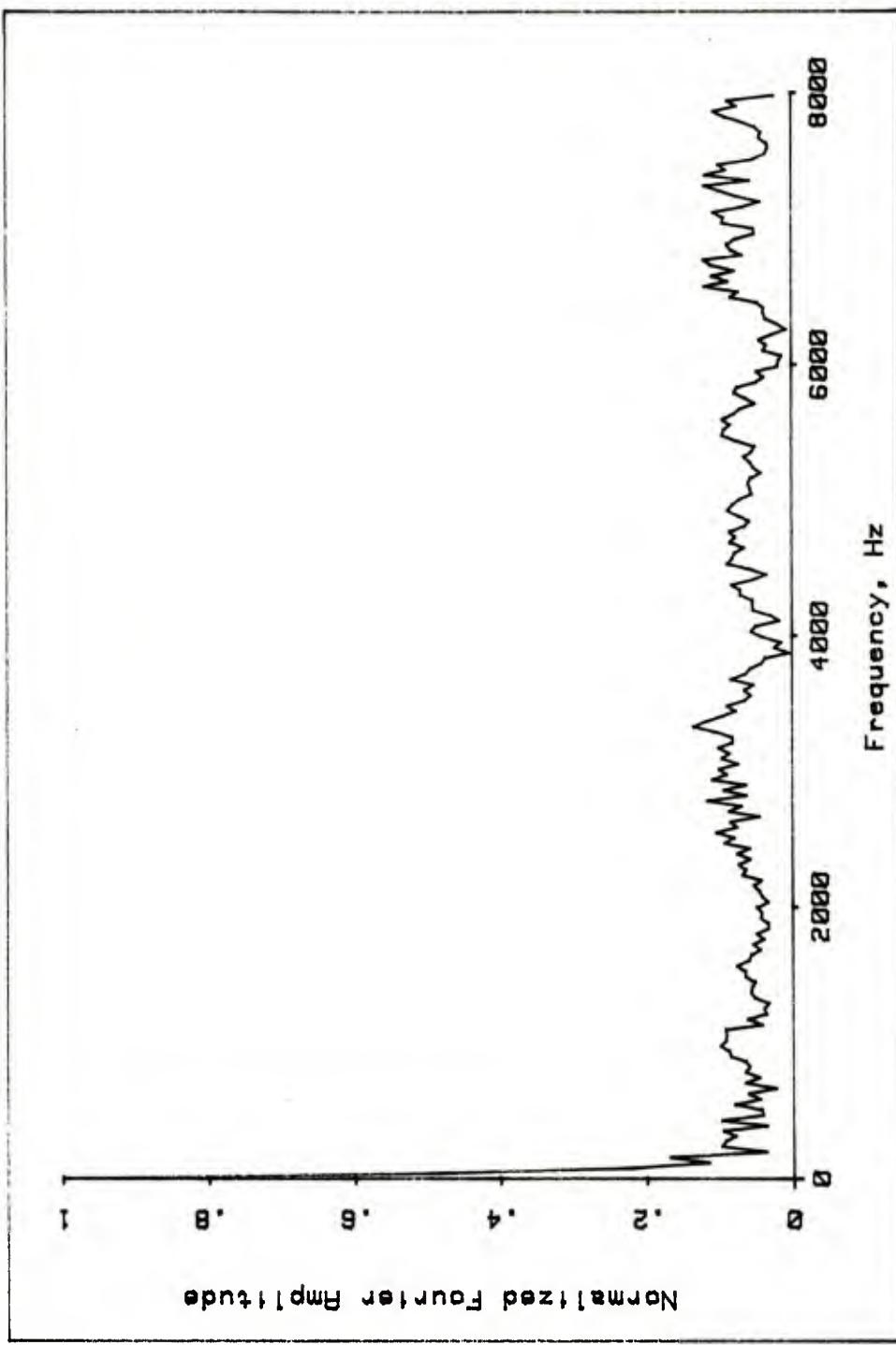
Figure 33. Spectrum of Uncorrected Acceleration Data

52
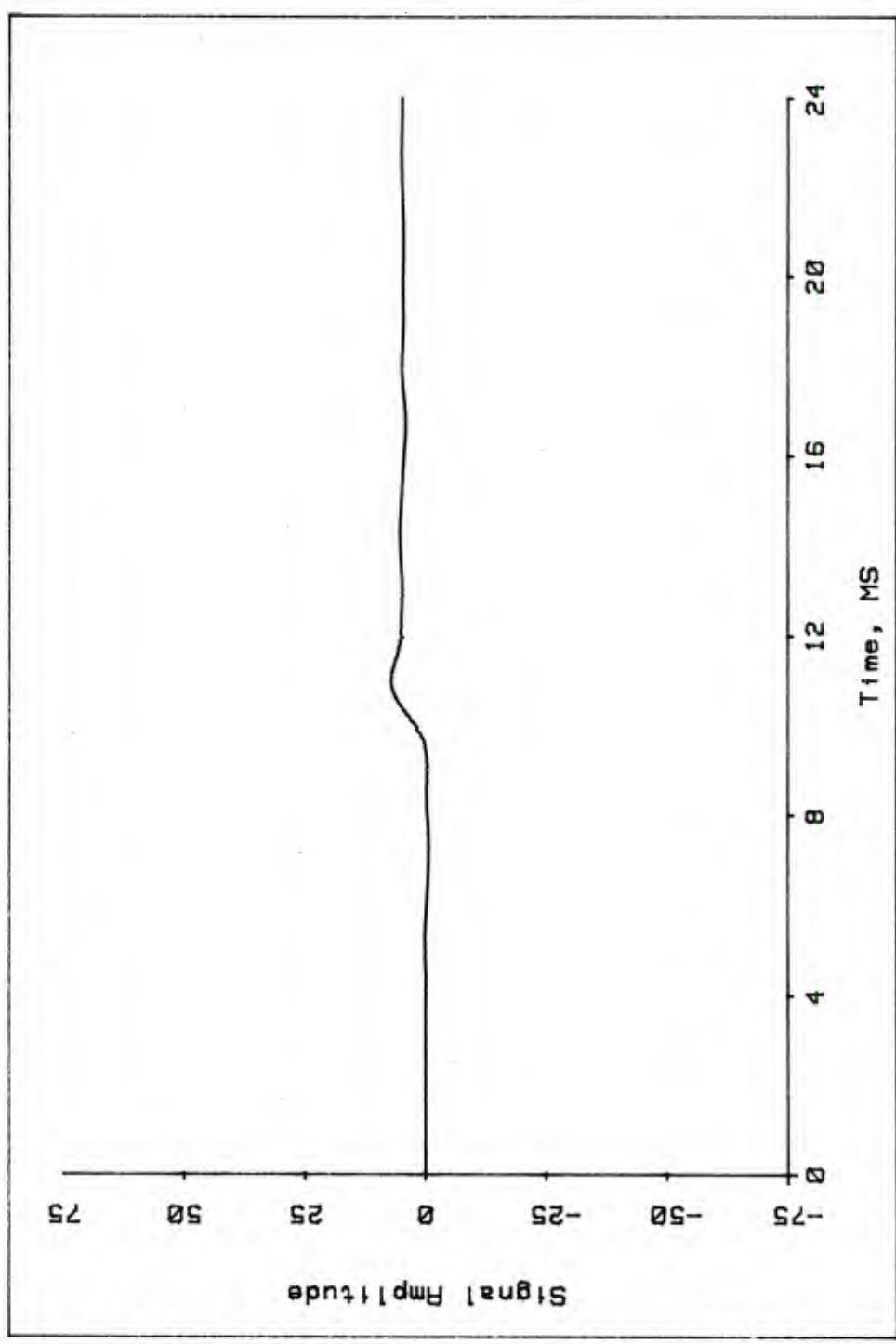
Figure 34. Baseline of Acceleration Data
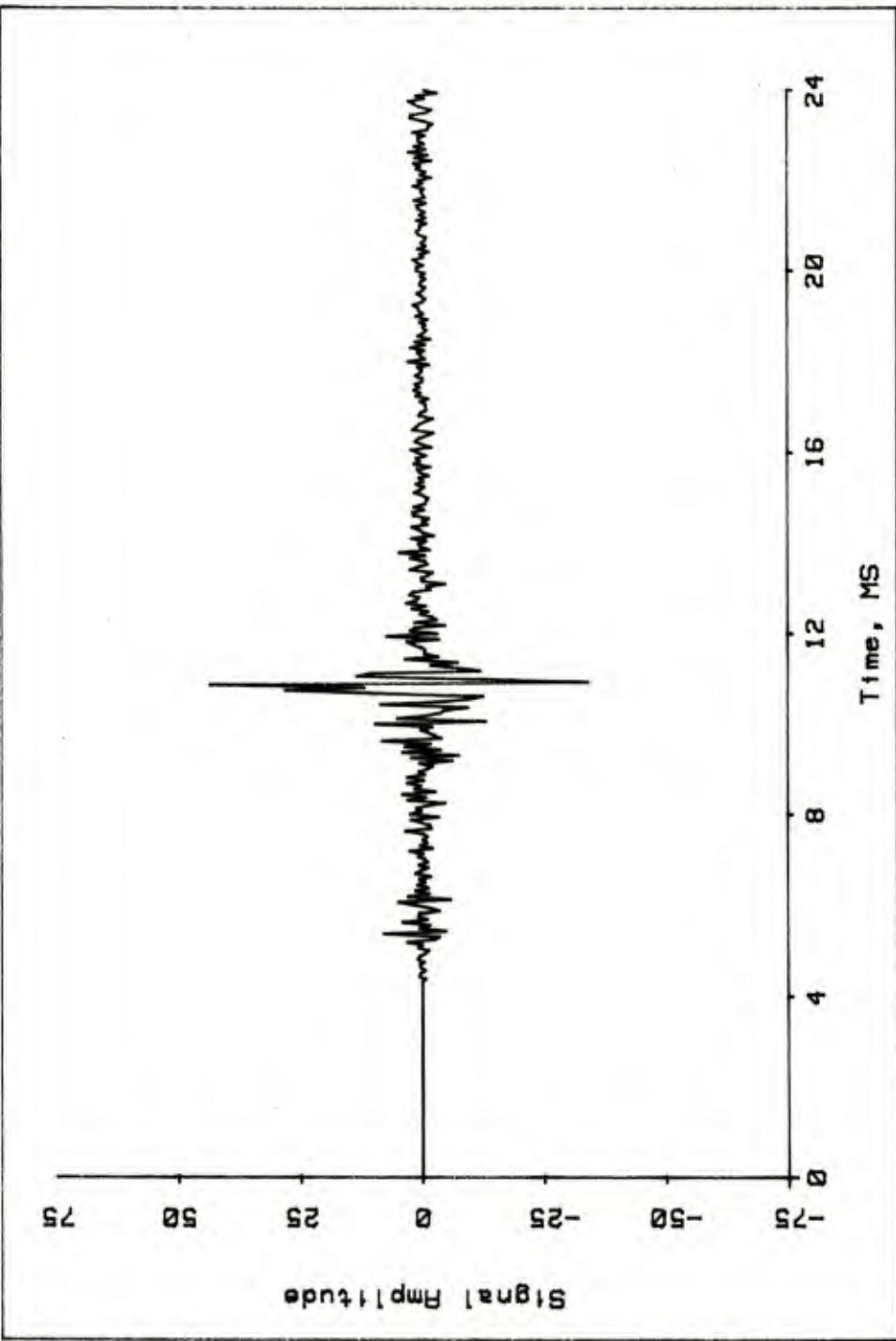
Figure 35. Corrected Acceleration Data
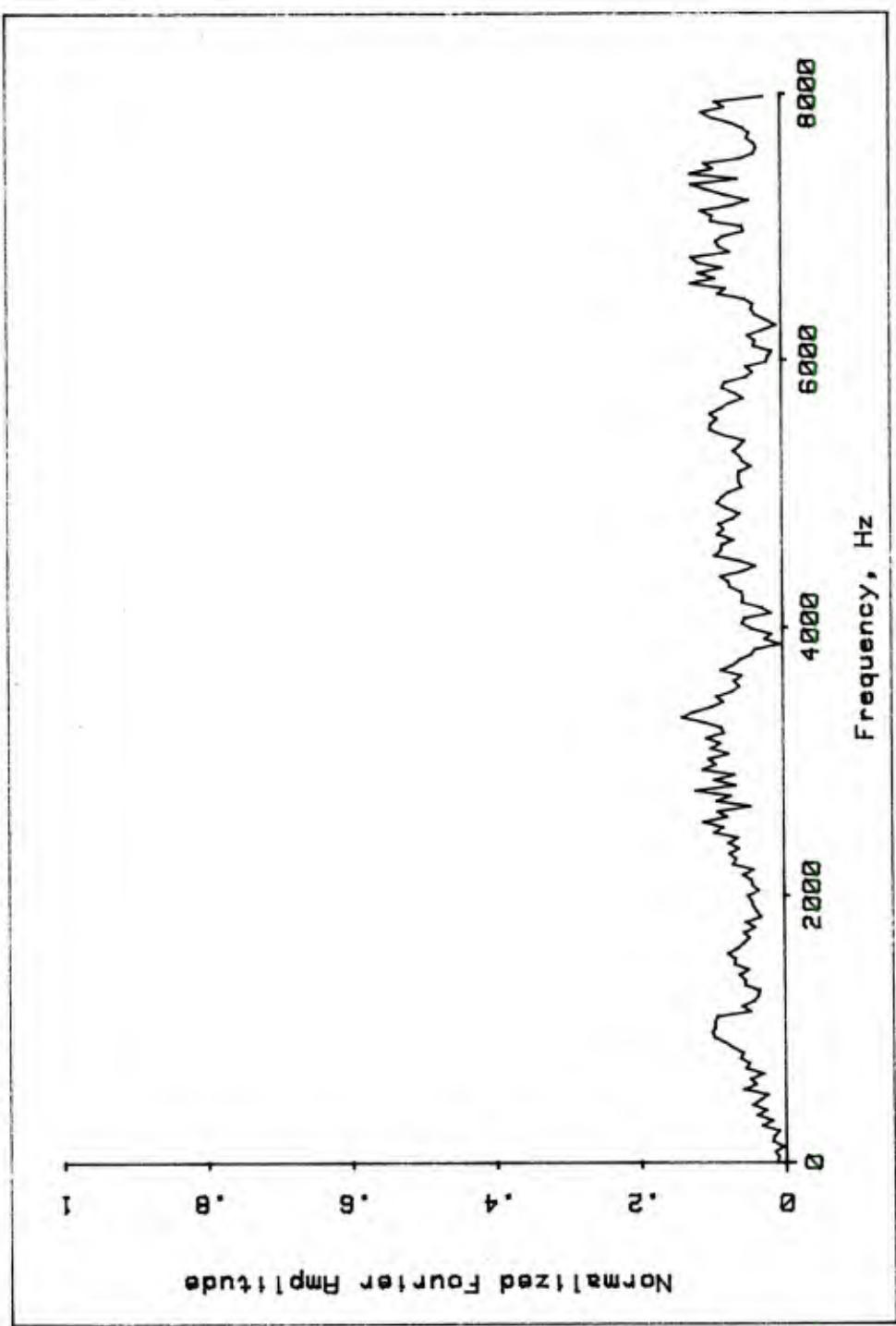
Figure 36. Spectrum of Corrected Acceleration Data
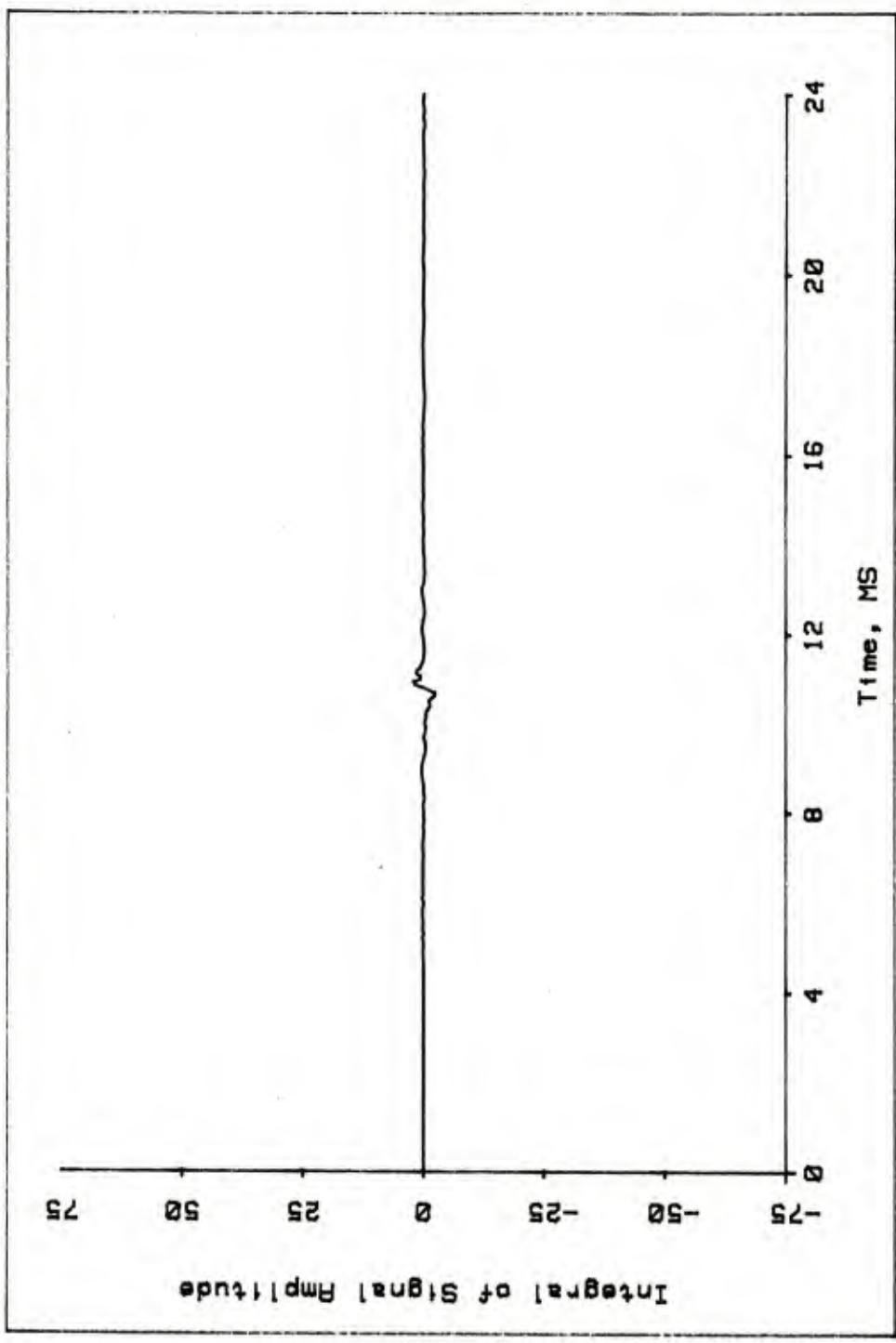
Figure 37. Integral of Corrected Acceleration
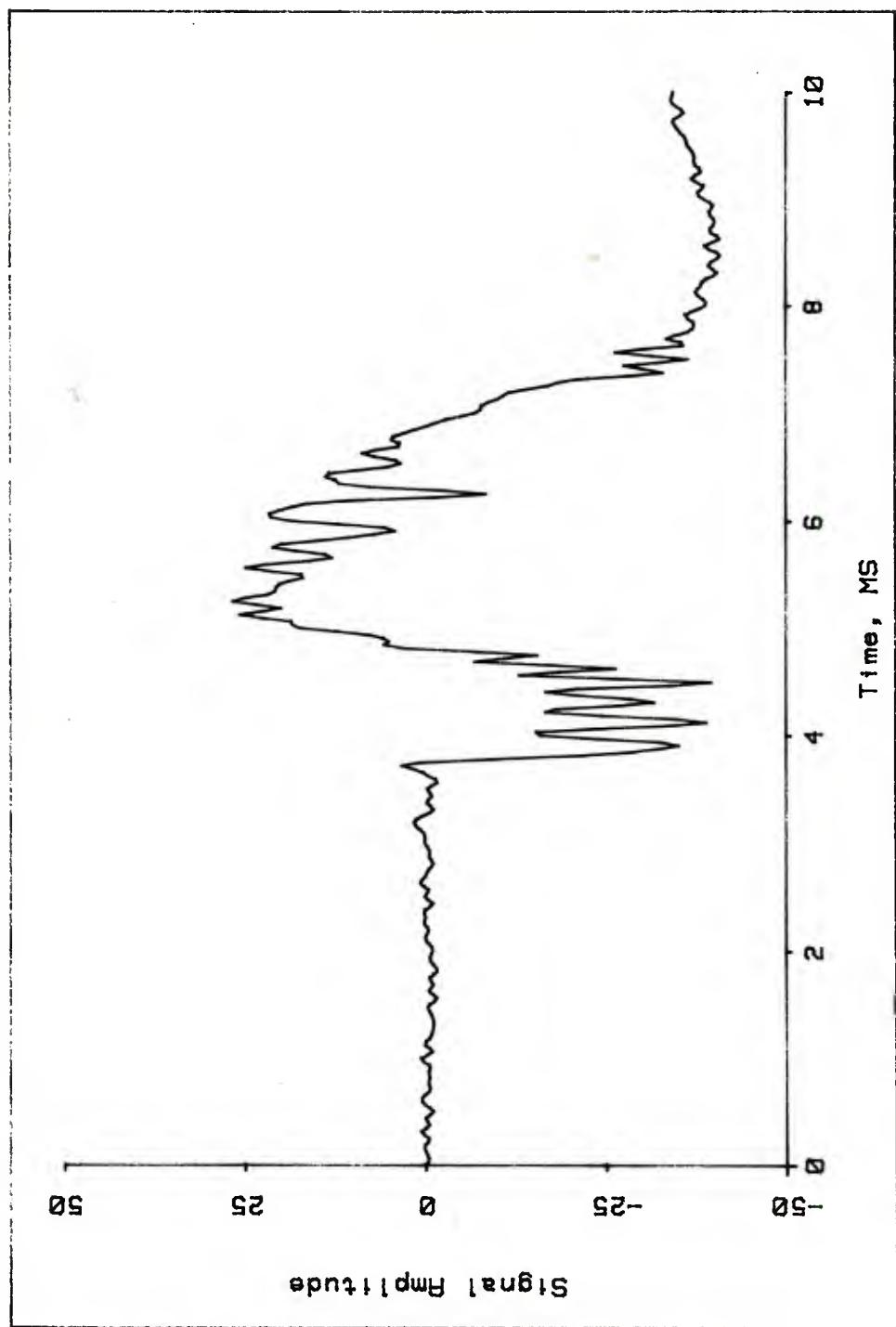
Figure 38. Pressure Difference, Aft Gage Minus Forward Gage

57

phenomenon, since the difference curve does not return to the zero level.

The spectrum of this data, Figure 39, shows the large zero Hz peak, reflecting the problem noted in the data. There are well defined spectral peaks: 200 Hz, 420 Hz, and 650 Hz. Based on the appearance of the original data, the 200 Hz is the gross cyclic variation in the curve. There is a higher frequency present in the data which is not noticeable in the spectrum. The 420 and 650 Hz components are not apparent in the original data.

Nevertheless, if one applies a band pass filter to the data, passing frequencies from 400 to 600 Hz, the result is the curve shown in Figure 40. This relatively pure waveform, decaying in both frequency and amplitude, is a typical example of pressure waves found behind the projectile in-bore. What is especially interesting here is that although the original record was of questionable validity, the wave structure remained intact.

VIII. SPECIAL TECHNIQUES FOR DIGITAL FILTER APPLICATION

In the foregoing examples, frequent reference has been made to the use of band pass filtering. As indicated in Example 2, the band pass filters employed were actually two filters, a low pass and a high pass, applied in succession. The reason for using a two-stage process is simply that low pass and high pass filters with the required frequency response were readily available. The assumption here is, of course, that it is accuracy and not time which is of the essence, since it takes twice as long to apply the two filters.

This process is shown graphically in the frequency domain in the next two illustrations. In Figure 41 is a spectrum containing three peaks (solid lines). Suppose it is desired to isolate the middle spectral peak. One begins by applying a low pass filter (dashed lines) with a transition band situated so as to exclude all of the spectral peak on the far right and to include all of the spectral peak in the middle. The second step, shown in Figure 42, is to apply a high pass filter (dashed lines) with a transition band situated so as to exclude all of the spectral peak on the far left and to include all of the sole remaining spectral peak to the right. Note that the original peak on the far right is gone, having been removed by step 1. Obviously, the same thing could have been accomplished by using the high pass filter first, followed by the low pass filter.

In Figures 41 and 42, the spectral peaks were sufficiently far apart to allow the filter transition bands to fit between them. Suppose this is not true. That is, suppose the spectrum of a particular data set has peaks too close to allow the transition band of a given filter to fit between them. In particular, the spectrum of Figure 43 has four peaks (solid lines), and it is desired to remove the two peaks at the right. Using the same low pass filter as in Figure 41 (dashed line), it will be

58
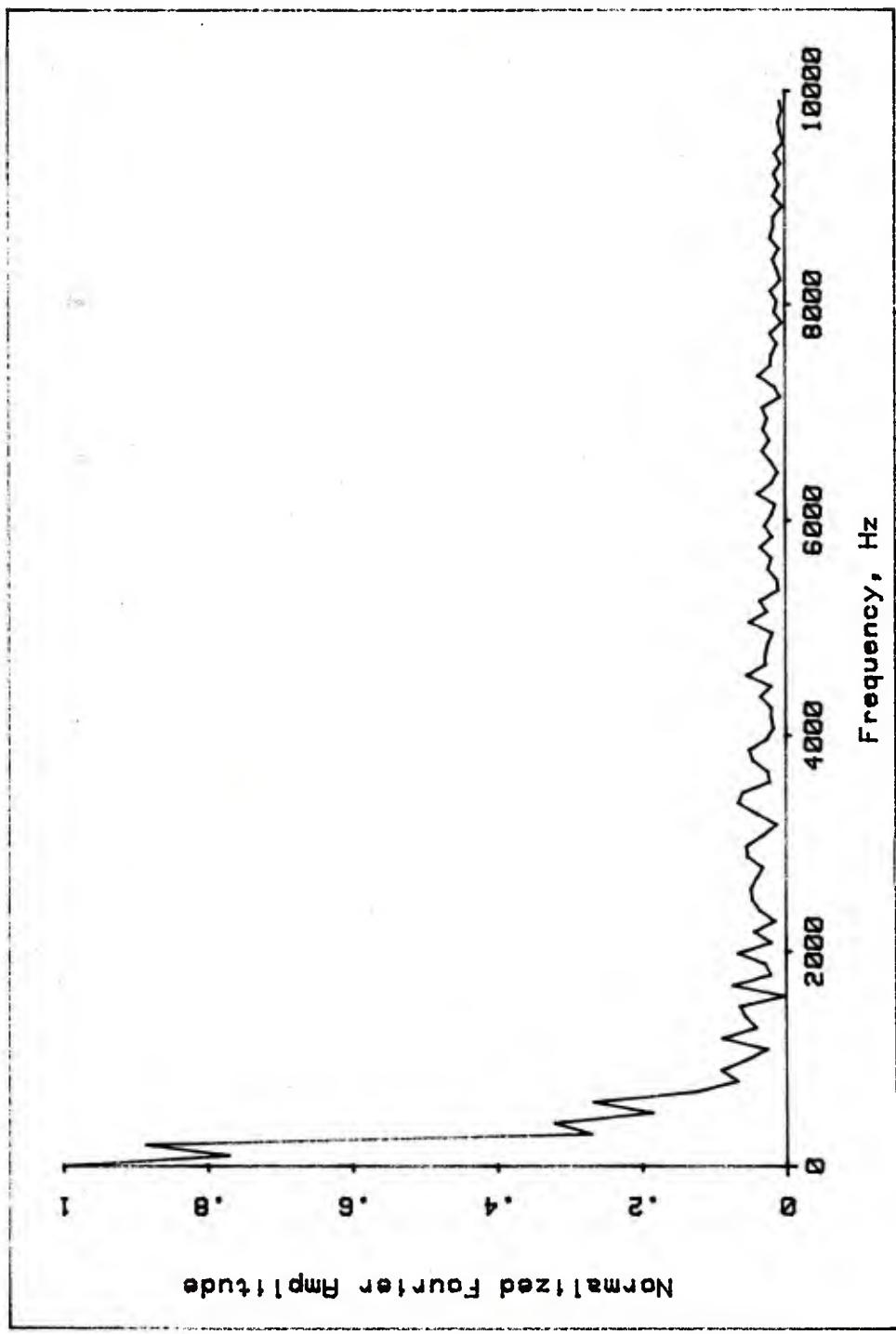
Figure 39. Spectrum of Pressure Difference
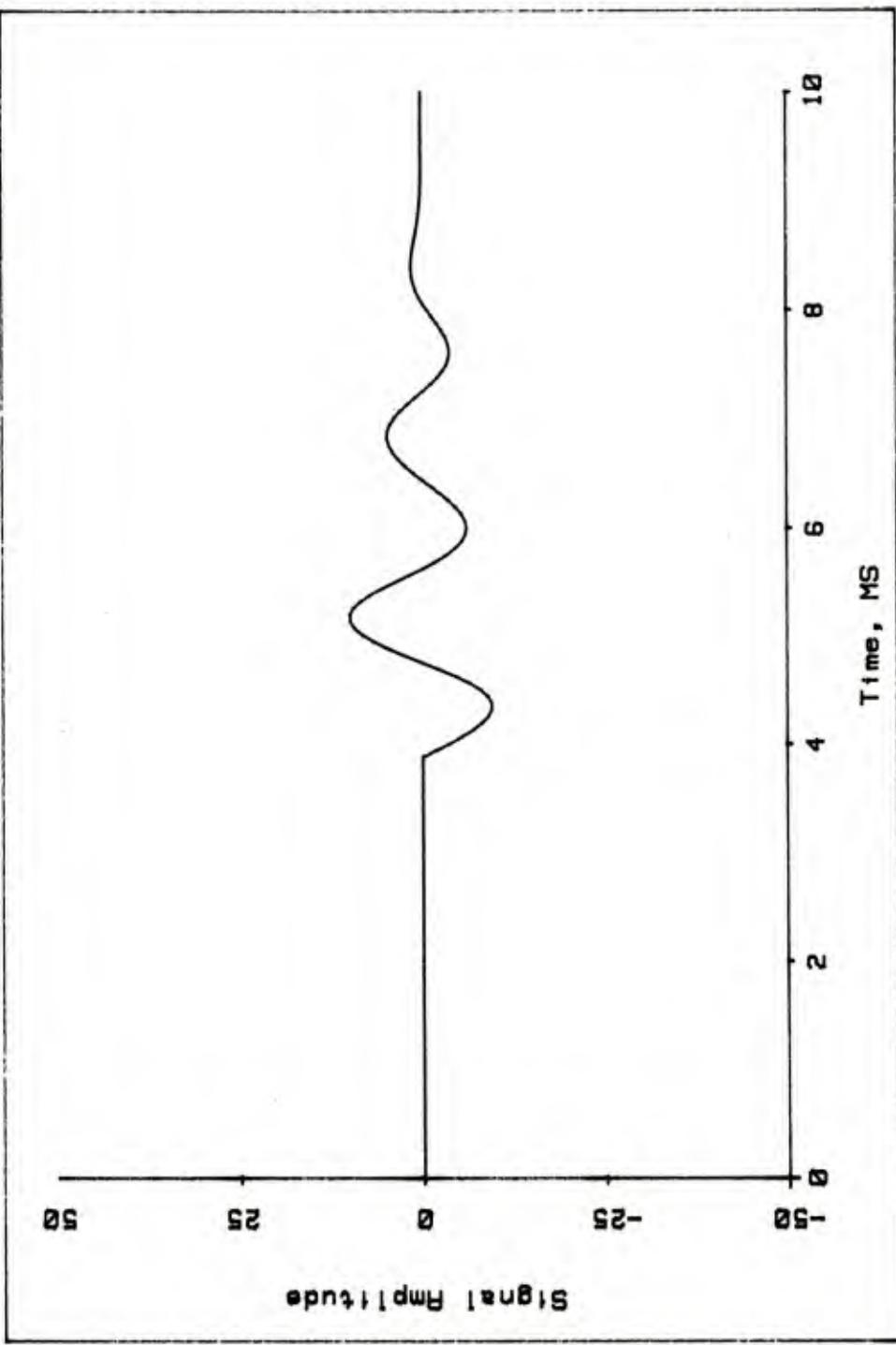
Figure 40. Pressure Waves Embedded in Pressure Difference
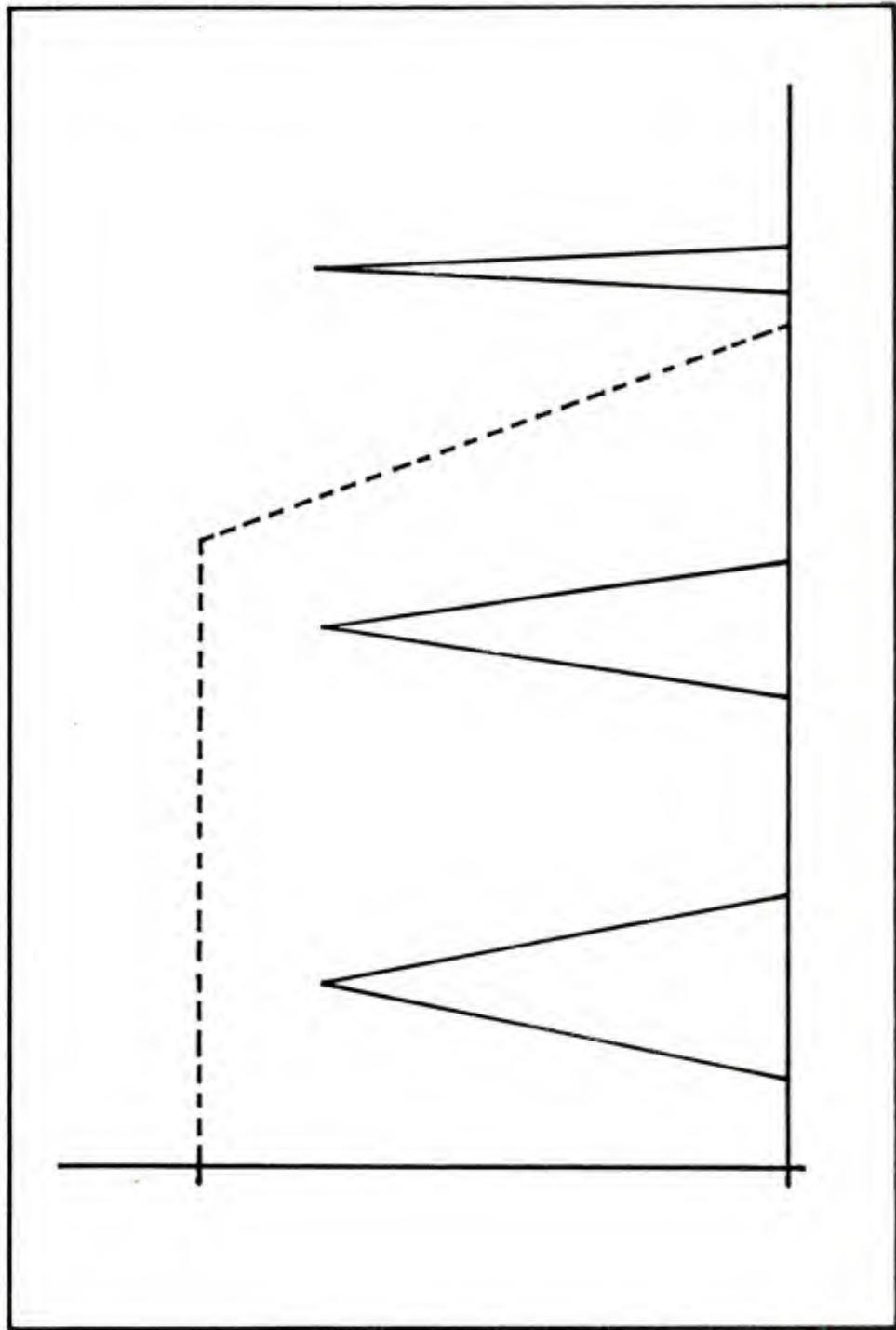
Figure 41. Band Pass Filter: Step 1

61
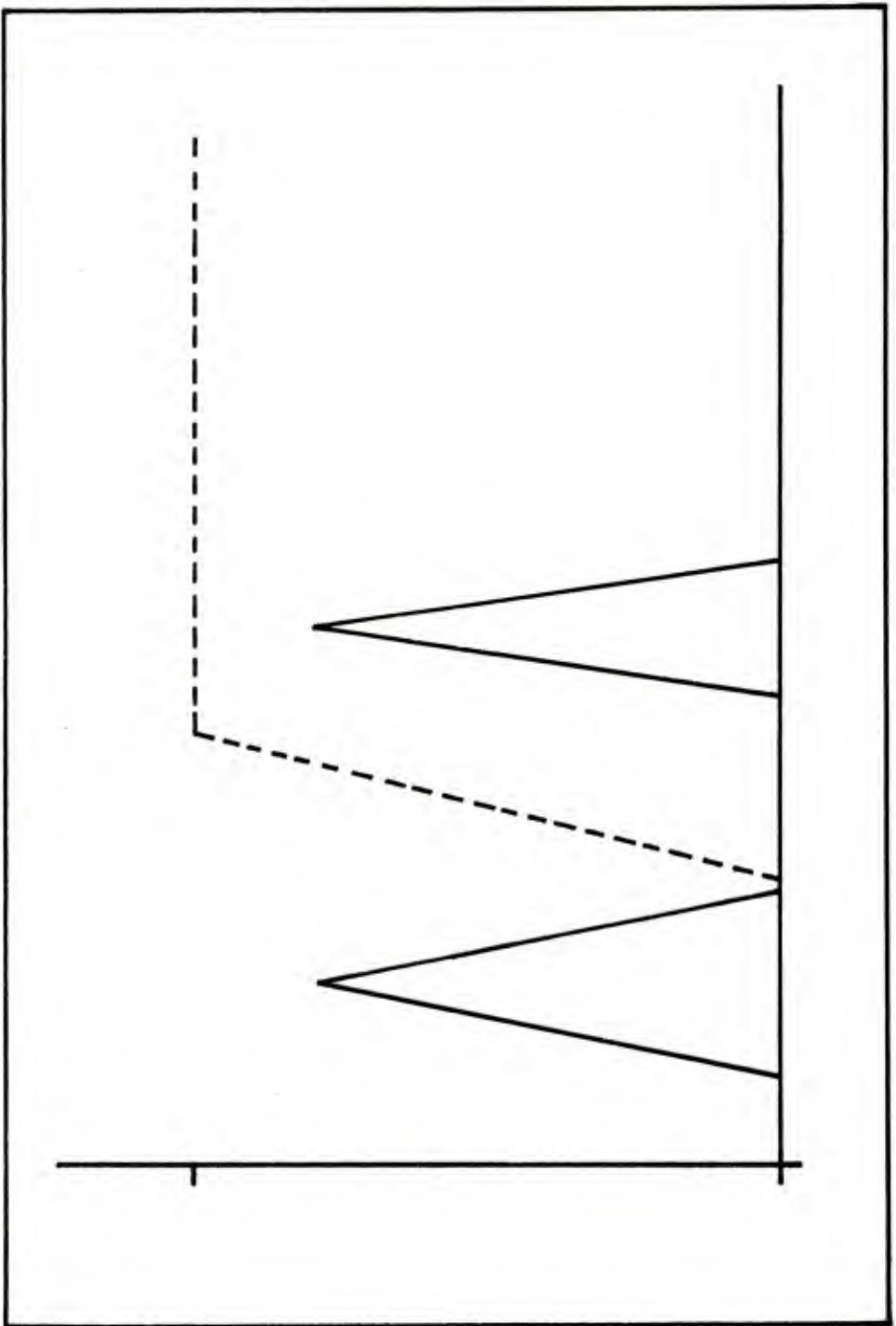
Figure 42. Band Pass Filter: Step 2
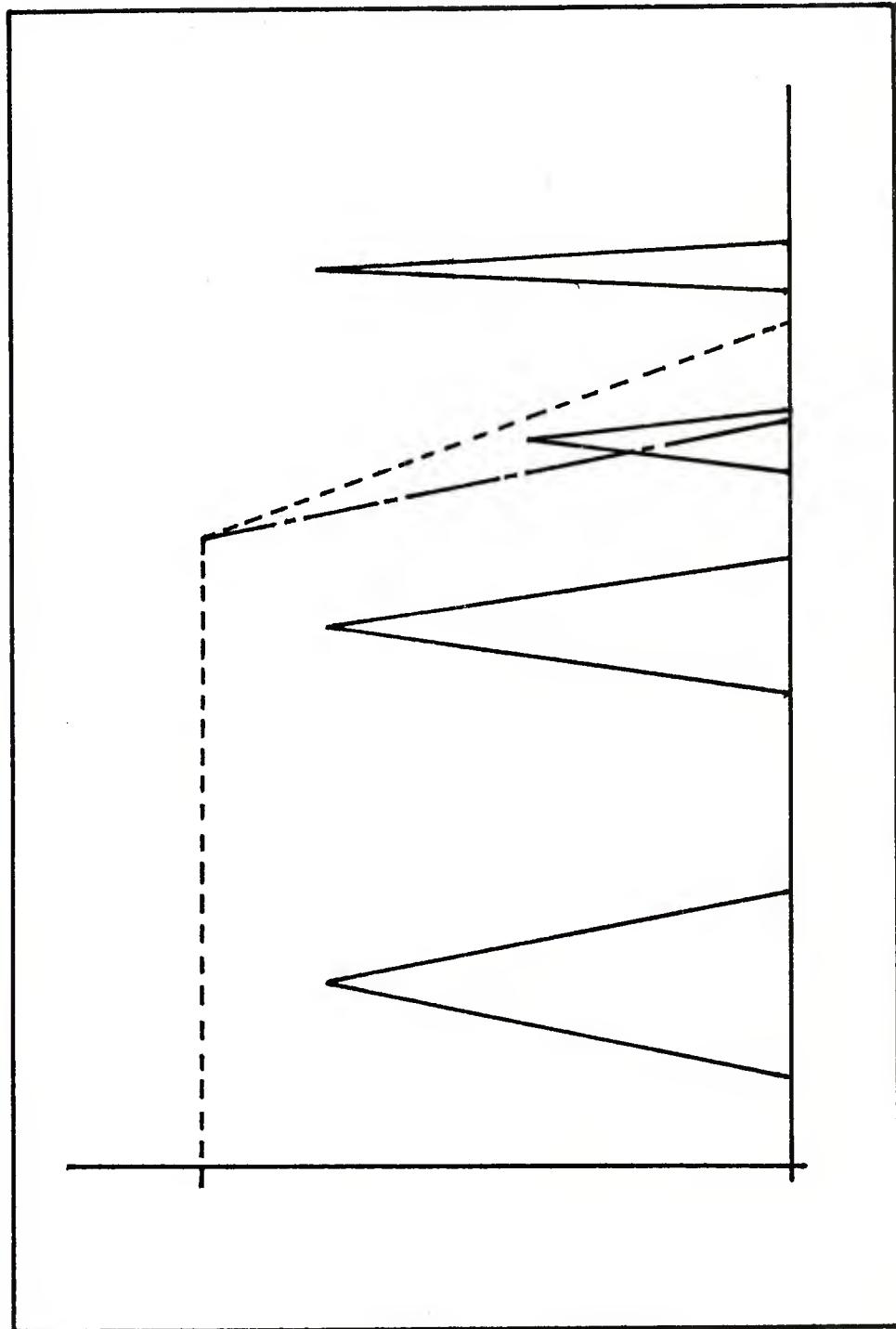
Figure 43. Multiple Applications of the Same Filter

63

seen that the peak on the far right is removed, but the second peak from the right is not completely removed. It will instead be reduced in magnitude by about half.

One option is to design a new low pass filter with a more narrow transition band. Another option which is very convenient is simply to apply the same low pass filter a second time. This has the effect of squaring the magnitude response. In the pass bands, where the magnitude is nearly 1, the squared response will remain nearly 1 (the ripple, or deviation, will of course be squared, but if it is small to begin with, this is of no consequence). In the stop bands, similarly, the values are nearly 0 and, when squared, remain nearly 0. It is in the transition bands where the significance of the procedure becomes apparent. Positive numbers less than 1, when squared, decrease in value. The net effect of two filter applications, or squaring the magnitude response, is that the transition band is more narrow, as shown by the broken line (not drawn to precise scale) in Figure 43.

Thus, if the second peak from the right is multiplied by 0.5 in each application of the filter, the net effect of two applications is to leave the peak with 0.5x0.5=0.25 times its original amplitude.

In general, a filter may be applied as many times as desired, provided the amplified deviation in the pass bands can be tolerated. If the spectrum of the data is sufficiently clean, even large amplitude deviations in the pass band of a filter can be corrected. For example, suppose, as in Figure 44, a relatively narrow spectral peak (solid lines) has been isolated by repeated application of a low pass filter (dashed lines). The resulting excessive deviation is shown by the arrows. The output of this filter process, being a single frequency, can then be multiplied in the time domain by the amount necessary to offset the deviation. This is, in effect, a digital amplifier. It must be emphasized that this works only at isolated frequencies and not across a band of frequencies.

The precise amplification factor is relatively simple to determine. Construct a time series representation of a sine wave with amplitude varying between +1 and -1 at the same sampling rate as the original data and with the same frequency as the isolated component. Apply the digital filter to this sinusoidal data; the maximum positive output amplitude is the inverse of the amplification factor. For example, if the output sinusoid has maximum positive amplitude 0.9, then the data component must be multiplied by 1/.9 to correct for its amplitude distortion.

In cases such as in Example 1, where the frequency of a spectral component varies during the event, this amplification correction is of no value since the spectral peak is likely to be wide with respect to the period of deviation in the filter pass band as shown in Figure 45. It is clear that no single amplification factor will correct the distortion resulting here. It should also be clear that, if there is more than

64
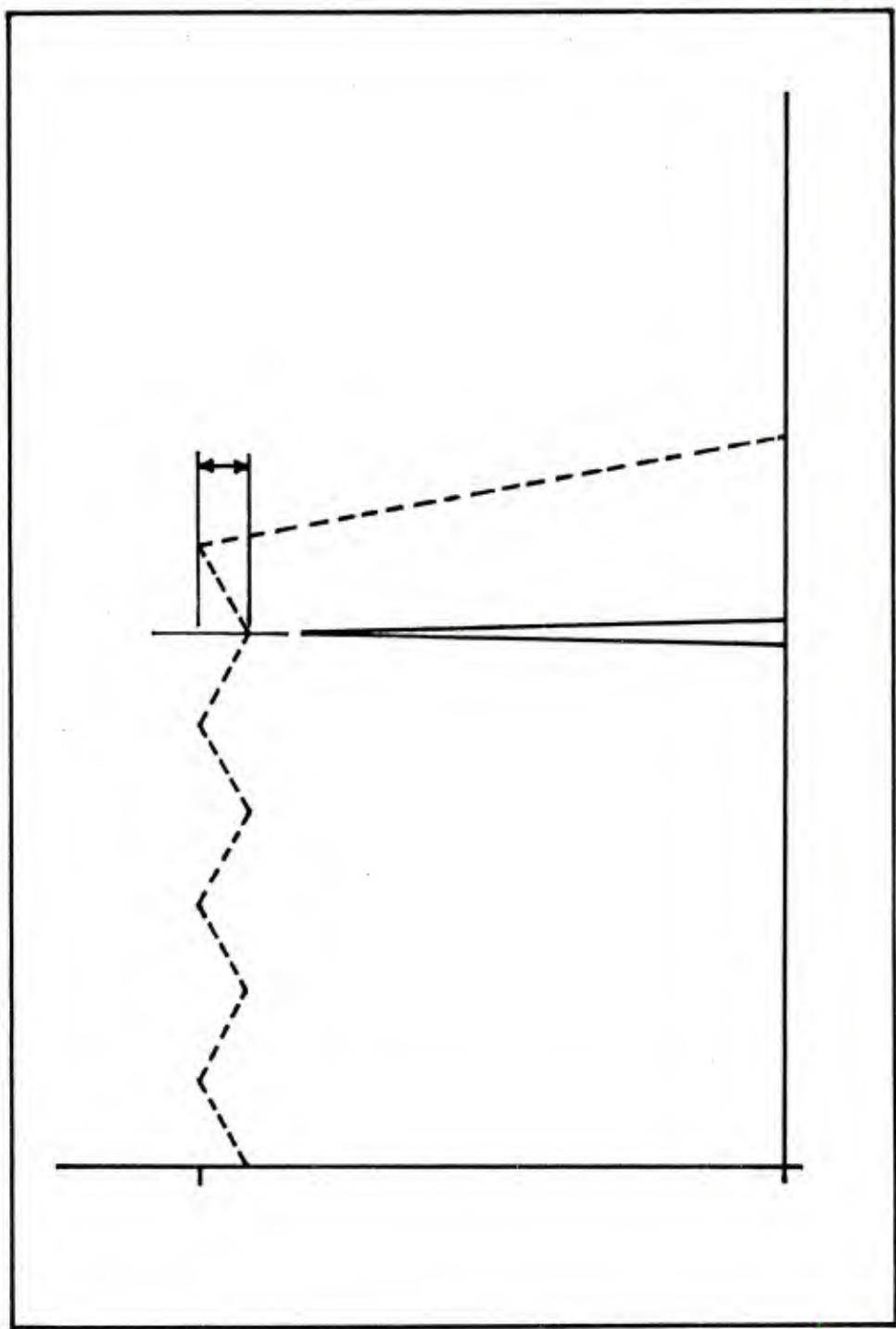
Figure 44. Amplitude Correction for Excessive Pass Band Deviation
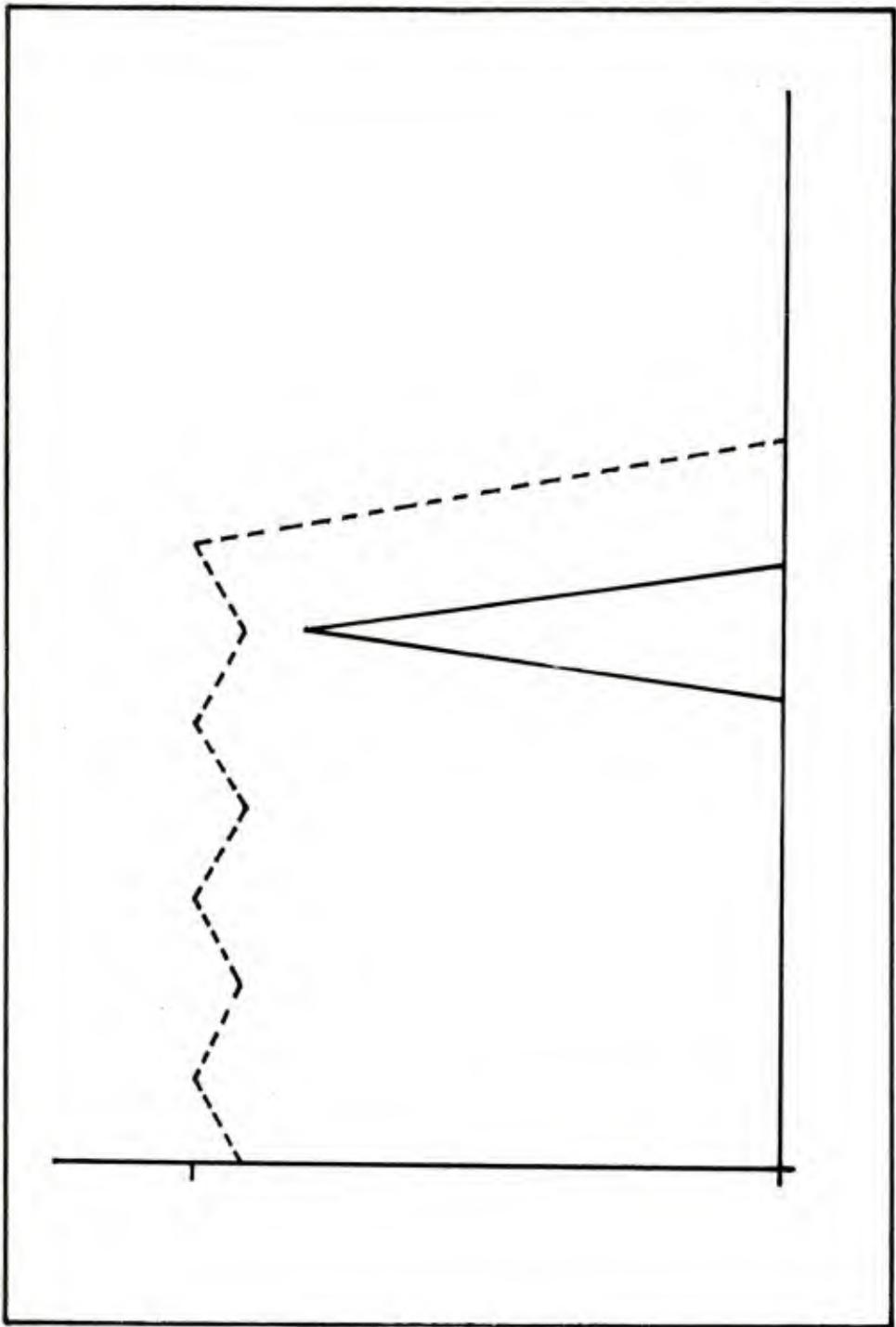
Figure 45.   Noncorrectable Amplitude Distortion (I)

one distinct frequency that has been isolated, the distortion may not be correctable. In Figure 46, for example, each peak will be distorted by a different amount; no single correction factor can be applied to the output to correct this distortion.

IX. NUMERICAL DIFFERENTIATION BY DIGITAL FILTER

Numerical differentiation has always been at best a tenuous process. The primary difficulty with most numerical schemes is their inherent instability at high frequencies. In this section it will be shown that digital filters designed as differentiators are stable and highly accurate. The theoretical basis for the design of a differentiating filter is quite simple. Let f(t) denote a differentiable function of time t, and suppose $F(\omega)$ is the Fourier transform of f, where ω is the circular frequency.

Then

$$f(t) = \frac{1}{2\pi} \int_{-\infty}^{\infty} e^{i\omega t} F(\omega) d\omega$$

Similarly, if $G(\omega)$ is the Fourier transform of the derivative of f(t) with respect to t, f'(t), then

$$f'(t) = \frac{1}{2\pi} \int_{-\infty}^{\infty} e^{i\omega t} G(\omega) d\omega$$

From the first of these two equations,

$$f'(t) = \frac{1}{2\pi} \int_{-\infty}^{\infty} e^{i\omega t} (i\omega F(\omega)) d\omega,$$

so that

$$G(\omega) = i\omega F(\omega).$$

It follows, then, that differentiation in the time domain corresponds in the frequency domain to multiplication by ω and positive rotation of the phase angle through $\pi/2$ radians. In particular, the amplitude response is just $|\omega|$, since $|i|=1$. Now, the variable ω is the circular
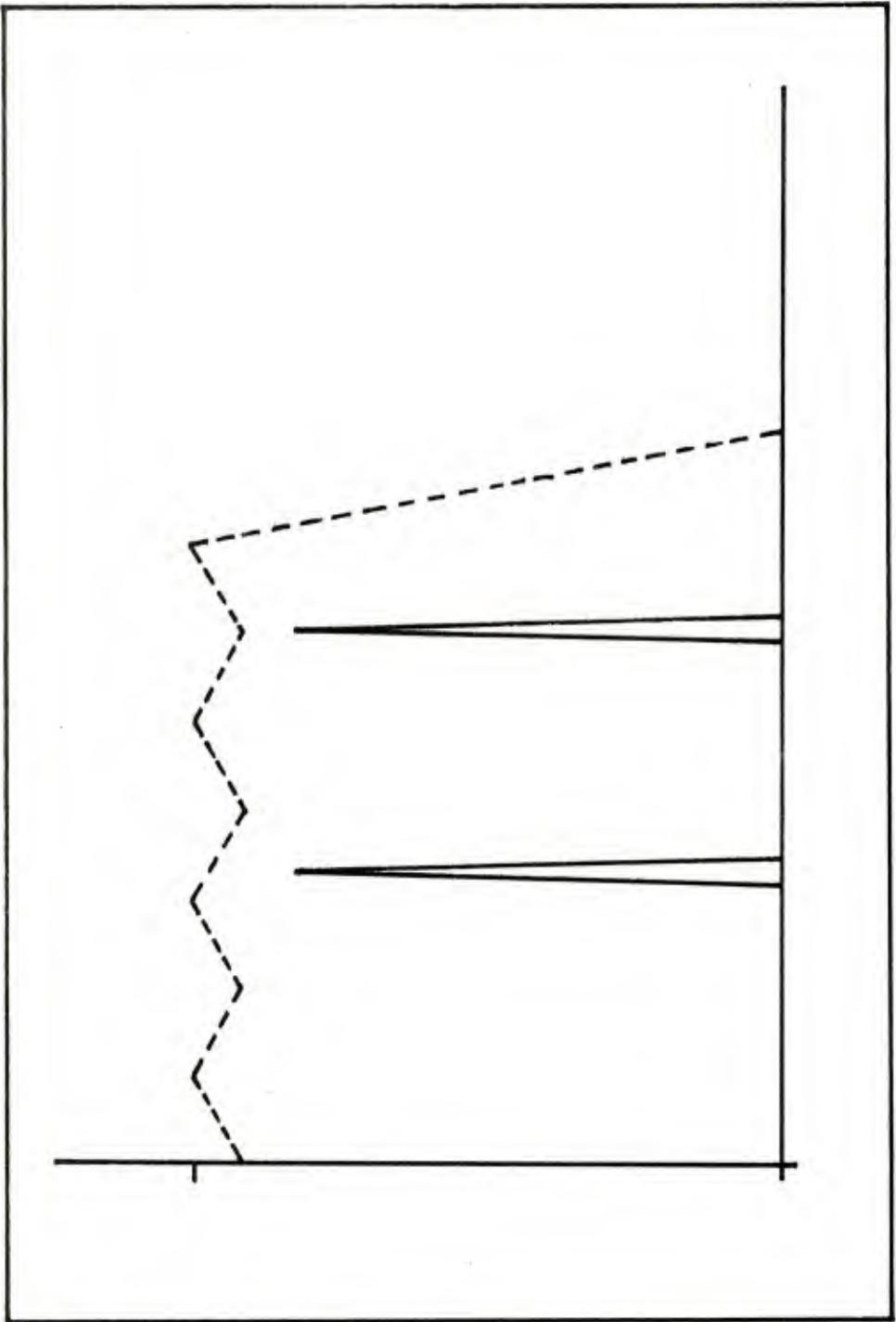
Figure 46. Noncorrectable Amplitude Distortion (II)

frequency, expressed in radians per second. One could write

$$\omega = 2\pi f,$$

where f is the frequency in units of cycles per second, or Hz.

In the case of the discrete Fourier transform, the Nth discrete frequency f_N is given by

$$f_N = (N-1)/[M(\Delta t)],$$

where M is the number of time series points spaced Δt apart. Then

$$\omega_N = \left(\frac{2\pi}{\Delta t}\right)\left(\frac{N-1}{M}\right),$$

and $(N-1)/M$ is the fraction of the sampling frequency. The amplitude response of a differentiating filter can then be represented as in Figure 47. It is an approximation to the straight line through the origin and through the point $(\frac{1}{2},\frac{1}{2})$, where the first coordinate is amplitude and the second coordinate is fraction of sampling frequency. After applying this differentiating filter to a data set, the differentiated data is multiplied by $2\pi/\Delta t$ to correct the amplitude.

The filter response of Figure 47 is a good approximation to the ideal differentiator out to about 80% of the bandwidth. Beyond that point, the amplitude falls off rapidly to 0. It is this return to zero amplitude that provides the stability at high frequencies. Clearly, the amplitudes of frequencies above 80% of bandwidth are greatly decreased. Instead of increasing the noise content of the differentiated signal, the high frequencies are actually suppressed. Since the magnitude response of the filter is constrained by design to be odd periodic, it must return to zero at each end; it is not possible to design a stable differentiator over the full bandwidth.

As long as the data set contains no useful information beyond 80% of the bandwidth, this differentiator performs admirably well. For example, if one computes by the trapezoidal rule the integral of the data in Figure 17, the result is shown in Figure 48. On applying the differentiating filter of Figure 47 to the integral in Figure 48, one obtains the curve shown in Figure 49. This curve is virtually identical to that of Figure 17; in fact, the difference between the two curves is shown in Figure 50. Indeed, the spectrum in Figure 18 shows that there is very little content beyond 80% of the bandwidth (8kHz).

69
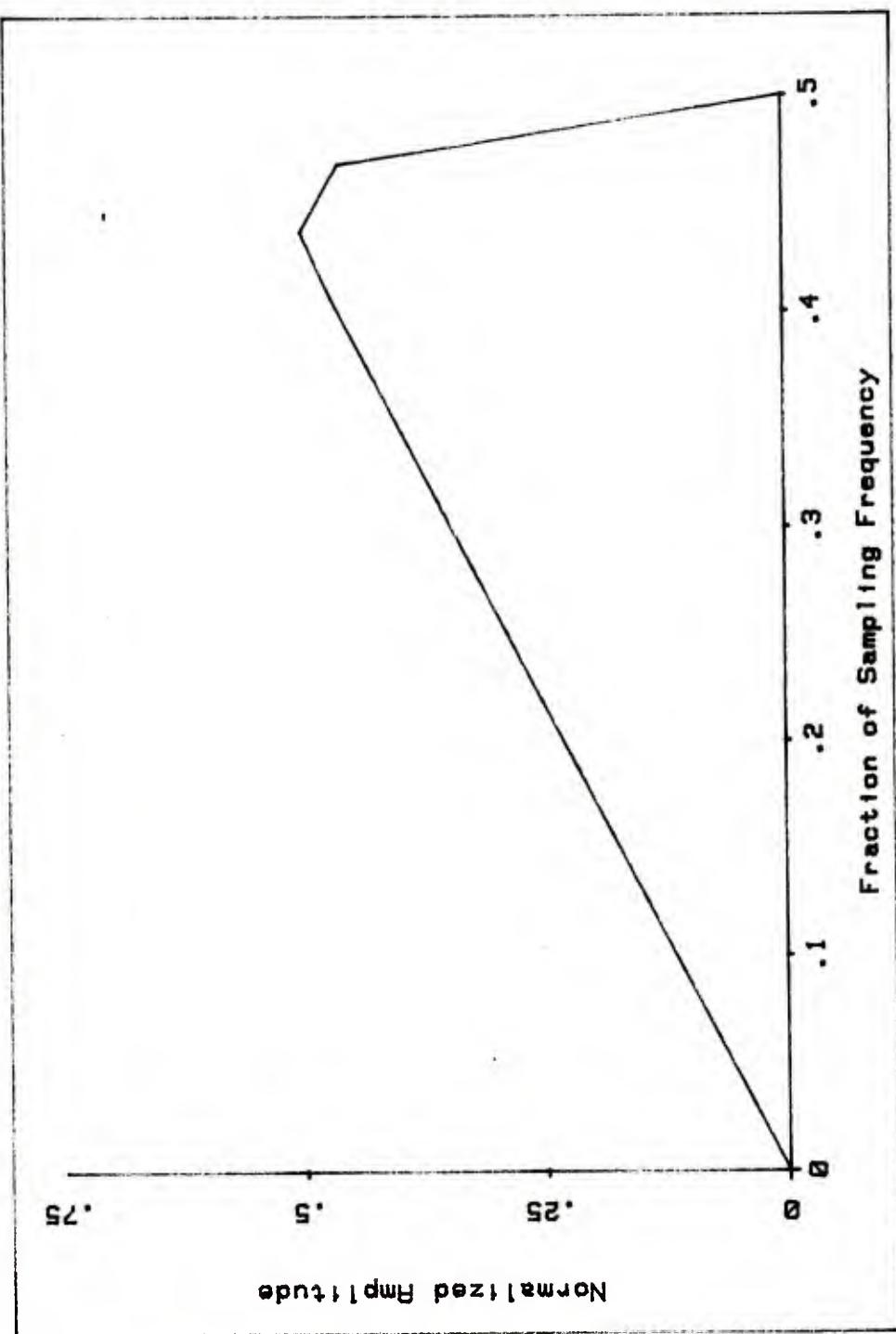
Figure 47. Frequency Response of a Differentiating Filter
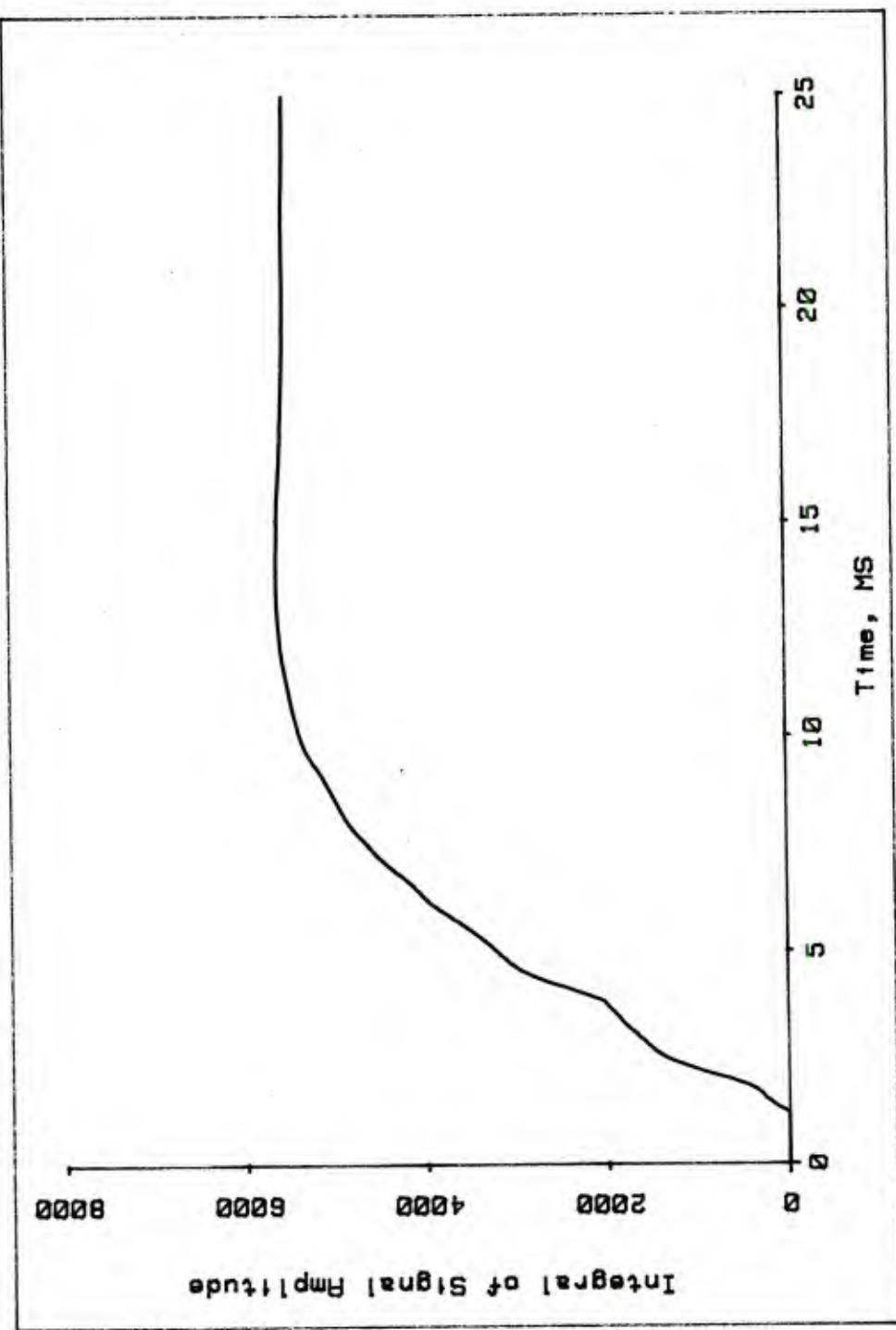
Figure 48. Integral of Blast Pressure Data
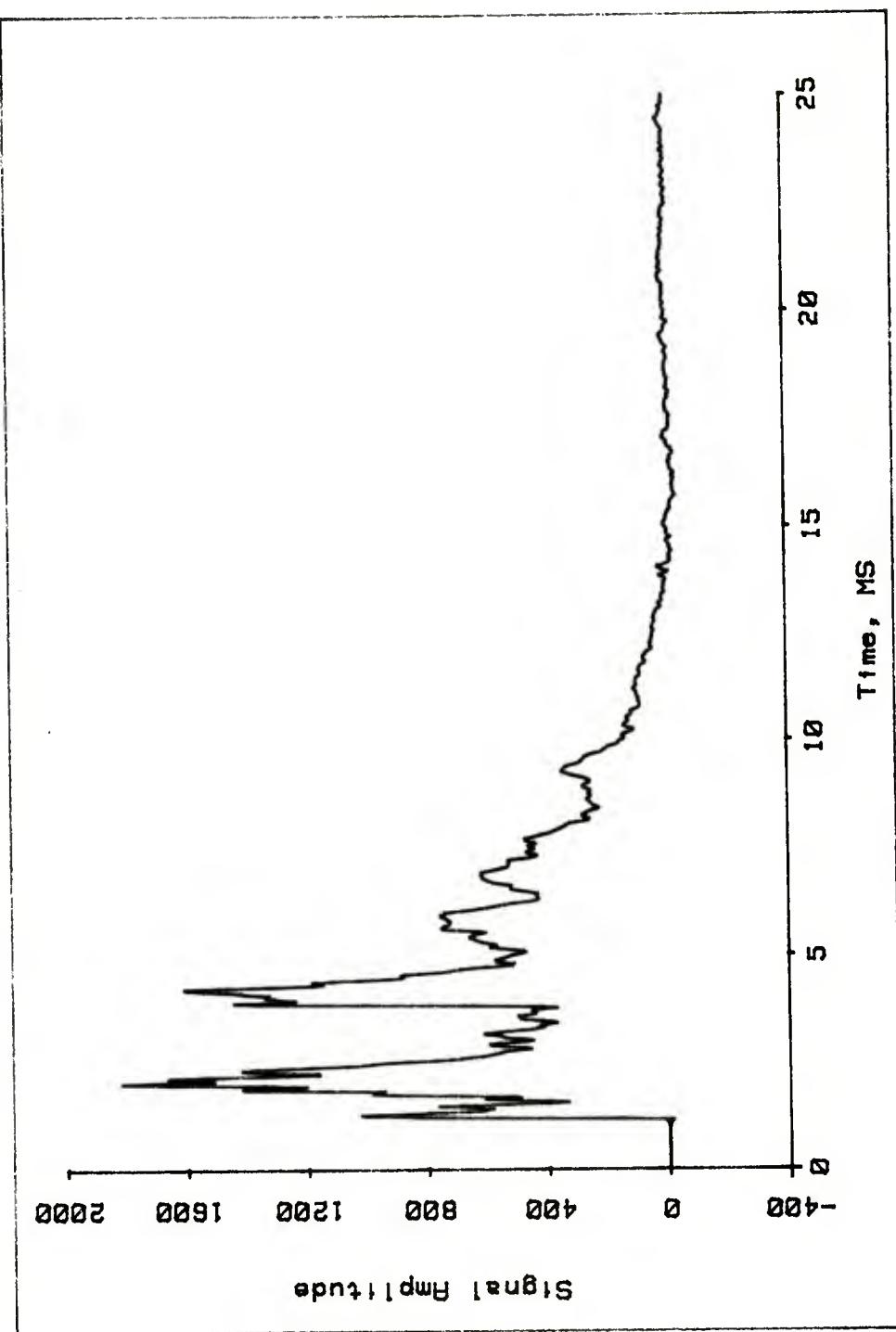
Figure 49. Derivative of Integral of Blast Pressure Data
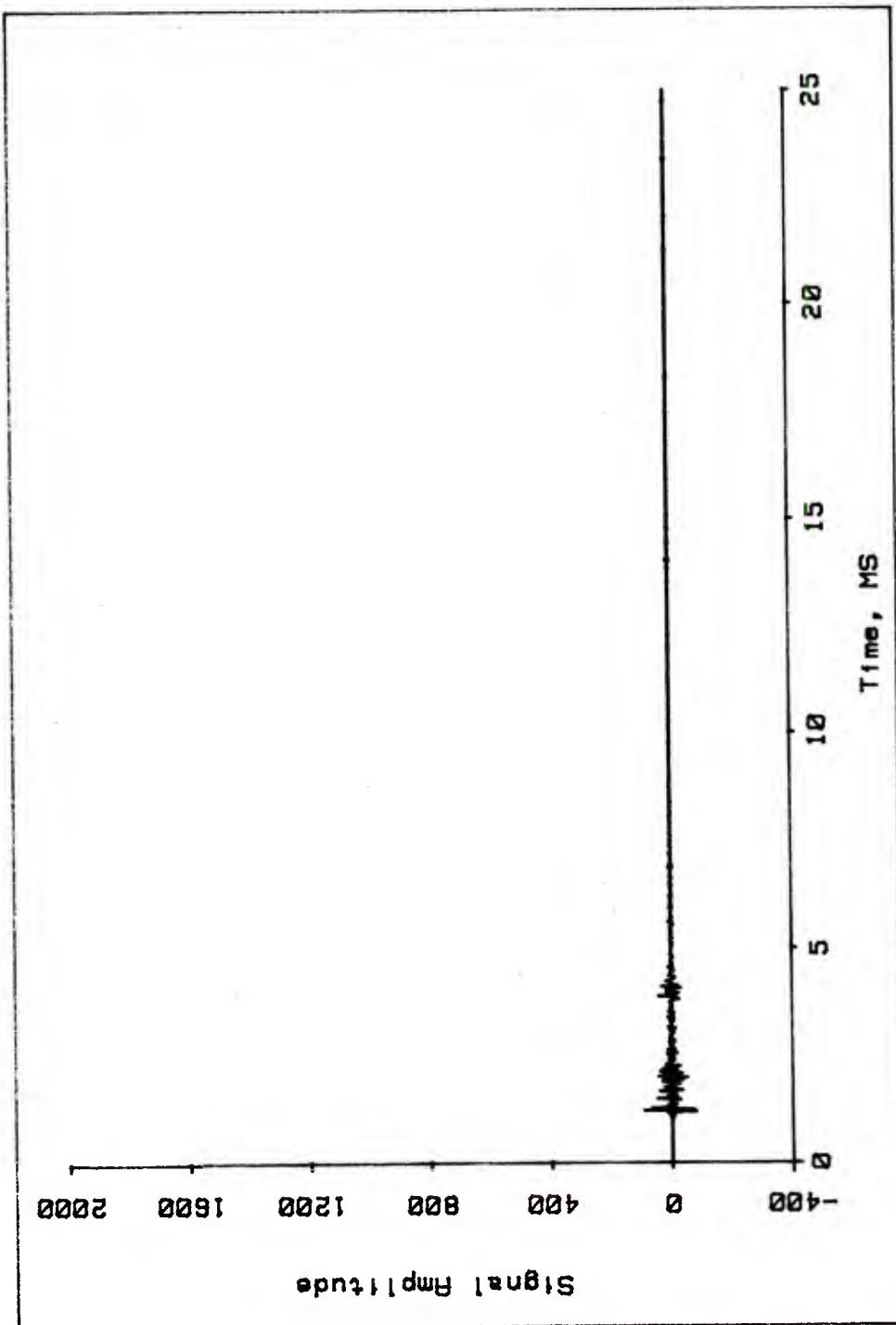
Figure 50. Difference: Figure 17 Minus Figure 49

73

One could not expect the differentiating filter to do as well if the input data contained significant frequencies beyond the 80% point. For example, the acceleration data of Example 4 was deliberately sampled sparsely so that its spectrum (Figures 33 and 36) has significant content out to the very end. Therefore, applying the differentiating filter to the integral in Figure 37 results in the curve in Figure 51. While this curve is similar to that of Figure 35, it is obvious that some high frequency content was lost. In fact, the difference curve of Figure 52 has nearly the same maximum and minimum amplitude as that of Figure 51.

If it should become necessary, in the course of analysis, to differentiate the data in Figure 37, there is a straightforward method by which this may be accomplished. If, in a particular time series, one interpolates between data points to double the total number available, then the apparent sampling rate is doubled, as is the bandwidth of the data. Using a simple linear interpolation on the data of Figure 35, its spectrum now is as shown in Figure 53. This spectrum is identical to that of Figure 36 up to the 8 kHz point. The "fabricated" part of the data, from 8 kHz to 16 kHz, shows a relative symmetry about the 8 kHz point, but with a rapidly decreasing amplitude. The important point to note is the absence of significant spectral content beyond 80% of the new bandwidth.

Applying the differentiating filter to the integral of the expanded acceleration data, and then incrementing the output by two to return to the original bandwidth, results in the curve shown in Figure 54. This curve is much closer to that of Figure 35 than was that in Figure 51. In fact, Figure 55 shows the difference between Figure 35 and Figure 54 to be insignificant except for the two high frequency peaks, one positive and one negative, at the center of the actual data event. While this technique has been relatively successful, it does demonstrate that using a sampling rate with only two samples per cycle at the highest frequency of interest may be enough to represent the data, but not enough to analyze it.

More precisely, sampling rate and useful frequency content can be linked as follows: at the 100% of bandwidth point in the spectrum, one has two samples per cycle, while at the 50% bandwidth point, one has four samples per cycle. It follows that at 80% of the bandwidth, one has about 2.5 samples per cycle (although the relationship is nonlinear). That is, a minimum reasonable data sampling rate is 3 samples per cycle at the highest frequency of interest. In actual practice, especially for analysis purposes, it is not desirable to have significant spectral content too close to the 80% point, and hence a much more useful minimum sampling rate is 4 or even 5 samples per cycle. Moreover, it has been shown that components, the frequency of which changes through the data event, can be isolated from the data for further study. If this additional analysis includes advanced Fourier techniques such as overlapping transforms for precise frequency determination, 8 to 10 samples

74
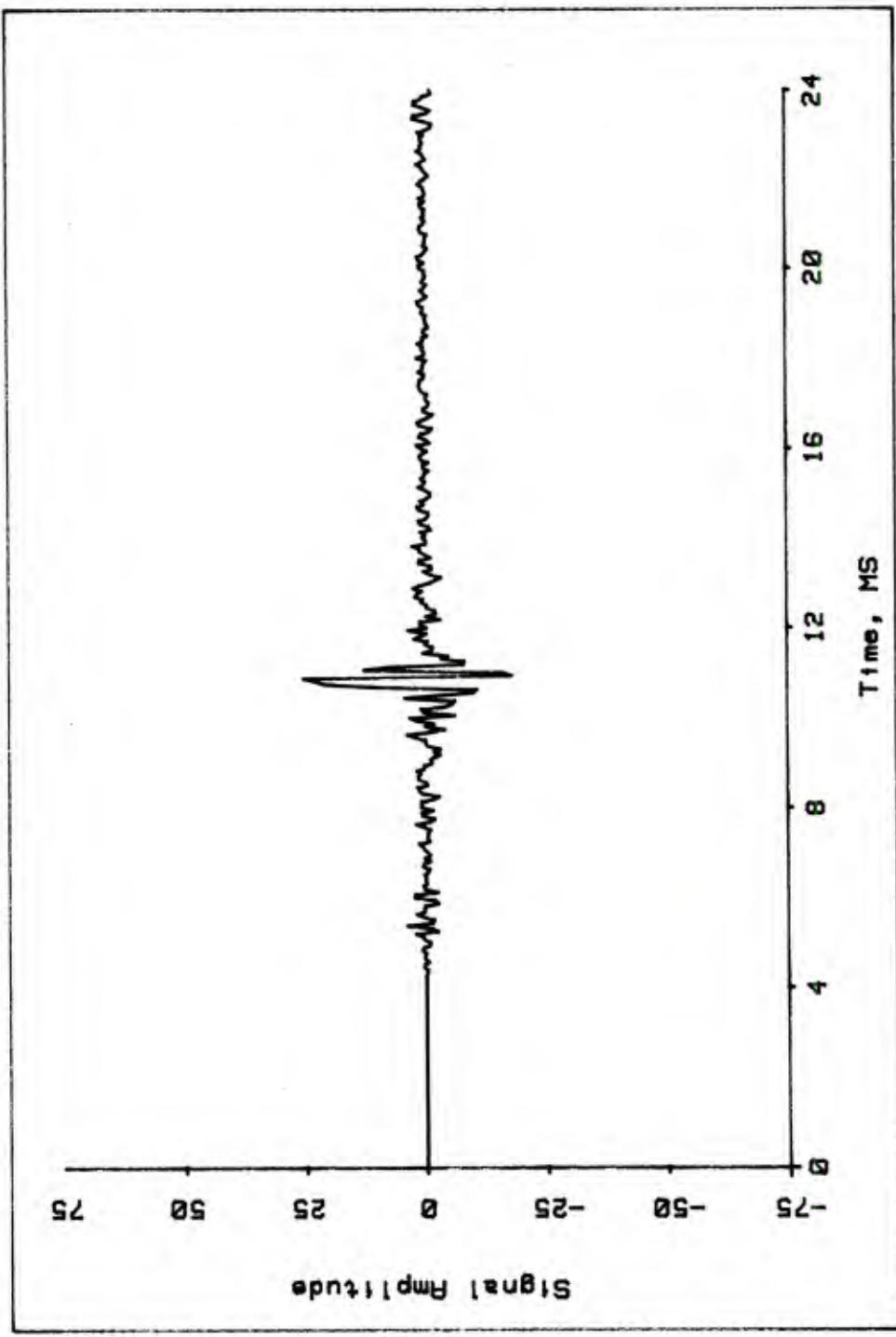
Figure 51. Derivative of Integral of Acceleration Data

75
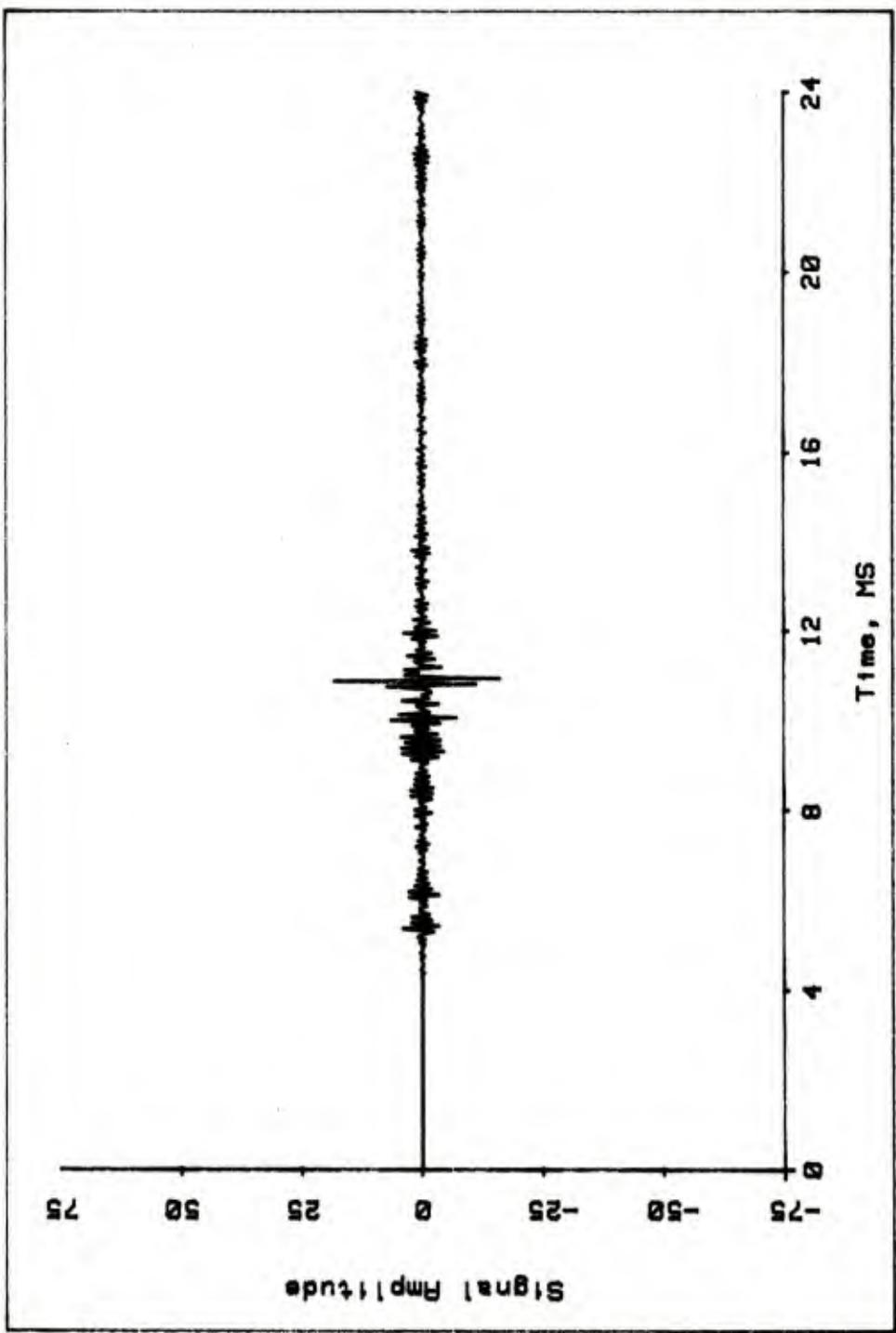
Figure 52. Difference: Figure 51 Minus Figure 35

76
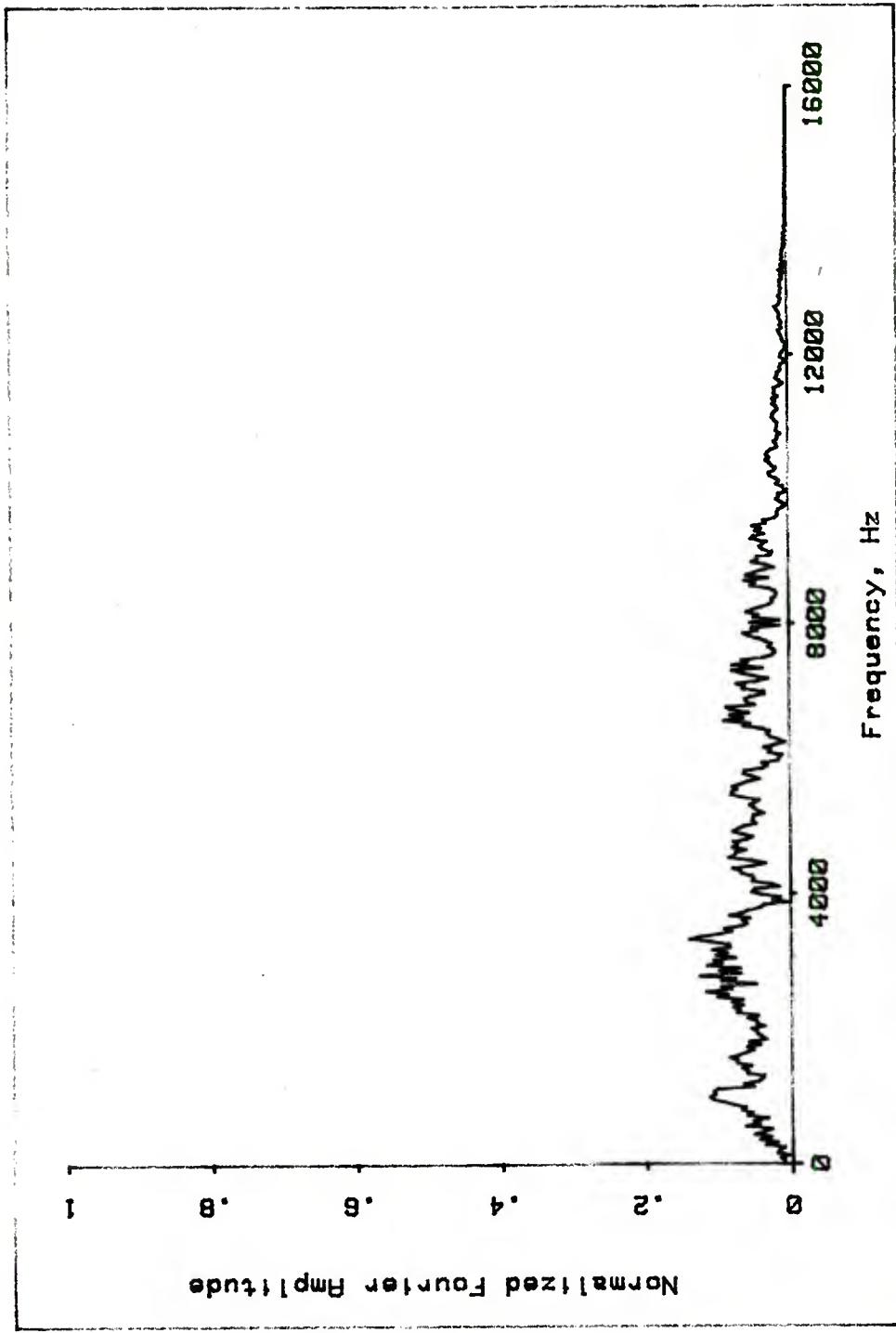
Figure 53. Spectrum of Expanded Acceleration Data
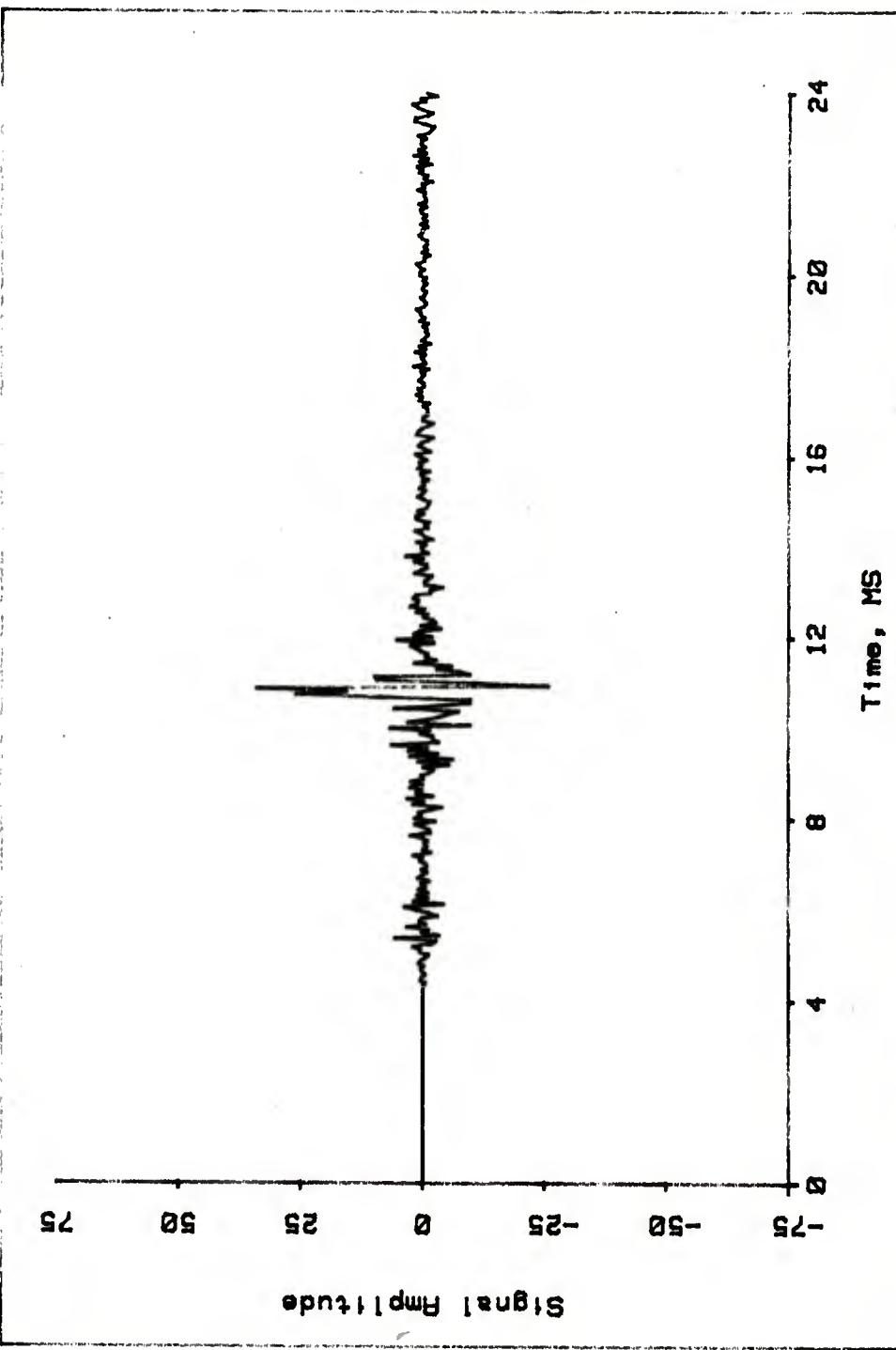
Figure 54. Derivative of Integral of Expanded Acceleration Data

78
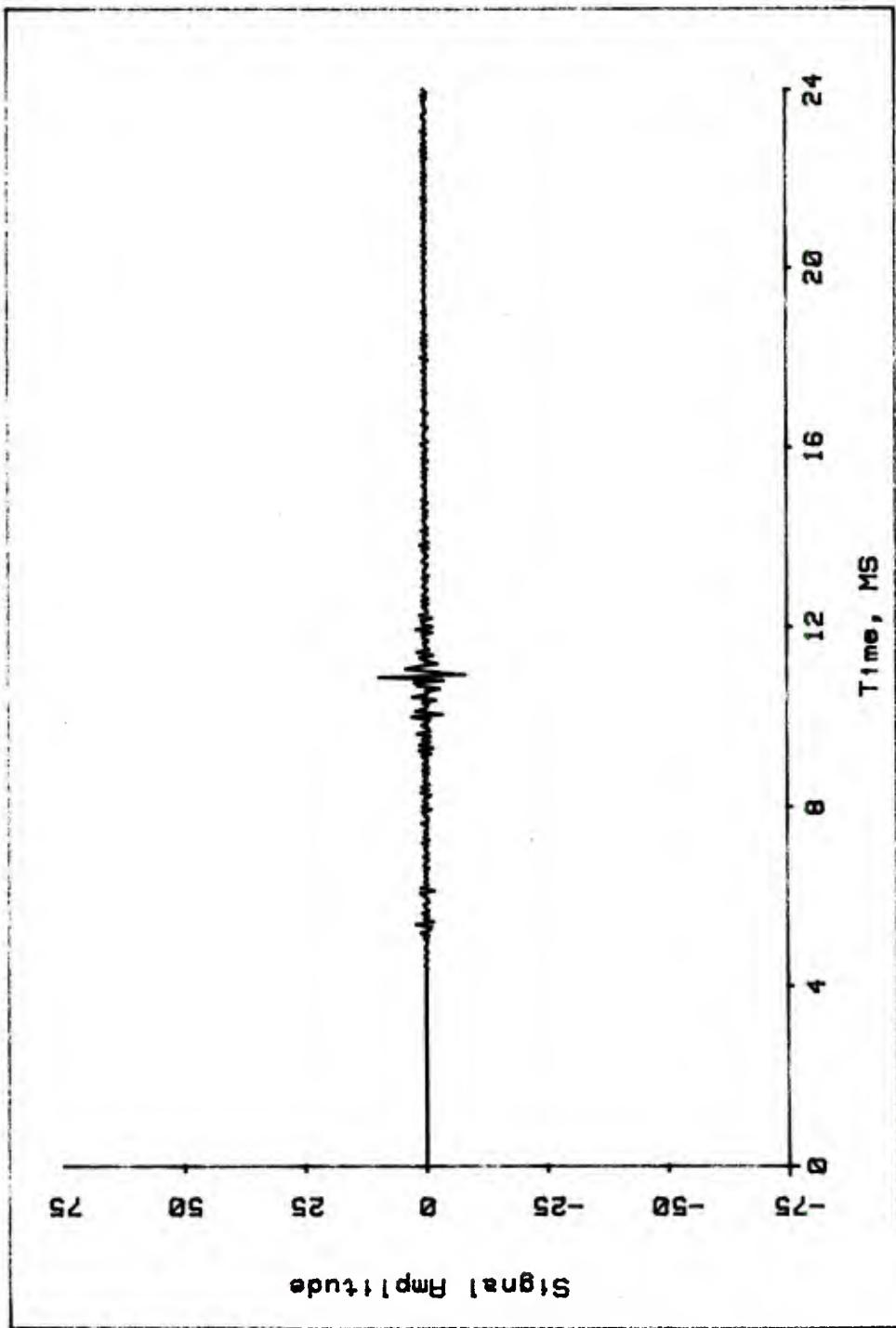
Figure 55. Difference: Figure 35 Minus Figure 54

79

per cycle at these frequencies may be necessary.

To further complicate the picture, it may not be possible to determine an appropriate sampling rate prior to conducting an experiment, since some or many of the frequency ranges may be unknown. In this respect, sampling rates should be tailored primarily to the frequency responses of the various record/playback devices and to the capabilities of the transducers involved. Total system frequency response cannot be increased by higher sampling rates, but data can certainly be lost by sampling rates which are too low. In short, instrumentation frequency responses and sampling rates must be chosen in consideration of the overall analytical plan in order to provide truly useful data. References 7, 8, and 9 contain more detailed discussions of these concepts.

X. CONCLUSIONS

In the analysis of ballistic data such as pressure, strain, and acceleration, the Fourier spectrum is an extremely useful tool. For nonreal-time data analysis, various numerical manipulations can be performed to enhance the applicability of Fourier techniques. These manipulations include odd periodic continuation, linear interpolation, and multiple-pass digital filter applications. While several less than successful examples have been presented, one can nonetheless conclude that Fourier analysis is applicable even in the presence of nonstationary frequencies. It can also be used to isolate aperiodic phenomena such as baseline variations.

Numerous methods have been presented by which the validity of the results of Fourier analysis can be verified, and by which amplitude errors can, in some cases, be corrected. It must be emphasized that in any such application, a great deal of engineering judgment is required for successful analysis. There is no substitute for thorough knowledge of engineering and physical principles as well as mathematical theory. Finally, specific results concerning the mechanical behavior of a system or revealing some fundamental physical or chemical property should be repeatable. The Fourier spectrum is a statistic; specific conclusions based on this type of analysis must be made from a sufficiently large sample of data.

---

[7] R.K. Otnes, L. Enochson, *Digital Time Series Analysis*, Wiley Inter-science, 1972.

[8] R.W. Hamming, *Numerical Methods for Scientists and Engineers*, McGraw-Hill, 1962.

[9] A. Papoulis, *The Fourier Integral and its Applications*, McGraw-Hill, 1962.

ACKNOWLEDGMENTS

REFERENCES

1. J.N. Walbert, "Computer Algorithms for the Design and Implementation of Linear Phase Finite Impulse Response Digital Filters", BRL Technical Report (to be published).

2. Bede-Liu, editor, Digital Filters and the Fast Fourier Transform, Halsted Press, 1975.

3. L.R. Rabiner, B. Gold, Theory and Application of Digital Signal Processing, Prentice-Hall, 1975.

4. R.B. Blackman, J.W. Tukey, The Measurement of Power Spectra, Dover Publications, 1958.

5. C.K. Yuen, D. Fraser, Digital Spectral Analysis, Pitman Publishing, 1979.

6. J.S. Bendat, A.G. Piersol, Randon Data: Analysis and Measurement Procedures, Wiley Interscience, 1971.

7. R.K. Otnes, L. Enochson, Digital Time Series Analysis, Wiley Interscience, 1972.

8. R.W. Hamming, Numerical Methods for Scientists and Engineers, McGraw-Hill, 1962.

9. A. Papoulis, The Fourier Integral and its Applications, McGraw-Hill, 1962.

APPENDIX A

A COMPUTER SUBROUTINE FOR THE FFT

```
10   OPTION BASE 0
20   COM SHORT Workin(1:2,1:4096),Workout(1:2,1:4096),Delta_time,Nrec
30   COM SHORT Delta_f,Maxx,Minx,Maxy,Miny,Call_point
40   COM Prime(1:12),Filename$(32),Label$(64),Prog$,Format$
50   COM INTEGER Array(0:16380),Nwords,Start,Stop,Inc,First_word
60   COM SHORT Data(1:4133),Complx(1:2,1:4133)
70   COM INTEGER Flag
80   BEEP
90   REDIM Workin(1:2,1:Nwords),Workout(1:2,1:Nwords)
100  PRINT "FOURIER TRANSFORM IN PROGRESS"
110  !   FFT ROUTINE COURTESY OF Dr. Carl DeBoor, MRC
120  !   GIVEN TO Dr. James Walbert IN MAY, 1979
130  Nextmx=12
140  Prime(1)=2
150  Prime(2)=3
160  Prime(3)=5
170  Prime(4)=7
180  Prime(5)=11
190  Prime(6)=13
200  Prime(7)=17
210  Prime(8)=19
220  Prime(9)=23
230  Prime(10)=29
240  Prime(11)=31
250  Prime(12)=37
260  Twopi=2*PI
270  RAD
280  Inzee=1
290  After=1
300  Before=Nwords
```

84

```
310  Next=1
320  IF INT(Before/Prime(Next))*Prime(Next))=Before THEN 380
330  Next=Next+1
340  IF Next<=Nextmx THEN 320
350  Now=Before
360  Before=1
370  GOTO 400
380  Now=Prime(Next)
390  Before=INT(Before/Prime(Next))
400  IF Inzee>1 THEN 430
410  CALL Fftstp(After,Now,Before,Twopi,Workin(*),Workout(*))
420  GOTO 440
430  CALL Fftstp(After,Now,Before,Twopi,Workout(*),Workin(*))
440  Inzee=3-Inzee
450  IF Before=1 THEN 480
460  After=After*Now
470  GOTO 320
480  IF Inzee=1 THEN 500
490  MAT Workin=Workout
500  BEEP
510  PRINT "FFT COMPLETED"
520  END
530  SUB Fftstp(After,Now,Before,Twopi,SHORT Zin(*),SHORT Zout(*))
540  PRINT "BEFORE=";Before;"AFTER=";After;"NOW=";Now
550  Nowmone=Now-1
560  Third=After*Now
570  Fourth=Third*(Before-1)
580  Angle=Twopi/Third
590  Omegar=COS(Angle)
600  Omegai=-SIN(Angle)
```

```
610    Argr=1
620    Argi=0
630    Second=Before*After
640    First=Nowmone*Second
650    FOR Index3add=0 TO Nowmone*After STEP After
660    FOR Ia=1 TO After
670    Index1=First+Ia
680    FOR Index3=Index3add+Ia TO Index3add+Ia+Fourth STEP Third
690    Valuer=Zin(1,Index1)
700    Valuei=Zin(2,Index1)
710    FOR Index2=Index1-Second TO Index1-First STEP -Second
720    Real=Valuer*Argr-Valuei*Argi+Zin(1,Index2)
730    Valuei=Valuer*Argi+Valuei*Argr+Zin(2,Index2)
740    Valuer=Real
750    NEXT Index2
760    Zout(1,Index3)=Valuer
770    Zout(2,Index3)=Valuei
780    Index1=Index1+After
790    NEXT Index3
800    Real=Argr*Omegar-Argi*Omegai
810    Argi=Argi*Omegar+Argr*Omegai
820    Argr=Real
830    NEXT Ia
840    NEXT Index3add
850    SUBEND
```

-86

DISTRIBUTION LIST

No. of Copies	Organization	No. of Copies	Organization
12	Commander Defense Technical Info Center ATTN: DDC-DDA Cameron Station Alexandria, VA 22314	9	Commander US Army Armament Research and Development Command ATTN: DRDAR-LC, T. Moore W. Williver K. Reuben H. Fair S. Bernstein G. Demitrack W. Benson B. Knutulski G. Bubb Dover, NJ 07801
1	Director Defense Advanced Research Projects Agency 1400 Wilson Boulevard Arlington, VA 22209		
1	Director Defense Nuclear Agency Arlington, VA 22209	2	Commander US Army Armament Research and Development Command ATTN: DRDAR-SC, B. Shulman Mr. Webster Dover, NJ 07801
1	Commander US Army BMD Advanced Technology Center ATTN: BMDATC-M P. O. Box 1500 Huntsville, AL 35807	2	Commander US Army Armament Research and Development Command ATTN: DRDAR-SE Dover, NJ 07801
1	Commander US Army Materiel Development and Readiness Command ATTN: DRCDMD-ST 5001 Eisenhower Avenue Alexandria, VA 22333	1	Commander US Army Armament Research and Development Command ATTN: DRDAR-FU Dover, NJ 07801
2	Commander US Army Armament Research and Development Command ATTN: DRDAR-TSS Dover, NJ 07801	2	Commander US Army Armament Research and Development Command ATTN: DRDAR-DP Dover, NJ 07801
1	Commander US Army Armament Research and Development Command ATTN: L. Goldsmith Dover, NJ 07801	2	Commander US Army Armament Research and Development Command ATTN: DRDAR-QA Dover, NJ 07801

DISTRIBUTION LIST

No. of Copies	Organization	No. of Copies	Organization

1	Commander
	US Army Armament Materiel
	  Readiness Command
	ATTN: DRSAR-LEP-L, Tech Lib
	Rock Island, IL 61299
		1	Commander
			US Army Electronics Research
			  and Development Command
			Technical Support Activity
			ATTN: DELSD-L
			Fort Monmouth, NJ 07703

1	Director US Army ARRADCOM Benet Weapons Laboratory ATTN: DRDAR-LCB-TL Watervliet, NY 12189	1	Commander US Army Harry Diamond Labs 2800 Powder Mill Road Adelphi, MD 20783
2	Director US Army ARRADCOM Benet Weapons Laboratory ATTN: DRDAR-LCB, T. Simkins T. Davidson Watervliet, NY 12189	1	Commander US Army Missile Command ATTN: DRSMI-R Redstone Arsenal, AL 35809
1	Commander US Army Aviation Research and Development Command ATTN: DRDAV-E 4300 Goodfellow Blvd. St. Louis, MO 63120	1	Commander US Army Missile Command ATTN: DRSMI-RBL Redstone Arsenal, AL 35809
2	Director US Army Research and Technology Laboratories (AVRADCOM) Ames Research Center Moffett Field, CA 94035	1	Commander US Army Missile Command ATTN: DRSMI-YDL Redstone Arsenal, AL 35809

1	Director
	US Army Air Mobility Research
	  and Development Laboratory
	Ames Research Center
	Moffett Field, CA 94035
		2	Commander
			US Army Mobility Equipment
			  Research & Development Command
			Fort Belvoir, VA 22060

1	Commander
	US Army Communications Research
	  and Development Command
	ATTN: DRDCO-PPA-SA
	Fort Monmouth, NJ 07703
		2	Commander
			US Army Tank Automotive Research
			  and Development Command
			ATTN: DRDTA-UL
			            Technical Director
			Warren, MI 48090

		2	Project Manager Division Air Defense Gun ATTN: DRCPM-ADG Dover, NJ 07801

DISTRIBUTION LIST

No. of Copies	Organization	No. of Copies	Organization
2	Project Manager Cannon Artillery Weapons System ATTN: DRCPM-CAWS Dover, NJ 07801	1	Director US Army TRADOC Systems Analysis Activity ATTN: ATAA-SL, Tech Lib White Sands Missile Range NM 88002
2	Project Manager Nuclear Munitions ATTN: DRCPM-NUC Dover, NJ 07801	1	Commander Naval Air Systems Command Washington, DC 20360
2	Project Manager Tank Main Armament Systems ATTN: DRCPM-TMA Dover, NJ 07801	2	Commander Naval Ordnance Systems Command Washington, DC 20360
1	Product Manager for 30mm Ammo. ATTN: DRCPM-AAH-30mm Dover, NJ 07801	1	Commander Naval Sea Systems Command Washington, DC 20362
2	Product Manager M110E2 Weapon System, DARCM ATTN: DRCPM-M110E2 Rock Island, IL 61299	2	Commander Naval Ship Research and Development Command Bethesda, MD 20084
3	Commander US Army Research Office P.O. Box 12211 ATTN: Technical Director Engineering Division Metallurgy & Materials Division Research Triangle Park NC 27709	1	Commander Naval Air Developmentment Center, Johnsville Warminster, PA 18974
1	Commander US Army Research Office ATTN: Dr. J. Chandra Research Triangle Park NC 27709	1	Commander Naval Missile Center Point Mugu, CA 95041
		2	Commander Naval Surface Weapons Center Dahlgren, VA 22448
4	Director US Army Mechanics and Materials Research Center ATTN: Director (3 cys) DRXMR-ATL (1 cy) Watertown, MA 02172	2	Commander Naval Surface Weapons Center Silver Spring, MD 20910
		2	Commander Naval Weapons Center China Lake, CA 93555

DISTRIBUTION LIST

No. of Copies	Organization
1	Commander Naval Research Laboratory Washington, DC 20375
1	Superintendent Naval Postgraduate School ATTN: Dir of Lib Monterey, CA 93940
1	Commander Naval Ordnance Station Indian Head, MD 20640
2	AFRPL ATTN: W. Andrepont T. Park Edwards AFB, CA 93523
2	AFATL Eglin AFB, FL 32542
2	AFWL Kirkland AFB NM 87117
2	ASD Wright-Patterson AFB OH 45433
1	Director Lawrence Livermore Laboratory Livermore, CA 94550
1	Director Los Alamos Scientific Laboratory Los Alamos, NM 87544
1	Headquarters National Aeronautics and Space Administration Washington, DC 20546

No. of Copies	Organization
2	Director National Aeronautics and Space Administration Langley Research Center Hampton, VA 23365
1	Director National Aeronautics and Space Administration Manned Spacecraft Center ATTN: Lib Houston, TX 77058
1	BLM Applied Mechanics Consultants ATTN: Dr. A. Boresi 3310 Willett Drive Laramie, WY 82070
1	CALSPAN Corp. ATTN: E. Fisher P. O. Box 400 Buffalo, NY 14225
1	S&D Dynamics, Inc. ATTN: Dr. M. Soifer 755 New York Avenue Huntington, NY 11743
1	Southwest Research Institute ATTN: P. Cox 8500 Culebra Road San Antonio, TX 78228
1	Stanford University Stanford Linear Accelerator Center ATTN: Eric Grosse, Numerical Analysis Consultant ALAC, P. O. Box 4349 Stanford, CA 94305
1	Towson State University Department of Mathematics ATTN: Miss Margaret Zipp Towson, MD 21204

DISTRIBUTION LIST

No. of Copies	Organization	No. of Copies	Organization
2	University of Delaware Department of Mathematics Department of Mechanical Engr. Newark, DE 19711		**Aberdeen Proving Ground**
		2	Dir, USAMSAA ATTN: DRXSY-D DRXSY-MP, H. Cohen
1	University of Illinois Department of Mathematics ATTN: Dr. Evelyn Frank Urbana, IL 61801	2	Dir, MTD ATTN: H. King P. Paules
		1	Cdr, USATECOM ATTN: DRSTE-TO-F

1	University of Kentucky
	Department of Computer Science
	ATTN: Prof. H. C. Thacher, Jr.
	915 Patterson Office Tower
	Lexington, KY 40506
		6	Cdr/Dir
			USACSL, EA
			ATTN: DRDAR-CL
			        DRDAR-CLB
			        DRDAR-CLB-PA
			        DRDAR-CLD
			        DRDAR-CLN
			        DRDAR-CLY

3	University of Wisconsin-Madison
	Mathematics Research Center
	ATTN: Dr. John Nohel
	        Dr. Carl de Boor
	        Dr. George Box
	610 Walnut Street
	Madison, WI 53706		

1	Virginia Commonwealth Univ. Department of Math. Sciences ATTN: Mr. V. Benokraitis 901 W. Franklin Richmond, VA 23284		
1	Virginia Polytechnic Institute Dept. of Aerospace Engineering ATTN: Prof. G. Inger Blacksburg, VA 24061		

USER EVALUATION OF REPORT

Please take a few minutes to answer the questions below; tear out this sheet, fold as indicated, staple or tape closed, and place in the mail. Your comments will provide us with information for improving future reports.

1. BRL Report Number_____

2. Does this report satisfy a need? (Comment on purpose, related project, or other area of interest for which report will be used.)

_____

_____

_____

3. How, specifically, is the report being used? (Information source, design data or procedure, management procedure, source of ideas, etc.)_____

_____

_____

4. Has the information in this report led to any quantitative savings as far as man-hours/contract dollars saved, operating costs avoided, efficiencies achieved, etc.? If so, please elaborate.

_____

_____

5. General Comments (Indicate what you think should be changed to make this report and future reports of this type more responsive to your needs, more usable, improve readability, etc.)_____

_____

_____

_____

6. If you would like to be contacted by the personnel who prepared this report to raise specific questions or discuss the topic, please fill in the following information.

Name:_____

Telephone Number:_____

Organization Address:_____

_____

_____